



Full-scale fire tests with a commuter train in a tunnel

Anders Lönnermark, Alexander Claesson, Johan Lindström, Ying Zhen Li, Mia Kumm, Haukur Ingason

SP Technical Research Institute of Sweden



Full-scale fire tests with a commuter train in a tunnel

Anders Lönnermark, Alexander Claesson, Johan Lindström, Ying Zhen Li, Mia Kumm, Haukur Ingason

Abstract

Full-scale fire tests with a commuter train in a tunnel

Three large scale fire tests were performed with a commuter train inside a tunnel. Two of the tests used an ignition source inside the train carriage and in one test a pool fire was placed under the carriage. Both tests where a fire initiated inside the carriage developed to flashover conditions. The difference between the two cases was that in one test a standard X1 carriage was used, while in the second case an X1 carriage was refurbished with more modern seats and a non-combustible aluminium lining on the walls and in the ceiling. The time to flashover was significantly different between the two test cases. In the test with the original seats and linings (test 2) the maximum heat release rate (HRR) was 76.7 MW and occurred 12.7 min after ignition. The maximum HRR in the case where more modern seats and aluminium lining were used (test 3), was 77.4 MW and occurred after 117.9 min. For these HRR calculations, the maximum gas temperature near the tunnel ceiling was used. The corresponding HRR calculated with oxygen consumption calorimetry was approximately 75 MW in test 3. Based on the temperature measurements in the carriage, the carriage was flashed over after 12 min in test 2 and after 119 min in test 3.

The main reason for the difference was the difference in initial combustion behaviour between the case with combustible wall and ceiling lining, and the case with non-combustible (aluminium) lining as the exposed interior surface. In the case with combustible lining a ceiling flame was developed, radiating towards the seats and the luggage spreading the fire more rapidly than in the case without exposed combustible lining.

The maximum HRR calculated from the experimental results are significantly higher than those obtained in other documented test series. The luggage in, under or between different seats was found to increase the fire spread significantly in both cases. This conclusion was drawn from other tests performed within the same project prior to the full-scale tests which are reported in full elsewhere.

Key words: metro, train, full-scale experiments, fire tests, tunnel

Photograph on front page shows fire test in the Brunsberg tunnel, courtesy of Per Rohlén.

SP Sveriges Tekniska Forskningsinstitut
SP Technical Research Institute of Sweden

SP Report 2012:05
ISBN 978-91-87017-22-3
ISSN 0284-5172
Borås

Contents

	Abstract	3
	Contents	4
	Preface	6
	Summary	7
	Nomenclature	9
1	Introduction	11
2	Description of the Brunsberg test tunnel	12
3	Fire load	14
3.1	Description of the carriages	14
3.1.1	X1	14
3.1.2	Refurbished X1	15
3.2	Luggage	16
3.3	Estimation of the fire load	17
3.4	Summary of material tests	17
4	Experimental set-up	19
4.1	Position of train carriage	19
4.2	Ventilation	20
4.3	Test 1	21
4.4	Test 2	22
4.5	Test 3	23
5	Theoretical procedure	25
5.1	Oxygen consumption calorimetry	25
5.2	CO ₂ and CO technique	25
5.3	CO ₂ production method	25
5.4	Maximum ceiling temperature method	26
5.5	Possible HRR of the metro carriage	27
5.6	Mass flow rate	27
5.7	Time correction	28
5.8	Extinction coefficient	29
6	Instrumentation	30
6.1	Temperature measurements	31
6.2	Heat flux	32
6.3	Gas analysis	33
6.4	Smoke	35
6.5	Air velocity in tunnel	37
6.6	Signal collection with data loggers	37
6.7	Instrumentation in the railway carriage - test 1	37
7	Test procedure	40
8	Results and discussion	42

8.1	Air velocity	42
8.2	Estimation of flow rate	44
8.2.1	Test 3	44
8.2.2	Test 2	46
8.3	Estimation of the HRR	46
8.3.1	Test 3	46
8.3.2	Test 2	48
8.4	Flashover of the carriage	51
8.5	Gas temperatures	51
8.6	Gas concentrations	61
8.7	Radiant heat Flux	64
8.8	Extinction coefficient	66
8.9	Pulsations	67
9	Conclusions	68
10	References	69
Appendix 1 - Test Protocols		71
Test 1		71
Comments and test Conditions		71
Notes before test start		71
Observations		71
Test 2		72
Comments and test Conditions		72
Notes before test start		72
Observations		72
Test 3		74
Comments and test Conditions		74
Notes before test start		74
Observations		74
Appendix 2 – Test Results		77
Temperature		77
Plate thermometers		86
Gas concentrations		87
Air velocity in the tunnel		90
Appendix 3 – Drawings		92
Appendix 4 – Photos from the tests		95
Test 1		95
Test 2		97
Test 3		102
Luggage		107
Appendix 5 – Results from material tests		111

Preface

METRO is a Swedish research project about infrastructure protection of rail mass transport systems, such as tunnels and subway stations. It is an multidisciplinary project with six different work packages (WP), where researchers from different national disciplines cooperate with practitioners with the common goal to make underground rail mass transport systems safer in the future. The nine partners were:

- **Mälardalen University** – School of Sustainable Development of Society and Technology, Project responsible
- **SP Technical Research Institute of Sweden** – Fire Technology
- **Lund University** – Department of Fire Safety Engineering and Systems Safety
- **Swedish Defence Research Agency (FOI)** – Defence and Security, Systems and Technology
- **Gävle University** – Department of Technology and Built Environment
- **Swedish National Defence College** – CRISMART
- **Swedish Fortifications Agency**
- **Greater Stockholm Fire Brigade**
- **Stockholm Public Transport (SL)**

METRO was a three year project which started in 15 December 2009 and finished 15 December 2012. The total budget was 19 million SEK. The full-scale tests presented in this report were a part of work package one (WP1) about design fires. The report summarises the results from the large scale fire tests carried out within the frame of WP1. It was the largest single WP and SP was WP leader of WP1. SP was together with Mälardalen University responsible for the performance of the full-scale tests in the Brunsberg tunnel.

METRO was funded by six organisations:

- Stockholm Public Transport (SL),
- the Swedish Research Council Formas
- Swedish Civil Contingencies Agency (MSB),
- the Swedish Transport Administration (STA),
- the Swedish Fortifications Agency (SFA),
- and the Swedish Fire Research Board (BRANDFORSK).

The project group wants to acknowledge the financiers of the project.

The following persons and organisations are acknowledged for their valuable contribution to the performance of the large scale fire tests presented in this report: fire fighters from Greater Stockholm Fire Brigade, geologist Anders Högrelius from Earth Consultants, Jari Antinluoma from Composite Media for the video documentation, Per Rohlén for photo documentation, students from Mälardalen University, the Fire Brigades from Arvika and Höga Kusten-Ådalen, and last but not least the technicians from SP who were instrumental in preparing for the tests and spent a lot of time at the test site making the experiments possible.

Summary

Three fire tests were performed under and inside commuter train carriages in a 276 m long abandoned railway tunnel, test 1 was a pool fire ignited under the carriage while test 2 and test 3 had a similar ignition source inside the carriage. Test 2 was conducted using a original X1 carriage with combustible interior wall lining while test 3 was conducted in a modified X1 carriage with non-combustible (aluminium) lining. The two tests with a fire initiated inside a carriage, developed to flashover conditions. In the test conducted with the original seats and linings (test 2), the maximum heat release rate (HRR) was 76.7 MW and occurred 12.7 min after ignition. In the test conducted on the refurbished carriage (test 3), the maximum HRR occurred after almost 118 min and was approximately 77.4 MW. This means that the maximum heat release rate was approximately the same in both tests, but the time to reach maximum HRR differed significantly. For these HRR calculations, the maximum gas temperature near the tunnel ceiling was used. The corresponding HRR calculated with oxygen consumption calorimetry was approximately 75 MW in test 3.

The main reason for the difference in fire growth rate between these two tests was due to the involvement of the combustible wall and ceiling lining in the test conducted in the original X1 carriage. This proves the importance of the lining material. A non-combustible interior lining material can increase the time available for evacuation significantly (almost a factor of 10 in these experiments). It should, however, be noted that the lining material in the original X1 also were of relative good quality (classified as HL2 according to CEN/TS 45545-2:2009).

The maximum HRR calculated from the experimental results are significantly higher than those obtained in other documented test series. The luggage in, under or between different seats was found to increase the fire spread significantly in both cases. Clearly, it is necessary for train owners to consider this transient load when conducting risk assessments and designing response tactics.

Different methods of estimating HRR are compared and good agreement has been obtained. The temperature method is quite robust, but dependent on the correct measurement of the maximum ceiling gas temperature. This method was used when deriving the HRR curves for the tests. The use of the CO₂/CO technology and the CO₂ production method underestimated the HRR at the first peak and slightly overestimate the HRR in the decay period (compared to the O₂ consumption calorimetry), but predict the HRR quite well in other periods.

To estimate the time for flashover of the carriage, the time when the gas temperature reached 600 °C in various positions and at different heights was evaluated. From this study the conclusion was drawn that the carriage was flashed over after 12 min in test 2 and after 119 min in test 3.

The gas temperature inside the carriage reached approximately 1000 °C in both test 2 and test 3 and despite the large difference in fire development, as discussed above, the temperature development for the parts when the entire carriage becomes involved in the fire are similar to each other

In the tunnel, the maximum temperature near the ceiling in test 3 was approximately 1120 °C measured above the centre of the carriage, compared to the maximum temperature in test 2 which was approximately 1080 °C, measured at the position +10m (10 m downstream the centre of the carriage).

During the periods of most intense fire in test 2 and test 3, pulsations in the tunnel were observed. The pulsations could be seen, felt and heard also outside the tunnel. The pulsations were identified as thermoacoustic instabilities.

Nomenclature

A	Area (m^2)
b	Equivalent radius of the fire source (m)
c_p	Heat capacity (kJ/kg/K)
c_{PT}	Lumped heat capacity coefficient ($\text{kJ/m}^2/\text{K}$)
C_s	Extinction coefficient ($1/\text{m}$)
h	Heat transfer coefficient ($\text{kW/m}^2/\text{K}$)
H	Height (m)
I	Intensity of light
k	Calibration coefficient (-)
k	Thermal conductivity (kW/m/K)
K_{cond}	Conduction correction factor ($\text{kW/m}^2/\text{K}$)
L	Distance between fire and measurement station (m)
L	Distance between transmitter and receiver in the smoke measurement system (m)
m	mass (kg)
\dot{m}	mass flow rate (kg/s)
M	Mole mass (g/mol)
Nu	Nusselt number (-)
p	Pressure (Pa)
P	Perimeter of the tunnel (m)
Pr	Prandtl number (-)
q''_{inc}	Incident heat flux (kW/m^2)
Q	Heat release rate (kW)
Re	Reynolds number (-)
T	Temperature (K)
u	Velocity (m/s)
V'	Dimensionless ventilation velocity (-)
W	Width (m)
x	Length (m)
X	Volume (mole) fraction (-)
ΔX	Volume (mole) fraction difference referring to ambient (-)
y	Distance from the wall closest to the point of interest (m)

Greek symbols

α	See Eq. (5.19)
β	See Eq. (5.19)
ε	Surface emissivity (-)
ρ	Density (kg/m^3)
σ	Stefan-Boltzmann constant ($5.67 \times 10^{-11} \text{ kW/m}^2/\text{K}^4$)
τ	Actual time (s)
ν	Kinematic viscosity (m^2/s)
ξ	Factor taking into account the combustion outside openings (-)
ζ	Ration between mean and maximum velocity

subscript

a	Air
c	Convective
c	Centre
fo	Fire source
i	i^{th} layer

j j^{th} species
k k^{th} segment
0 Ambient conditions

Abbreviations

DTR1 Delta temperature in region I
DTR2 Delta temperature in region II
HRR Heat release rate
PTC Plate thermometer

1 Introduction

Society is highly dependent on access to mass transport systems, e.g. metro systems, in order to facilitate transportation of people in populated urban areas. One example of such a metro system is the Stockholm underground. Fires, incidents or terror attacks not only potentially cost human lives and injuries, but also damage the environment, influence citizens' daily life and represent a significant cost in economic terms. Authorities and engineers working on safety and security aim to provide users with a high level of confidence in public systems, but safety and security come only at significant cost and it is often necessary to compromise between cost and benefits. One could, e.g., install water spray systems in the entire metro system to prevent the development of a fire, but this is in some cases unfavourable from a cost-benefit point of view.

Numerous fires and terror attacks have occurred in metro related systems throughout the world. A total of 289 people were killed and 265 severely injured in an accidental fire in the subway of Baku, the capital of Azerbaijan, 28th of October 1995 [1]. Similarly, some 198 people were killed and 146 injured in the Daegu subway arson attack of February 18, 2003 [2].

The mass transport system must be constructed so that people feel safe and secure when travelling. A lack of confidence in the system is devastating for both society and mass transport companies. Knowledge of the consequences of a fire incident or a terror attack in a metro system is therefore of utmost importance. There is a great need to improve the knowledge in many different fields of fire safety and security in metro systems.

Therefore, a large research project (METRO) was conducted 2009-2012 where a number of large-scale test were performed. The METRO project (www.metroproject.se) was an interdisciplinary collaborative research project between universities, research institutes, tunnel infrastructure owners and fire departments in Sweden. The main objective of METRO was to create a safer environment for passengers, personnel and first responders in the event of fire or terror attack in underground mass transport systems. A central part of the project is large-scale fire tests with commuter train carriages in a tunnel. The main aim of the large-scale tests is to illustrate the limitations, consequences and risks when such a carriage starts to burn, or is subject to a terrorist attack in a mass transport system. Such large-scale tests can give information on fire spread and development, the limit for flashover, radiation towards people, structures and equipment, conditions and possibilities for the fire and rescue services, and much more.

The large amount of resources needed (personnel, material, equipment, transportation, etc.) to perform large-scale fire tests with trains means that the number of full-scale tests that have been performed is limited. Still such full-scale tests are very important both for understanding of the fire behaviour and for comparison with computer simulations and model-scale tests. One example of tests performed with a metro car is from the extensive EUREKA 499 test series [3, 4]. In that test series, a German metro car was used giving a maximum HRR of 35 MW. In the same test series, tests were performed with different types of railway cars with maximum HRR between 13 MW and 43 MW [5]. Given the range of HRR and the diversity of railway carriages and tunnel dimensions, there is clearly a need for further large-scale data.

In this report the set-up and results of the large-scale fire tests performed within the METRO project are presented.

2 Description of the Brunenberg test tunnel

The full scale tests were performed in the old Brunenberg tunnel, located between Kil and Arvika in western Sweden (see Figure 2.1). This abandoned, 276 m long tunnel lies on a siding about 1 km long. It was taken out of service when a new tunnel was constructed to reduce the sharpness of a bend in the route (see Figure 2.2).



Figure 2.1 The location of the Brunenberg tunnel (from RIB with permission from the Swedish Civil Contingencies Agency, MSB).

The ground was not horizontal and the carriage in the tests was leaning somewhat sideways (towards south) corresponding to 3 mm over a distance of 60 cm. The tunnel had a slight downhill slope from east to west in the tunnel. The cross-section of the tunnel varies along the tunnel and to obtain a better view of this variation the cross-section was registered using a laser equipment at 21 different positions along the tunnel. The width 33 cm above the ground varied between 5.9 m and 6.8 m, with an average of 6.4 m and a median value of 6.3 m. The maximum tunnel height in the same positions varied between 6.7 m and 7.3 m with an average of 6.9 m and a median value of 6.8 m.



Figure 2.2 The old (left) and the new (right) Brunenberg tunnel. The picture was taken towards the western entrance.

The carriages used in the fire tests (see Section 3.1) were centred around a position 96 m from the eastern tunnel entrance (180 m from the western entrance). In Table 2.1 the width and height of the tunnel cross-sections at locations along or near the carriage are presented. The variation in the numbers can to a large extent be explained by local variation and the roughness of the tunnel, but one can see that the tracks were closer to the northern tunnel wall.

Table 2.1 Width and height of the tunnel near the location of the carriage.

Position ^{c)}	W _{north} ^{a)} (m)	W _{south} ^{a)} (m)	W _{total} ^{b)} (m)	H (m)
160 m	2.89	3.94	6.83	6.98
180 m	3.06	3.24	6.30	6.84
190 m	2.76	3.37	6.13	6.78
200 m	2.71	3.60	6.31	7.25

a) Measured from the centreline between the rails.

b) The width was measured 0.33 m around the ground between the rails.

c) Measured from the western entrance. The train carriage was centred around the position 180 m from the western entrance.

3 Fire load

3.1 Description of the carriages

3.1.1 X1

For the tests, X1 commuter trains, placed at the METRO project's disposal by the Stockholm Public Transport, were used. These trains consisted of two carriages each: one motor carriage and one control carriage. In the fire tests only the control carriage (control car) in each train set was used. The control carriage was approximately 24 m long. There was a driver's compartment at one end and the length of the passenger compartment was 21.7 m. The width of the inside of the carriage was 3 m and the height along the centreline was 2.32 m. The height at the wall was 2.06 m. The horizontal part of the ceiling was approximately 1.1 m wide. The carriage had six double doors, three on each side. The carriage had 22 double seats and 18 triple seats giving seating for a total of 98 passengers.

The passenger compartment had in total eight doors: six wide double door on the long sides (three on each side), one door to the next carriage (only one carriage was used in the each test) and one to the driver's compartment. At the start of the full scale tests the three doors on the southern side of the carriage were open, simulating a scenario where the train was stationary at a platform.

The X1 train was manufactured by Asea and owned by Stockholm Public Transport (SL). SL ordered 104 sets of X1 trains from Asea with delivery between 1967-1975 [6]. In 2006 an intensive outsourcing was started and trains were sent to disposal. At the end of 2009 as many as 20 X1 sets were still used as reserve trains. In April 2011 the last X1 trains were taken out of service. X1 3019 can be seen at the railway museum in Gävle. Bombardier still uses one X1 as a test train. The interior design of a X1 is shown in Figure 3.1. The standard X1 train was used in tests 1 and 2.



Figure 3.1 Interior design of a X1 train.

3.1.2 Refurbished X1

The X1 carriage used in Test 3 was refurbished to be similar to a modern C20 carriage used in the Stockholm Metro today. The underlying flooring material both in the X1 and C20 carriages consists of plywood board >18 mm with a minimum capacity in terms of an ultimate limit state of 750 kg/m² according to manufacturing documents. In the C20 carriage the surface flooring material consists of bitumen rubber carpets while the flooring in the older X1 carriage consisted of mipolam type (PVC) glued carpets. No changes were made from the X1 interior regarding the floor covering.

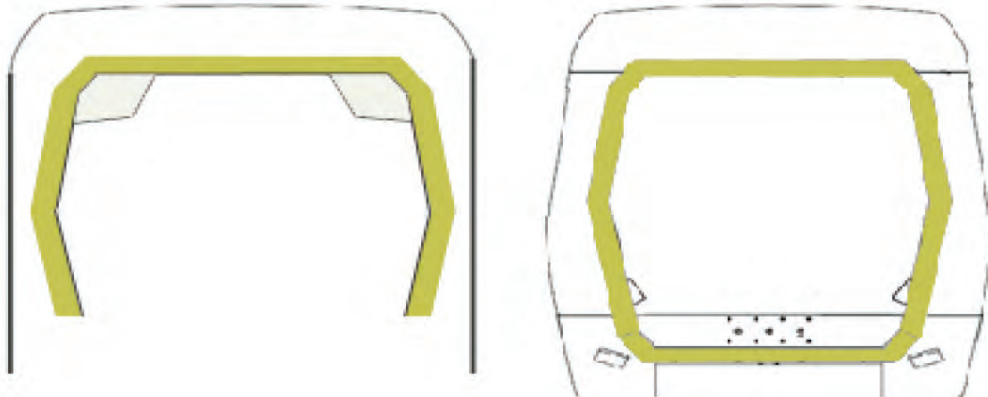


Figure 3.2 Inner shape of modern C20 wagon shown in X1 external measures (left) and original C20 external measures (right).

The new tilted walls in the refurbished X1 carriage were made of shielding panels of 1.5 mm thick SS 4007-14 aluminium panels with under-laying insulation of stone wool with a density of 100 kg/m³ similar to the original C20 fitting. The walls between the windows were covered with 0.6 mm thick aluminium metal sheets of the same quality. No under-laying isolation was mounted between the windows. The full interior of the refurbished X1 carriage was covered with incombustible surface material except for the driver's cabin, which was left in its original state. The dividing wall and door was fitted with aluminium metal plates with 50 mm stone wool of above-mentioned density. All joints, pop rivet and interstices were covered with aluminium tape in order to minimize the risk of early smoke and fire spread behind the panels. The refurbished width at the floor was 298.5 cm and the smallest width between the rounded walls below the windows was 283.5 cm.

The seats were changed to seats taken from a later X10 commuter train with the same fire resistance and measures as the seats in a C20 carriage. The set-up of the seats in the refurbished X1 was according to drawings of a C20 mid-section. The C20 carriages are fitted with glass partitions on each side of the doors. The partitions cover the entire floor to ceiling except for the aisle. In C20 the partitions are made of hardened glass, but in the refurbished X1 test carriage the partitions were made of 1.5 mm thick aluminium plates with aluminium taped wall and roof angles to cover the interstices between the pop rivets.



Figure 3.3 Interior X1 (left), C20 (middle) and refurbished X1 (right).

3.2 Luggage

It has been shown in fire tests carried out by the authors, in a fire laboratory using 1/3 of a train carriage, that luggage plays a very important role in the fire development [7]. Further, in investigations of some of the most hazardous fire accidents in railway and metro systems in modern time it has been shown that the luggage carried on by train passengers plays a very important role in the fire development [1, 8, 9]. Therefore, when planning the full scale fire tests, the influence of the transitional fire load in mass transport systems carried on by passengers was one of the most important parameters to evaluate.

To obtain a good estimation of what passengers in the Stockholm metro and commuter trains carry with them on the trains, a field study was carried out by Mälardalen University [10]. The field study was performed between the 12th of April 2010 and the 28th of May 2010, with an additional visit in June. Random passengers were asked if they wanted to be a part of this study and if they would allow their bags to be examined, the contents documented and weighed. The type of bag and position in the train were also noted. To obtain results that were as representative as possible, metro lines, times, days, age of the passenger etc. were varied. In total 323 bags in the metro and 299 on the commuter train were examined. The average weight of each carried piece of luggage on the commuter trains were at weekdays 4.4 kg, travel days and weekends 4.9 kg and over all a total of 4.65 kg. For the metro the corresponding numbers are: on weekdays 3.5 kg, travel days and weekends 4.5 kg and overall a total of 4.2 kg. On the commuter trains approximately 87 % of the passengers carried bags, while the corresponding value for the metro was 82 %. In average two prams were brought per train set during 75 % of the studied time (rush hours and daytime). Approximately 28 % of the passengers asked carried some sort of pressurized cans, like hairspray or other cans, mostly pressurized with flammable gas. A train set in Stockholm can carry approximately 1200 passengers during rush hours. This implies that an additional fire load corresponding to 85 GJ can be present on the train. If the carried fire load is left on the train or if the passengers bring their luggage with them in case of a fire depends mainly on the following parameters: the speed of the fire development, the design of the exits in the carriage (the distance down to the track) and the weight and importance of the bags. If the bags are left in the carriages it will lead to an increased fire load; if they instead are brought along they could constitute a factor that could slow down the flow of people through doors or decrease the walking speed in the tunnel.

In the full-scale tests, a total of 79 pieces of luggage was used in each test. This corresponds to approximately 81 % of the number of passenger seating positions for the original X1 (corresponding to 98 seats). The weight and the estimated energy content of the luggage is presented in Section 3.3. Photos of the luggage and information on type of luggage and the distribution of luggage in the carriages are presented in Sections 4.4 and 4.5. Photos of examples of the different types of luggage used are also included in Appendix 4.

3.3 Estimation of the fire load

Information concerning the total fire load of the commuter train X1 is relatively sparse, but the total fire load was estimated from the information that was available to be 35.4 GJ. This estimation is based on the materials in the walls, ceiling, floor and seats. Cables, batteries, other electric components, etc. are not included in this estimation.

In addition to the fire load of the carriages, the added luggage needs to be taken into account when estimating the total fire load in the tests. In total 79 pieces of luggage were used with an average mass of 4.44 kg. This corresponds to a total extra fire load of 351 kg. The different types of bags were filled with clothes and paper (reports and brochures). In total, the content of textile and plastics for each bag was approximately 60 % while the rest (40 %) was cellulosic material. If an average energy content of 20 MJ/kg is assumed, the extra fire load corresponds to 7.2 GJ, which represents 17 % of the new total fire load (42.6 GJ).

3.4 Summary of material tests

In connection with the full-scale tests it is of interest to know what classification the interior and furniture of the trains tested would achieve according to technical specification CEN/TS 45545-2:2009. In order to estimate the classification, a number of materials from the carriages were tested using the small scale fire test methods: ISO 5658-2, ISO 5659-2, ISO 5660-1 and ISO 9239-1. Further, the fire behaviour of passenger seats was evaluated according to CEN/TS 45545-2:2009, Annex B.

Two types of carriages were involved in the METRO project: the original X1 carriage here called type "X1" and a combination of train types "C20" and "X10", here referred to as "C20/X10". The "C20/X10" carriage was created by refurbishing an X1 carriage. The "C20/X10" designation signifies interior material simulating train type "C20" (with the exception of the floor coverings) with ceiling and walls covered with an aluminium layer, while passenger seats were from train type "X10". Materials tested in this study were wall linings, floor linings from "X1" and passenger seats from both train types. Ceiling lining was not tested due to lack of material.

The material tests are described in detail in Appendix 5. The results are summarized in Table 3.1 and Table 3.2 below.

Test results regarding the furniture and interior of the carriage called "X1" indicates Hazard Level HL2 for wall lining and Hazard Level HL3/HL1 for passenger seats. The floor did not achieve any Hazard Level rating due to too high values for CIT_G .

Table 3.1 Indicated Hazard Levels for "X1".

"X1"	Product Number	Requirement Set	Hazard Level
Wall lining	IN1	R1	HL2
Complete passenger seat	F1	R17	HL3
Passenger seat, upholstery	F1A	R20	HL1
Floor	IN16	R9	Not Classified

Test results regarding the furniture and interior of the carriage called "C20/X10" indicates Hazard Level HL3 for wall lining and Hazard Level HL3/HL1 for passenger seats.

Table 3.2 Indicated Hazard Levels for "C20/X10".

"C20/X10"	Product Number	Requirement Set	Hazard Level
Wall lining + Aluminium sheet	IN1	R1	HL3
Complete passenger seat	F1	R17	HL3
Passenger seat, upholstery and back shell	F1A	R20	HL1
Floor	Not tested since the same as for "X1".		

4 Experimental set-up

4.1 Position of train carriage

The carriages (see Figure 4.1) used in the fire tests were centred around a position 96 m from the eastern tunnel entrance (180 m from the western entrance). This location is referred to as ‘0 m’ (see Figure 4.2). Negative distance numbering refers to positions upstream of the fire, while positive numbers refer to positions downstream. Since the ventilation flow is coming from the eastern entrance, upstream of the fire means on the eastern side of the carriage and downstream means towards the western entrance of the tunnel. A more detailed description of the measurement positions is included in Chapter 6 and a large version of the drawing is included in Appendix 3. In some cases the “right” side or the “left” side of the carriage are referred to in the text. In these cases the carriage is viewed towards the front of the carriage (from outside) from the eastern entrance (see Figure 4.1), which means that the right side of the carriage faces north.

To protect the concrete lining of the tunnel (approximately 10 cm of reinforced shotcrete), the tunnel ceiling was covered with 630 m² insulation between -15 m and +35 m (see Figure 4.1). The insulation used was 50 mm thick U Protect Wired Mat 2.0 with a density of 55 kg/m³.



Figure 4.1 The carriage at its position in the tunnel before test 2.

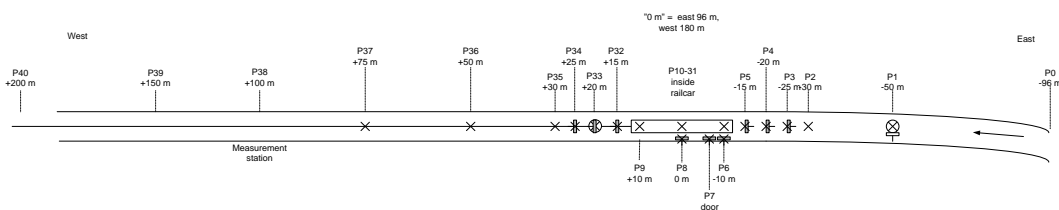


Figure 4.2 Positions in the Brunnsberg tunnel. A larger version of the drawing is included in Appendix 3.

4.2 Ventilation

When using PPV (Positive Pressure Ventilation) a common recommendation in enclosure fires is to place the mobile ventilator at a distance correlating to the opening height. As mobile ventilation of tunnels in case of fire is less common than in traditional enclosure fires, the same recommendation is typically used in tunnel situations as well. Neither openings in buildings nor tunnel entrances correlate well to the shape of the air cone from a mobile ventilator. If the air cone meets the wall outside the tunnel, much momentum is lost before the air even enters the tunnel. Outside the the tunnel the air can be turbulent due to the outside wind and the ejector effect, when the primary airflow through the ventilator pulls additional air into the tunnel, can be disturbed.

Prior the full scale fire tests, the optimal location of the ventilator, with respect to the tunnel entrance, was investigated at the Ådalen Line tunnels in the north of Sweden [11]. The tunnels used for the ventilation pre-tests were: the Gårdberg Tunnel (820 m), the Murberg Tunnel (1689 m) and the Kroksberg Tunnel (4551 m). The tests were performed with the ventilator placed at the downstream end of the tunnel. During the tests the counteracting wind induced air velocity inside the tunnel varied between 0.1 and 0.5 m/s. For the three tested locations - outside the tunnel, in the tunnel opening and inside the tunnel - the difference in counteracting airflow for the same tunnel varied ≤ 0.09 m/s. The distance outside the tunnel entrance was chosen with respect to the cone angle so the air cone from the ventilator should cover the tunnel opening but meet the rock wall outside the tunnel as little as possible. The same distance from the tunnel entrance was then chosen for the location inside the same tunnel. The variation of the distance between the tunnel opening and the location of the ventilator was ≤ 1.0 m for the three different tunnels.



Figure 4.3 The tested locations; outside the tunnel, at the tunnel entrance and inside the tunnel. (Photo: Mia Kumm)

The same ventilator, a trailer mounted Mobile Ventilation Unit, MGV L125/100FD (see Figure 4.3), with the capacity of $217,000 \text{ m}^3/\text{h}$ (equal to $60.3 \text{ m}^3/\text{s}$) was used both in the ventilation pre-tests and in the later full-scale fire tests. The results clearly showed that the location inside the tunnel was more favourable with respect to the time to turn the airflow inside the tunnel and the final achieved air velocity. At the two tests in the Gårdberg and Murberg tunnels the ventilator induced air velocity increased with approximately 7 % from the outside location to the location at the tunnel entrance and approximately 18 % from the outside to the inside locations. From the Kroksberg tunnel tests, due to leakage around the evacuation doors between the main tunnel and the evacuation tunnel, no specific conclusions regarding the influence of the location on the re-directed air velocity inside the tunnel, could be drawn.

During the full-scale fire tests, the ventilator was placed at the east end of the tunnel in order to direct the smoke and make temperature and HRR measurements possible. Based on the results from the ventilation pre-tests the ventilator was positioned 4 m into the

tunnel from the eastern tunnel entrance. The mean air velocity in the tunnel, before ignition, varied between 2.0 and 3.0 m/s and was somewhat higher for Test 1.



Figure 4.4 The fan was positioned 4 m into the tunnel from the eastern tunnel entrance. (Photo: Per Rohlén)

The mobile ventilator also made it possible for the fire and rescue services to be located, up-stream, close to the fire. Without the ventilator the heat flux from the back-layering and the fire itself would have made it impossible for the fire fighters to stay close enough to the fire to make the desired observations. The sound level from the ventilator caused problems for the BA (breathing apparatus) Fire Fighters to communicate, both between themselves and with the BA Rescue Commander. For safety reasons the ordinary BA mask mounted microphones had to be changed for throat microphones, commonly used by military pilots, between Test 1 and Test 2. After the changes of microphones the communication worked satisfactory, except in the immediate surroundings of the ventilator itself. As the location, in a real life fire, of the ventilator and the BA Rescue Commander could be close or the same, fire and rescue services using mobile ventilation in tunnels should include communication tests in their contingency planning for the tunnels within their jurisdiction.

4.3 Test 1

The purpose of the fire scenario in test 1 was to evaluate the risk for fire spread underneath the railway carriage in case of a fire in for example the breaks or electrical devices. On the same time it was important that the fire did not spread to the inside of the carriage since it was to be used in a second fire test. Therefore, the temperature in the floor was measured during the test. Furthermore, a manually manoeuvred open sprinkler system with the nozzles pointing upwards was for safety reasons mounted between the rails beneath the carriage. The fire source was a pool of heptane positioned under the ATC receiver (see Figure 4.5). The pool area was 350 mm × 350 mm × 35 mm. The pool contained 3.2 L of heptane. The distance between the top of the pool (edge) and the ATC receiver was 155 mm. The test was performed inside the tunnel and with an air velocity over the pool fire under the carriage of approximately 2-3 m/s. The HRR from such a pool fire was measured in the laboratory (without ventilation) to increase to a plateau at 300 kW after 1 min. After 3 min the HRR increased further to a maximum of

approximately 500 kW after which the HRR decreases until it was self-extinguished after approximately 6 min.



Figure 4.5 Position of the heptane pan in test 1.

4.4 Test 2

In test 2 an X1 carriage with original interior materials was used. As described in sections 3.2 and 3.3, luggage was added to the carriage to simulated luggage left behind in a burning carriage. Table 4.1 shows the amount and type of each bag that were used in the railway carriage in fire test 2. Figure 4.6 shows how the different types of luggage was placed and distributed inside the carriage. The positions of different pieces of luggage in test 2 are also shown in the schematic in Figure 4.7 and the photo in Figure 4.7.

Table 4.1 Table of the luggage used in fire test 2.

Type of luggage	Amount	Weight (kg) / bag
Large duffel bag or suitcase	4	14
Middle size bag	5	10
Cabin bag	15	5.3
Sports bag, shoulder bag	27	3
Backpack	28	3
Total	79	4.44 in average

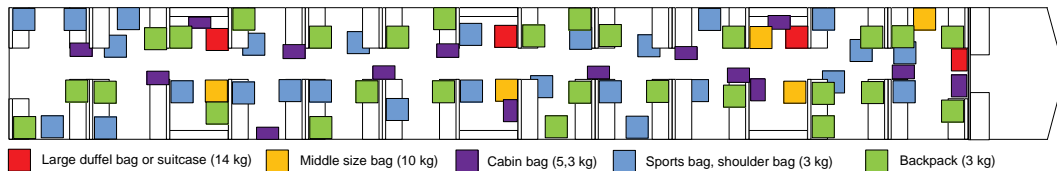


Figure 4.6 Placement of the luggage in fire test 2.



Figure 4.7 Pieces of luggage in, at or under different seats in the X1 carriage before the start of test 2. (Photo: Per Rohlén)

4.5 Test 3

In test 3, the refurbished X1 carriage (see section 3.1.2) was used. Luggage was added in the same way as in test 3, but the distribution between sports bags/shoulder bags and backpacks was not exactly the same in the two tests (see Table 4.1 and Table 4.2). The weight of these bags were, however, the same. Furthermore, the content was of the same type for all of the bags. This means that that the total weight of the luggage was the same in test 2 and test 3. The distribution of different types of luggage in the carriage were also the same in the two tests. The distribution of the luggage in test 3 can be seen in the schematic in Figure 4.8. The positions of different pieces of luggage in test 3 are also shown in the photo in Figure 4.9

Table 4.2 Table of the luggage used in fire test 3.

Type of luggage	Amount	Weight (kg) / bag
Large duffel bag or suitcase	4	14
Middle size bag	5	10
Cabin bag	15	5.3
Sports bag, shoulder bag	23	3
Backpack	32	3
Total	79	4.44 in average

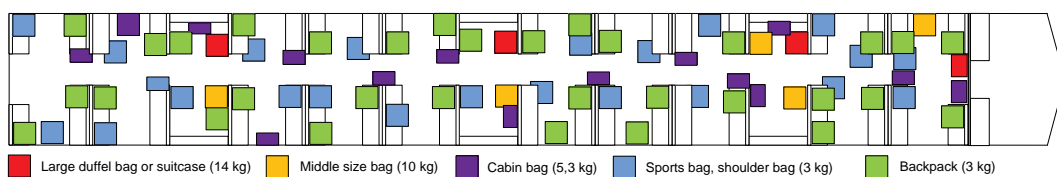


Figure 4.8 Placement of the luggage in fire test 3.



Figure 4.9 Pieces of luggage in, at or under different seats in the refurbished X1 carriage before the start of test 3. (Photo: Per Rohlén)

5 Theoretical procedure

5.1 Oxygen consumption calorimetry

In the analysis of the measured data, the heat release rate was determined by dividing the cross-section into several segments, each relating to a specific set gas analyses. The heat release rate produced by the vehicles burning inside the tunnel can be estimated by use of the following equation (without correction due to CO production) using oxygen consumption calorimetry [12, 13].

$$Q = 14330 \sum \dot{m}_i \left(\frac{X_{0,o_2} (1 - X_{CO_2,i}) - X_{O_2,i} (1 - X_{0,CO_2})}{1 - X_{O_2,i} - X_{CO_2,i}} \right) \quad (5.1)$$

where Q is the heat release rate (kW), \dot{m}_i is the mass flow rate of the i^{th} layer, X_{0,o_2} is the volume fraction of oxygen in the incoming air (ambient) or 0.2095, X_{0,CO_2} is the volume fraction of carbon dioxide measured at the measuring station or $X_{0,CO_2} \approx 0.00033$, carbon dioxide, X_{O_2} and X_{CO_2} are the downstream of the fire measured by a gas analyser (dry).

5.2 CO₂ and CO technique

There are other calorimetry methods available to determine the heat release rate, such as CO/CO₂ ratio method developed by Tewarson [14] and utilized in tunnel fires by Grant and Drysdale [13, 15]:

$$Q = 12500 \frac{M_{CO_2}}{M_a} \Delta X_{CO_2} \dot{m}_a + 7500 \frac{M_{CO}}{M_a} \Delta X_{CO} \dot{m}_a \quad (5.2)$$

where $M_{CO_2} = 44$ g/mol, $M_{CO} = 28$ g/mol and $M_a = 28.95$ g/mol. X_{CO_2} and X_{CO} are the increases above ambient, i.e. the 'background' levels should be subtracted from these measured values.

5.3 CO₂ production method

The production rate of the j^{th} species in a tunnel fire can be estimated by the following equations:

$$\dot{m}_j = \dot{m} \frac{M_j}{M_{air}} \Delta X_{j,avg} \quad (5.3)$$

where \dot{m}_j is the production rate of the j^{th} species, \dot{m} is the total mass flow rate, M is the molecular weight.

The production rate of CO₂ can be expressed as a function of the heat release rate in the following form [16]:

$$\dot{m}_{CO_2} = 0.000087Q \quad (5.4)$$

and the heat release rate can be estimated by:

$$Q = 11500\dot{m}_{CO_2} \quad (5.5)$$

5.4 Maximum ceiling temperature method

Li and Ingason [6-8] investigated the maximum ceiling temperature in a tunnel fire using most of the data available internationally, including the Runehamar test data [16]. They proposed that the maximum excess gas temperature beneath the ceiling in a tunnel fire can be divided into two regions depending on the dimensionless ventilation velocity, V' . Each region can be further subdivided into two regions with transition from linear increase to a constant plateau according to the fire size and ventilation. The maximum excess gas temperature beneath the ceiling can be expressed respectively as [6-8]:

Region I ($V' \leq 0.19$):

$$\Delta T_{\max} = \begin{cases} \text{DTR 1}, & \text{DTR 1} < 1350 \\ 1350, & \text{DTR 1} \geq 1350 \end{cases} \quad (5.6)$$

Region II ($V' > 0.19$):

$$\Delta T_{\max} = \begin{cases} \text{DTR 2}, & \text{DTR 2} < 1350 \\ 1350, & \text{DTR 2} \geq 1350 \end{cases} \quad (5.7)$$

where

$$\text{DTR 1} = 17.5 \frac{Q^{2/3}}{H_{ef}^{5/3}},$$

$$\text{DTR 2} = \frac{Q}{u_o b_{fo}^{1/3} H_{ef}^{5/3}}.$$

In Equation (5.6) and (5.7), DTR1 means Delta Temperature in Region I ($^{\circ}\text{C}$) and DTR2 means Delta Temperature in Region II ($^{\circ}\text{C}$), H_{ef} is the effective tunnel height (m), i.e. the vertical distance between the bottom of the fire source and tunnel ceiling, b_{fo} is the equivalent radius of fire source (m), u_o is the ventilation velocity (m/s).

The dimensionless ventilation velocity, V' , in Equations (5.6) and (5.7) is defined as:

$$V' = \frac{u_o (b_{fo} \rho_o c_p T_o)^{1/3}}{(gQ)^{1/3}} \quad (5.8)$$

where g is gravity acceleration (m^2/s), c_p is heat of capacity (kJ/kg/K), T_o is ambient temperature (K).

In our case, the dimensionless ventilation velocity, V' is higher than 0.19, and the maximum ceiling excess temperature is less than 1350°C . Thus, the heat release rate can be estimated by:

$$Q = u_o b_{fo}^{1/3} H_{ef}^{5/3} \Delta T_{\max} \quad (5.9)$$

In these specific cases, the entire horizontal cross-section is considered as the fire source in calculating the equivalent radius of the fire source.

5.5 Possible HRR of the metro carriage

For a fully developed metro carriage fire, the possible HRR can be estimated using:

$$Q_{\max} = 3000 \dot{m}_{a,\max} = 1500 \sum A_i \sqrt{H_i} \quad (5.10)$$

where A_i and H_i are the area and the height of the i^{th} window, respectively.

For a post-flashover fire, there could also be some part of combustion outside the openings. This increases the total heat release rate significantly. Ingason carried out a series of model scale (scale 1:10) railcar tests [17] and the results showed that the heat release rate for a post-flashover fire can be estimated using Equation (5.10) multiplied by a factor, ξ , ranging from 1.3 (Test 5) to 1.72 (Test 1). Note that the scaled-up fuel load density in test 1 in the model-scale test series [17] was quite high. Therefore, the lower factor of 1.3 is more reasonable for comparison with the full scale tests carried out in METRO project (presented in this report). The maximum heat release rate for a post-flashover fire in a metro carriage can be expressed as:

$$Q_{\max} = 3000 \xi \dot{m}_{a,\max} = 1500 \xi \sum A_i \sqrt{H_i} \quad (5.11)$$

5.6 Mass flow rate

Bi-directional probes [10] were used to measure the centreline velocity, u_c , which can be expressed as:

$$u_c = \frac{1}{k} \sqrt{\frac{2T\Delta p}{\rho_o T_o}} \quad (5.12)$$

where T is the gas temperature, T_o ambient temperature, k a calibration coefficient, Δp the measured pressure difference.

The calibration constant k is a function of the Reynolds number, where the characteristic length is the diameter of the probe. In the test the Reynolds number was found to be approx. 2000 – 5000 which means that the calibration constant is 1.08 [18]. The ambient temperature and air density used was, 286 K and 1.22 kg/m³, respectively.

Since the velocity measured in the tests is not the average velocity of the fresh air, u_o , one needs to determine a flow coefficient related to the measured velocity and the average velocity. In the analysis of the measured data the air mass flow rate was determined by dividing the flow into five along the height equally distributed horizontal area segments, where every area was related to each bi-directional probe and thermocouple. The total air mass flow rate, \dot{m} , was determined according to the following equation:

$$\dot{m} = \sum_k \zeta_k \frac{\rho_0 T_0}{T_k} u_k \Delta A_k \quad (5.13)$$

The theoretically determined mass flow correction factor (ratio of mean to maximum velocity), ζ_k , is dependent of the variation of temperature and velocity over the segment. Velocity and gas temperature difference profiles (ΔT) can be represented by the following expression for turbulent boundary layer flow in smooth pipes [11]:

$$\frac{u}{u_{\max}} = \left(\frac{y}{y_{\max}} \right)^{1/n} \quad (5.14)$$

where y is the distance from the wall closest to the position of interest, u is the velocity in this position, y_{\max} is the distance from the centre to the closest wall valid for the position of interest, and u_{\max} is the velocity in the centre of the cross-section. The ratio of mean to maximum velocity can then be calculated as

$$\zeta = \frac{u_0}{u_{\max}} \quad (5.15)$$

The exponent n in equation (5.14) varies with the Reynolds number ($n=7$ for $Re=1.1 \times 10^5$ and $n=8.8$ for $Re=1.1 \times 10^6$). For the present case the Reynolds number was between 7×10^5 and 8×10^5 . This indicates an n between 7 and 8.8, but since there was no information given for the values within this interval, a value of 7 was chosen for n . According to the literature [11] the ratio of mean to maximum velocity becomes 0.817 for $n = 7$. This coefficient are assumed to be valid for each area segment.

5.7 Time correction

Since the estimated HRR at the measuring station located 100 m downstream of the fire source does not represents the actual HRR at the fire source at a specific time, we need to correct the time scale to plot the right one.

The actual time, τ , can be approximated with aid of the following equation [12]:

$$\tau = t - \int_0^L \frac{dx}{u(x)} \quad (5.16)$$

where L is the distance between fire and measurement station.

The variation of the velocity along the tunnel can be approximated with aid of the mass balance equation and the ideal gas law assuming constant cross-sectional area and neglecting the fuel mass flow compared to the airflow in the tunnel:

$$u(x) = \frac{u_0}{T_0} T(x) \quad (5.17)$$

According to the analysis of Section 2.3, the average temperature of the smoke flow at a given distance, x , downstream of the fire can be estimated by:

$$T_{avg}(x, t) = T_0 + \frac{2}{3} \frac{Q(\tau)}{\dot{m}c_p} \exp\left[-\left(\frac{hP}{\dot{m}c_p} x\right)\right] \quad (5.18)$$

Therefore, the actual time can be expressed as:

$$\tau = t - \frac{L}{u_0} \left[\frac{1}{\alpha} \ln\left(\frac{\beta + e^\alpha}{\beta + 1}\right) \right] \quad (5.19)$$

where

$$\alpha = \frac{hPL}{\dot{m}c_p} \quad \text{and} \quad \beta = \frac{2}{3} \frac{Q}{\dot{m}c_p T_0}$$

Another simple method to correct the time is based on a direct estimation of the time consumed during the transport between the fire source and the measurement station using the ventilation velocity. This simple method is very useful when the distance is short, e.g. suitable in this report.

According to the relation between the measured time and the actual time, the actual heat release rate can be obtained. Note that the combustion products produced in a tunnel fire is carried by the flow. This suggests that one can obtain the actual heat release rate curve just by correcting the time index.

Further, note that the time index of the heat release rate curve based on ceiling gas temperature does not need to be corrected since the time delay of the ceiling gas temperature measurements, i.e. only some seconds, can be ignored.

5.8 Extinction coefficient

The smoke density was measured both in the carriage and at the measurement station, using laser and photo cell systems. The attenuation in the smoke can be described by the extinction coefficient.

The extinction coefficient of the smoke can be obtained by the following:

$$C_s = \frac{1}{L} \ln\left(\frac{I_0}{I}\right) \quad (5.20)$$

where

C_s	=	Extinction coefficient
L	=	Length between laser and photo cell receiver
I_0	=	Original intensity without smoke
I	=	Intensity with smoke

6 Instrumentation

During the tests, different parameters were measured in many different positions. All positions for measuring are numbered from P1 – P39 and shown in Figure 4.2. Positions P10 – P31 are measuring positions inside the railway carriage and are shown in more detail in section 6.7. For more details about each measuring point (P1-P39) see Appendix 3.

The data acquisition was comprehensive. Gas temperatures at numerous positions (both in the carriage and in the tunnel), heat release rate (HRR), gas concentrations and smoke inside the carriage and the tunnel, as well as radiant fluxes and gas velocities, were measured. In Figure 6.1 and Figure 6.2 the measurement positions in the tunnel are presented. The measurement positions inside the carriage are given in Figure 6.3. The details on the different types of measurements are presented in separate sections below.

The set-up of measurement equipment in the tunnel was the same in all three fire tests. The midpoint of the railway car was placed 96 m into the tunnel, measured from the eastern entrance. This position was used as the zero point for all distances measuring in the tunnel. Position P1 was therefore given the distance -50 m and P38 was given the distance +100 m.

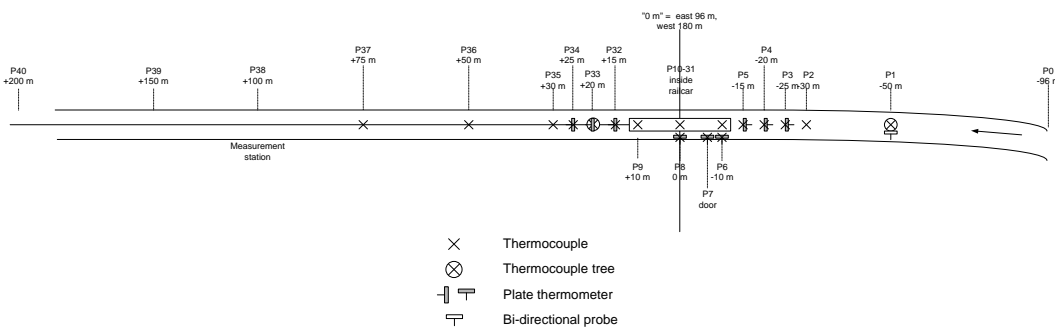


Figure 6.1 Instrumentation in the tunnel (for a larger drawing please see Appendix 3).

Figure 6.2 shows a drawing of the measurement station used in position P38. This measuring station was installed mainly to make it possible to calculate the heat release rate.

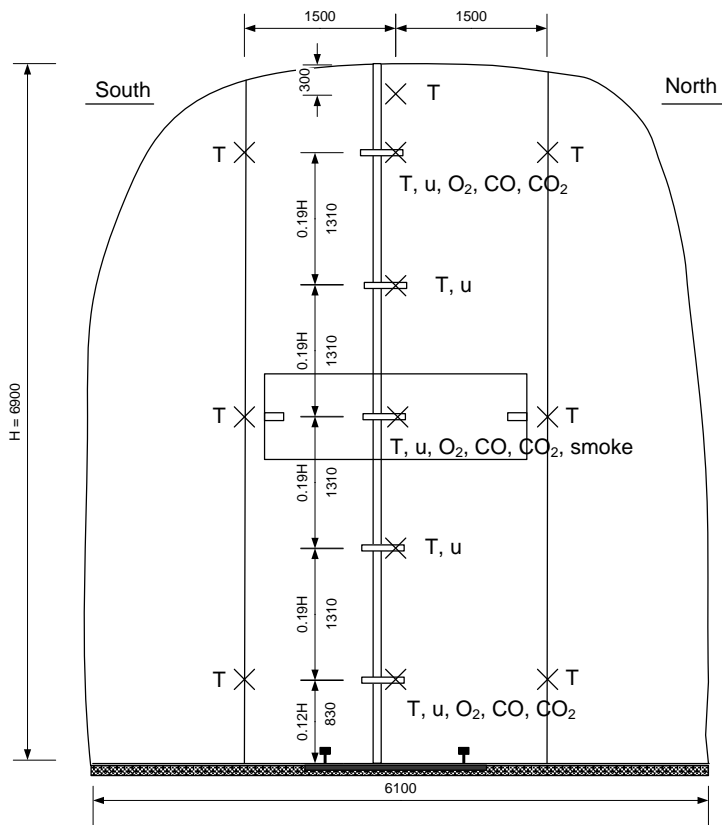


Figure 6.2 Instrumentation at the measurement station 100 m downstream of the fire, P38 (for a larger drawing please see Appendix 3).

The railway carriage contained position P10 – P31 shown in Figure 6.3. The distances to the thermocouples in the thermocouple trees were measured from the ceiling which means that the thermocouple 1.20 m from the ceiling was approximately 1.12 m from the floor. In the carriage gas temperature and smoke density were measured. Gas was sampled at three heights and analysed for O₂, Co and CO₂. Outside the carriage the radiation was measured with plate thermometers.

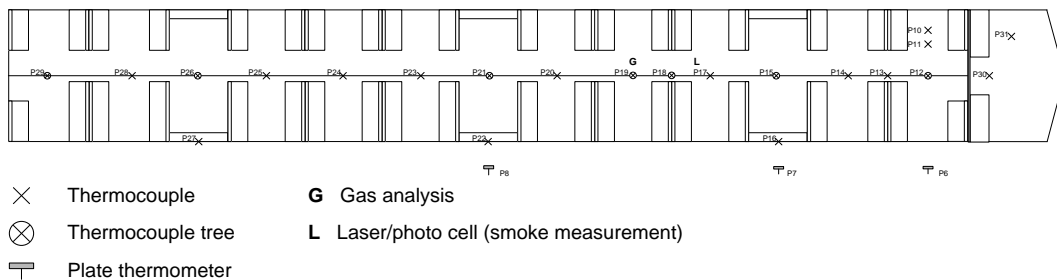


Figure 6.3 Instrumentation of the railway carriage (for a larger drawing see Appendix 3).

In total 139 sensors or sampling points were used, distributed as 67 in the carriage, 28 (temperature, velocity, optical density, CO, CO₂, O₂) at the measurement station (P38) and the remaining 44 at other positions in the tunnel. More details on the measurements can be found in the sections below.

6.1 Temperature measurements

The gas temperatures were measured at several positions along the tunnel (see Figure 6.3). Three different types of thermocouples were used in the tests to measure the

gas temperature. The majority of the gas temperatures were measured using unsheathed welded thermocouples, 0.5 mm type K. For reference measurements, e.g. to estimate the influence of radiation, extra unsheathed welded thermocouples, 0.25 mm type K were installed at positions P4, P7, P19, P33 and P38. At positions P6, P8 and P9 1 mm sheathed thermocouples were used 0.30 m from the tunnel ceiling, right above the commuter train carriage.

Where single thermocouples are indicated in the drawings they were positioned 0.3 m from the tunnel ceiling. For all measurements in the tunnel, the distances to the measurement positions were measured from the ground, except for the positions 0.3 m from the tunnel ceiling. This means that, since the ceiling height varies along the tunnel, the distance between the thermocouples in the thermocouple tree and the ceiling also varied somewhat depending on the position in the tunnel. One example, the thermocouple tree downstream of the carriage (P33), had the thermocouples positioned 0.83 m, 2.14 m, 3.45 m, 4.76 m and 6.07 m from the ground, in addition to the thermocouple 0.3 m from the ceiling. In this thermocouple tree channel 98 was 6.07 m from the ground and 0.88 m from the ceiling.

In the carriage both single thermocouples and thermocouple trees were used. The single thermocouples were placed 28.8 cm from the ceiling while the thermocouple trees had six thermocouples at the following distances from the ceiling: 5 cm, 28.8 cm, 74.4 cm, 120 cm, 165,6 cm, and 211,2 cm. In the tree at position P18 only three height were used for thermocouples: 28.8 cm, 120 cm and 211.2 cm from the ceiling, i.e. the same heights as for the smoke measurements.

In the three doors (on the left side) that were open at the start of the tests, a thermocouple was positioned along the centreline, 5 cm from the top of the door opening.

6.2 Heat flux

Heat fluxes were measured using plate thermometers (PTC), see P3 - P8, and P32 - P34 in Figure 6.1. PTC P3-P5 were placed in front of the train (1.6 m above the ground, along the centreline of the tracks, facing the carriage), at -25 m, -20 m and -15 m, respectively. PTC P6 – P8 were placed on the tunnel wall (see Figure 6.4) facing the side of the train carriage in such a way that PTC in P6 were facing the centre of the lower edge of the first passenger window on the left side, while PTC in P7 and P8 were facing the centre of the first and the second door on the left side of the carriage. PTC P32-P34 were placed behind the train carriage (1.6 m above the ground, along the centreline of the tracks, facing the carriage), at +15 m, +20 m and +25 m.

The Plate thermometer was developed to control the temperature in test furnaces when testing the resistance of construction specimens [19]. The Plate thermometer has a relatively large area (100 mm × 100 mm) and is therefore highly sensitive to radiation but relatively insensitive to convection.

The incident heat fluxes were calculated using the following equation [19, 20]:

$$[\dot{q}_{inc}'']^{j+1} = \sigma [T_{PT}^4]^j + \frac{(h_{PT} + K_{cond})([T_{PT}]^j - [T_{\infty}]^j) + C_{PT} \frac{[T_{PT}]^{j+1} - [T_{PT}]^j}{t^{j+1} - t^j}}{\varepsilon_{PT}} \quad (6.1)$$

where the conduction correction factor $K_{cond} = 0.00843 \text{ kW/m}^2/\text{K}$, the lumped heat capacity coefficient $C_{PT} = 4.202 \text{ kJ/m}^2/\text{K}$, and the surface emissivity of the plate thermometer $\varepsilon_{PT} = 0.8$.



Figure 6.4 Plate thermometer mounted on the wall to measure the radiation from the fire in the carriage.

The convective heat transfer coefficient (h_{PT}) is dependent on the airflow in the tunnel and how the PTC is placed in the airflow. Because of the complex geometry in the tunnel, the shifting forced airflow and the flow induced by the fire, it is very likely that h_{PT} has varied during the fire. Because of the complexity, h_{PT} is estimated to be $0.010 \text{ kW/m}^2/\text{K}$ (equals natural convection) for all PTC:s placed perpendicular to the airflow. For the PTC:s placed on the wall facing the carriage, P6-P8, forced convection is assumed and h_{PT} is calculated below, see equation (2-4) [21].

$$h_{PT} = \frac{Nu \times k}{x} \quad (6.2)$$

$$Nu = 0.66 \times Re^{1/2} \times Pr^{1/3} \quad (6.3)$$

$$Re = \frac{u \times x}{\nu} \quad (6.4)$$

where

k	=	Thermal conductivity of air [W/m/K]
x	=	Characteristic length of PTC [0.1 m]
Nu	=	Nussel number [-] (flow over flat plate)
Re	=	Reynolds number [-]
Pr	=	Prandtl number [-]
u	=	Air velocity [m/s]
ν	=	Kinematic viscosity of air [m^2/s]

The convective heat transfer coefficient was calculated on the basis of an air temperature of 900 K, the airflow was assumed to be 3 m/s, see Appendix 2, the characteristic length of the PTC is 0.1 m. The thermal conductivity of air at 900 K is 0.000062 kW/m/K , the Prandtl number is 0.72 and the kinematic viscosity is $1.029 \times 10^{-4} \text{ m}^2/\text{s}$. All of this results in a h_{PT} of approx. $0.020 \text{ kW/m}^2/\text{K}$

Equation 6.3 is restricted to Reynolds numbers larger than 20 and smaller than 3×10^5 . With a characteristic length of 0.1 m and an air velocity of 3 m/s the Reynolds number is approx. 3000 at 900 K.

6.3 Gas analysis

Gas was sampled for analysis, both inside the carriage and at the measurement station at +100 m (P38). Gas concentrations are of interest for studies of the evacuation conditions.

The gas analysis at the measurement station were used to calculate the heat release rate, but could also be used to calculate total production of different species.

Figure 6.5 shows one of the inlet pipes for gas analysis in the railway car. The gas samples were taken at three different heights, 28.8 cm, 120 cm and 211.2 cm from the ceiling. Figure 6.6 shows the placement of the gas analyse at the measuring station downstream the fire. Shown in Figure 6.6 is inlet pipe at 0.83 m and 3.45 m over the railway sleepers, the inlet pipe at 6.07 m is not visible at the picture.



Figure 6.5 Inlet pipe for the gas sampling inside the railway carriage.

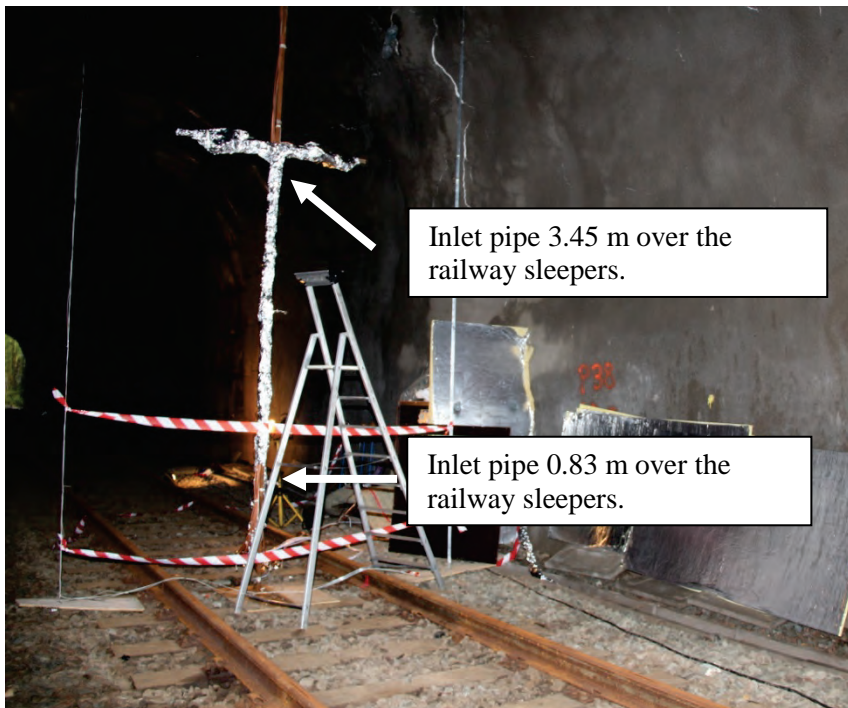


Figure 6.6 Gas sampling at the measuring station downstream the fire.

The following analysis instruments were used to measure the changes of O₂, CO and CO₂ concentrations in the air:

- Rosemount Analytical inv. No. 900863 (Ch131,Ch134,Ch137; P38; 3.45m), and No. 900865 (Ch130,Ch133,Ch136; P38; 6.07m), with a calibrated measuring range of 0-20.95 vol% O₂, 0-10 vol% CO₂ and 0-1 vol% CO. Inv. No. 900864 (Ch62,Ch65,Ch68;P19;211.2cm) and No. 900866 (Ch60,Ch63,Ch66; P19;28.8cm) with a calibrated measuring range of 0-20.95 vol% O₂, 0-30 vol% CO₂ and 0-10 vol% CO.
- M&C O₂ Analyser PMA10 inv. No. 201625 (Ch132;Pos38;0.83m), and No. 700173 (Ch61,Pos19;120cm) with a calibrated measuring interval of 0-30 vol%.
- Rosemount BINOS 100 CO and CO₂, inv. No. 701133 (Ch64,Ch67;Pos19;120cm) with a calibrated measuring interval of 0-10vol% for CO and 0-30vol% for CO₂.
- Rosemount 100 2M, inv. No. 700394(Ch135,Ch138;Pos38;0.83m) with a calibrated measuring interval of 0-1vol% for CO and 0-10vol% for CO₂.

The response time of the analysers inside the carriage was 30 s and the response time for the analysers at the measurement station was 23 s. This has not been corrected for in the graphs in this report.



Figure 6.7 One of the stations where the gas analysis instruments were placed.

6.4 Smoke

The smoke density was measured both in the carriage and at the measurement station (P38), using laser and receiver systems. The laser was a diode pumped laser module with an output wavelength of 635-680 nm and a output power of 5 mW. The receiver was a Hamamatsu GaAsP photodiode (G1737).

Figure 6.8 shows the arrangement of laser transmitters and receivers inside the train carriage. The distance between the transmitter and the receiver was 73.5 cm. In the railway carriage the thickness of the smoke was measured at three different heights: 28.8 cm, 120 cm and 211.2 cm from the ceiling. The position of the laser transmitter and receiver setup was 27.5 cm from position P17 (towards the rear end of the wagon).

Figure 6.9 shows the arrangement for the laser transmitter and receiver at the measuring station, position P38. The distance between the transmitter and receiver at this position was 40 cm. The smoke density was measured with the transmitter/receiver system at 3.45 m over the railway sleepers.

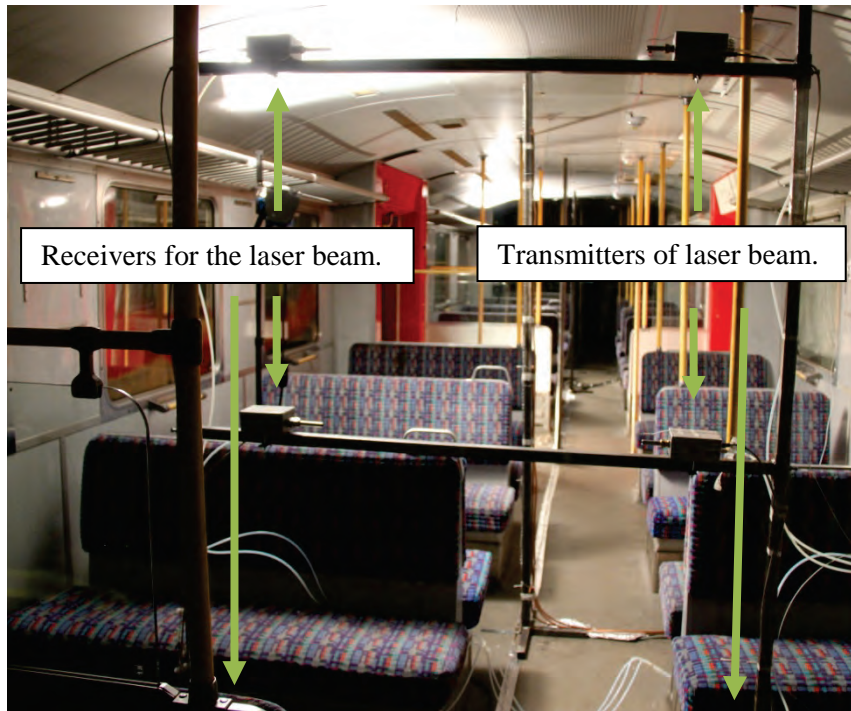


Figure 6.8 Measuring device (laser /photo cell system) to measure the thickness of the smoke inside the railway carriage.



Figure 6.9 Position of the laser equipment in the measurement station.

6.5 Air velocity in tunnel

The air velocity was measured using bi-directional probes [18] with a diameter of 16 mm. At 50 m upstream of the carriage (P1) the velocity was measured 3.45 m from the ground and at the measurements station the velocity was measured at five different heights: 0.83 m, 2.14 m, 3.45 m, 4.76 m, and 6.07 m above the ground

The pressure at P1 was measured with a Furness Controls Differential Pressure Transmitter model 332 (Inv 900875). The measuring range was ± 30 Pa for this equipment. At the measurement station the pressure was measured with five different channels (Ch 1 to 5) in a 20 channel Autotron 700D differential pressure transmitter (Inv 700313). the measuring range was ± 32 Pa.

The changes in differential pressure is converted, with equation (5.12) [18], to a velocity of the air in m/s by measuring the gas temperature at the same place.

6.6 Signal collection with data loggers

The signals from the measurements were collected by data loggers of the type Solatron E-IMP 5000 1KE (inv. No. 701054, 701051, 701050, 701052, 701242, 701243) and FLUKE 2645A NetDAQ – Networked Data Acquisition Units (inv. No. 700369). These data loggers were connected to D-Link DGS-1008D network hubs that sent all the data to computers via network cables.

6.7 Instrumentation in the railway carriage - test 1

Not included in the drawing shown in Figure 6.3 are four thermocouples shown in Figure 6.10 - Figure 6.13 for fire test 1. These measurements were connected to Ch89 – Ch92. These extra temperature measurement were positioned: 1) in a drilled hole in the carriage floor (Ch89; Figure 6.10), 2) at the lower edge of the door near the fire (Ch90; Figure 6.11), 3) at the steel frame above the Automatic Train Control (ATC) unit (Ch91; Figure 6.12), and 4) at the top of the ATC unit (Ch92 Figure 6.13).



Figure 6.10 Position of the thermocouple that was placed inside the floor (Ch 89).



Figure 6.11 Position of the thermocouple at the door step (Ch 90).



Figure 6.12 Position of the thermocouple placed right above the heptane pan and near the floor (Ch 91).



Figure 6.13 Position of the thermocouple right above the heptane pan (Ch 92).

7 Test procedure

The purpose of test 1 was to evaluate the risk for fire spread underneath the train carriage in case of a fire in for example electrical devices. A pool of heptane was placed approximately 15 cm under the ATC receiver, near the front of the carriage (the first double door). The pool of heptane was lit and temperatures were measured with in particular four thermocouples. These thermocouples were placed above the pool fire, on the door step of the train carriage and in a hole in the floor inside the train carriage, see also Figure 6.10 to Figure 6.13. To study the temperature development inside the carriage floor, also IR-camera was used.

The purpose of test 2 and 3 was to investigate a fully developed train carriage fire inside a tunnel to create basis for design fires. The same ignition scenario was used in both test 2 and 3, but two different train carriages were used. The most significant difference between the carriages were the combustible linings used in test 2 and non-combustible linings used in test 3, also see section 3.1.1 and 3.1.2.

The ignition scenario, in test 2 and 3, was supposed to simulate an arsonist igniting one of the seats in the corner. The ignition was achieved letting small ignition sources ignite petrol. An empty milk container (paper with an inner plastic lining) was filled with 1 L of petrol. The milk container was placed on a plywood board (36 cm × 36 cm × 1.2 cm), see Figure 7.1.

Three small ignition sources (fibre board with added paraffin) were used. One was placed on the seat just outside the plywood board and two on the floor (see Figure 7.1). One of the ignition sources on the floor was placed in position P11 and one between P10 and P11, in test 2 18.5 cm from P11 and in test 3 somewhat closer to P10. The small ignition sources were 23 mm × 30 mm × 15 mm in size. When pulling a string, the milk container tumbled over and the petrol flowed out on the seat and floor and was ignited by the burning fibre board ignition source.

Table 7.1 Test series.

Test no.	Ignitions source	Place of ignition	Train id.
1	Heptane pool	Underneath the carriage	X1, see section 3.1.1
2	Petrol	Inside carriage	X1, see section 3.1.1
3	Petrol	Inside train	Refurbished X1, see section 3.1.2



Figure 7.1 Positions of the fibre board pieces used to ignite the petrol.

The heptane pool fire in test 1 did locally ignite train dirt/paint at the surface (the protection plates are engulfed in the flames in Figure 7.2) of the ATC unit located above the fire, but the fire did not spread further and self-extinguished approximately 13.5 minutes after the pool fire burnt out.



Figure 7.2 The flames a few minutes into test 1.

In test 2 and test 3, the ignited petrol in one corner of the carriage spread on the floor and to nearby luggage and other material. The initial development was similar in the two tests, but very soon the development differed significantly. In test 2 the fire continued to develop very fast and soon the entire carriage was involved in the fire. In test 3, on the other hand, the initial development stopped and the fire spread slowed down. The fire did, however, not extinguish completely, but continued on a low and relatively constant level. More detailed information and a discussion of the differences between test 2 and test 3 are presented in chapter 8.

Since one of the aims of the fire tests was to study the effects (condition in the tunnel, radiation, etc.) of a fully developed fire it was in test 3 decided to assist the fire development by igniting some additional pieces of luggage. Two litres of Diesel fuel was added to each of five pieces of luggage in the vicinity of door 1, i.e. 10 L in total. However, when the first of these pieces of luggage (very close to door 1) was ignited approximately 110 min after the original ignition, the fire fighter igniting the luggage saw flames near the ceiling of the carriage and had to exit the carriage without igniting the other prepared pieces of luggage. The fire had spontaneously spread to the driver's cabin. The fire then spread back again to the passenger compartment shortly after the decision was made to intervene in the fire progress (but before this intervention was completed).

In all the tests the logging systems were started some minutes prior to ignition to check the instruments and to get background measurements. However, in the graphs, both in chapter 8 and in Appendix 2, the time has been shifted so that time zero corresponds to ignition.

8 Results and discussion

8.1 Air velocity

To estimate the air velocity in the tunnel, the differential pressure and gas temperature were measured at -50 m (test 1, 2 and 3) and +100 m (test 2 and 3) in the tunnel. The differential pressure was measured using bi-directional probes, $\phi = 16$ mm, and a pressure transmitter with a measuring range of ± 30 Pa. The air velocity was calculated with equation 5.12, see section 5.6.

The air velocity in test 1 (around 4 m/s) was higher than the velocity in test 2 and 3 (2-3 m/s), see Figure 8.1 and Figure 8.2.

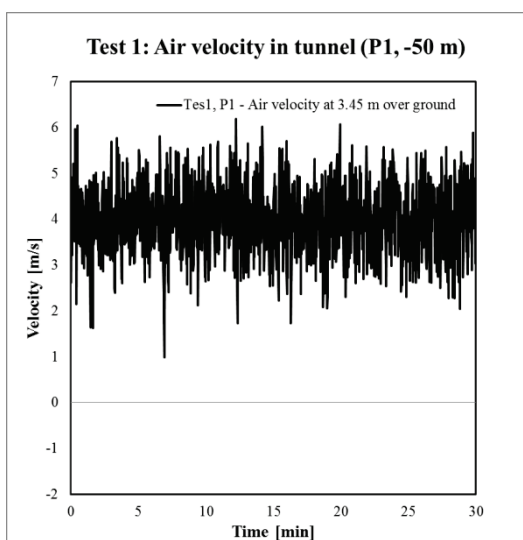


Figure 8.1 Air velocities in the tunnel during test 1, at -50 m.

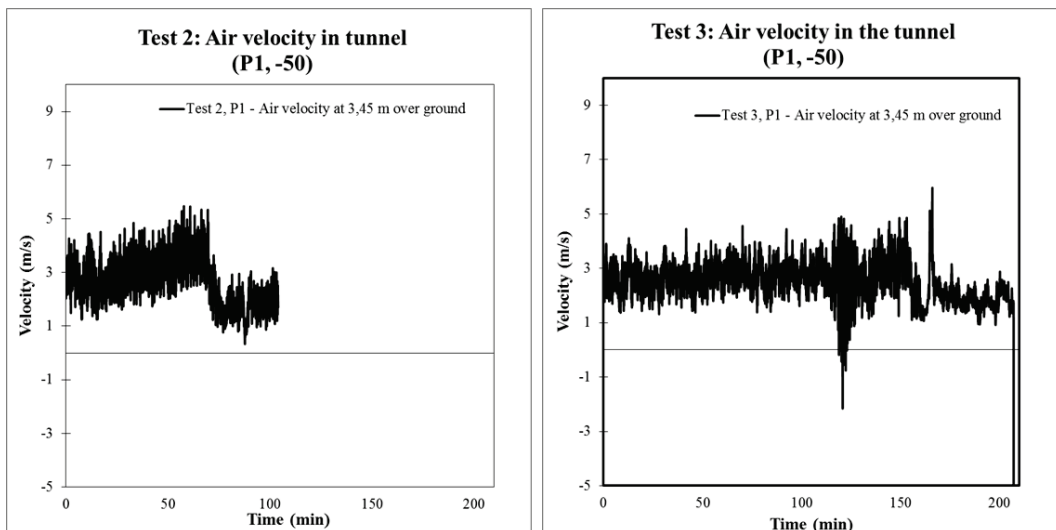


Figure 8.2 Air velocities at -50 m in the tunnel, test 2 (left) and test 3 (right). Negative velocities are flows in the opposite directions. Positive velocities are air/gas flows into the tunnel (from east to west) towards the train carriage.

Air velocities in the tunnel, upstream of the carriage, are in the magnitude of 2-5 m/s. The air velocity in test 1 (on average around 4 m/s) was higher than the velocity in test 2 and 3 (2-3 m/s), see Figure 8.1 and Figure 8.2. The negative velocities seen in Figure 8.2 (right)

are flows in the opposite direction, out of the tunnel. These flows occur about the same time as back-layering, see test 3 in Appendix 1. The back-layering is shown in Figure 8.3.



Figure 8.3 Developed backlayering in test 2 (left) and large flames and progressing backlayering in test 3 (right). (Photo: Per Rohlén)

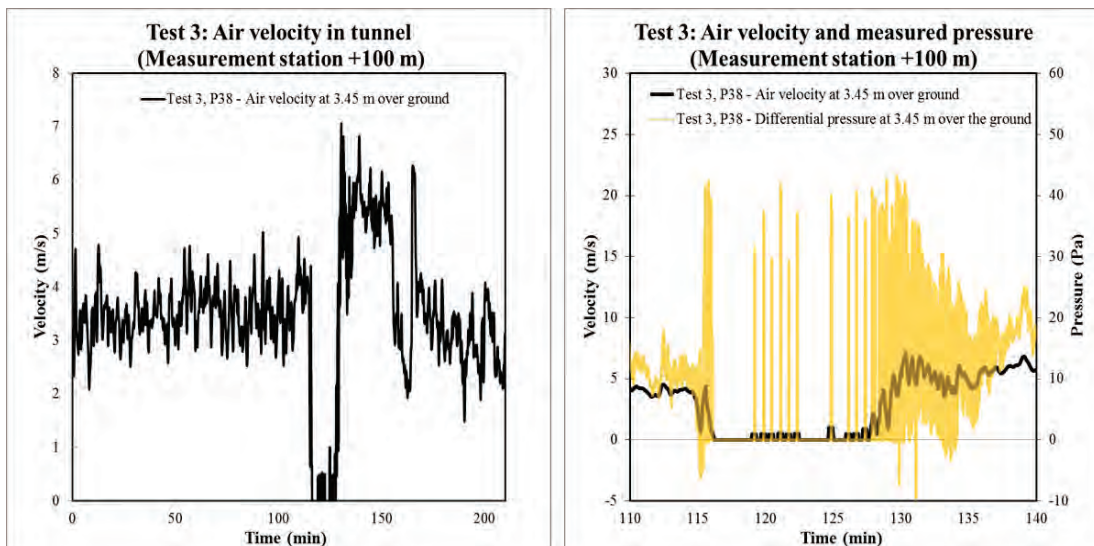


Figure 8.4 Calculated air velocity (left) and air velocity and measured differential pressure (right) at the measure station (+100 m). Positive pressure and velocities are air/gas flows from the train wagon and out of the tunnel.

The air velocity at +100 m in test 3 varied between 3–6 m/s (see Figure 8.4), where the highest velocities were measured after 110 min when the fire intensity increased.

The void data between 115–130 min is likely due to an insufficient measuring range of the pressure transmitter. It is very likely that the pressure during this time period was higher than +30 Pa because of the intense fire and the strong pulsations, see the right hand diagram in Figure 8.4 for the pressure measurement and Appendix 1 for a description of the course of the fire in test 3. Measured values over 30 Pa, plotted in Figure 8.4, should be regarded as highly uncertain.

8.2 Estimation of flow rate

During the tests, one bi-directional probe was placed at the centreline of the cross-section at -50 m and 5 pressure probes were positioned at different heights at +100 m. However, during test 2, the measured data at the downstream measurement station were lost due to electrical failures 9.4 min after ignition, i.e. before the fully developed stage.

Furthermore, in both tests strong pulsations were observed (see section 8.9) and this affected the velocity data measured at the downstream measurement station. As a consequence, the tested data measured upstream of the fire are more reliable. All the velocities discussed here refer to the average velocity of fresh air in the tunnel, u_0 .

8.2.1 Test 3

The fluctuation of the average upstream velocity is shown in Figure 8.5. The averaged values within 30 s were also plotted. Strong fluctuations in the velocity measurements could be observed due to the pulsations in the tunnel.

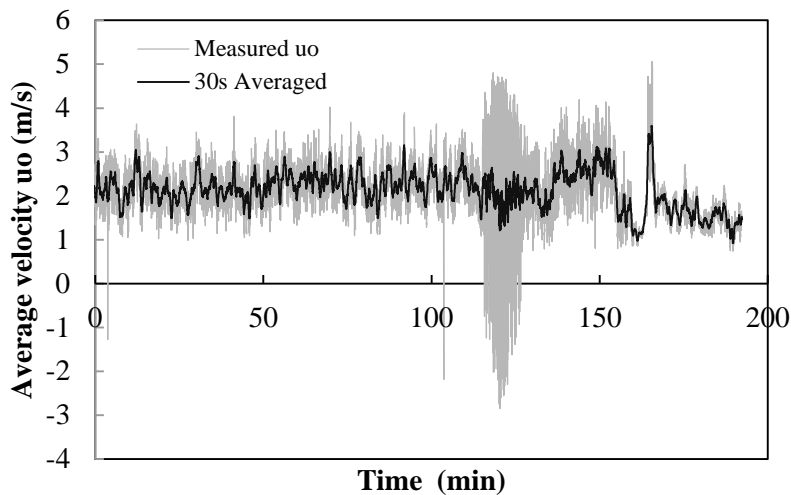


Figure 8.5. Average velocities measured upstream (-50m) in test 3.

The velocities measured upstream and downstream are compared in Figure 8.6. They are correlated with each other quite well.

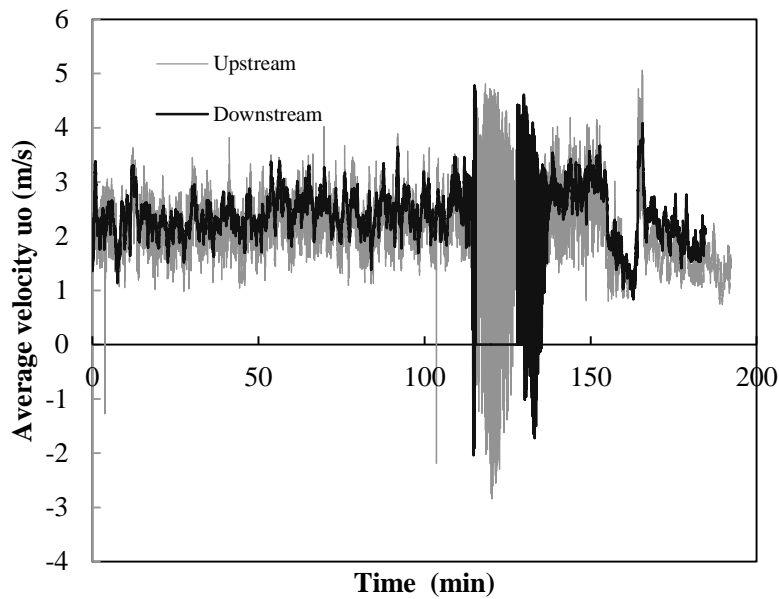


Figure 8.6. Comparison of average velocities measured upstream and downstream in test 3.

Local comparison of the measured values upstream and downstream between 150 min and 170 min was made, as shown in Figure 8.7. The comparison shows that they correlate quite well with each other. This verifies the correctness of the velocity measurement and that the data can be used in the analysis. Therefore, the velocity data measured upstream of the fire were used when the downstream data were not available.

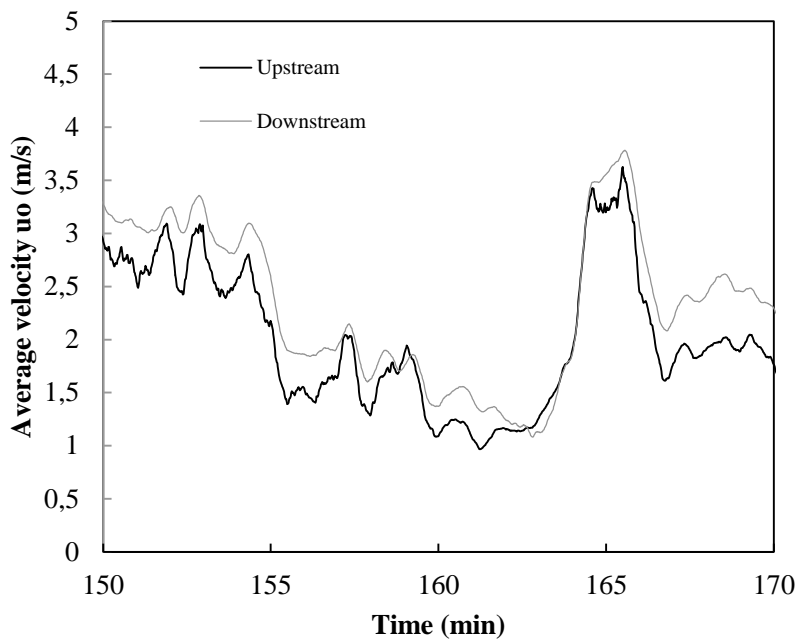


Figure 8.7. Average velocity in test 3 (30s averaged values, real time).

During the fully developed fire stages, the measured velocities varied significantly due to pulsation (see Section 8.9), 30 s average values of velocities were used in the analysis to reduce the effect of pulsation. There is no significant difference obtained when using 30 s or 60 s average values.

8.2.2 Test 2

Figure 8.8 shows the comparison of average velocities measured upstream in test 2 and test 3. The fire growth was delayed about 107 min in test 3, to make a comparison to test 2 relevant. The value of 107 min is roughly determined based on the comparison of the fire curves.

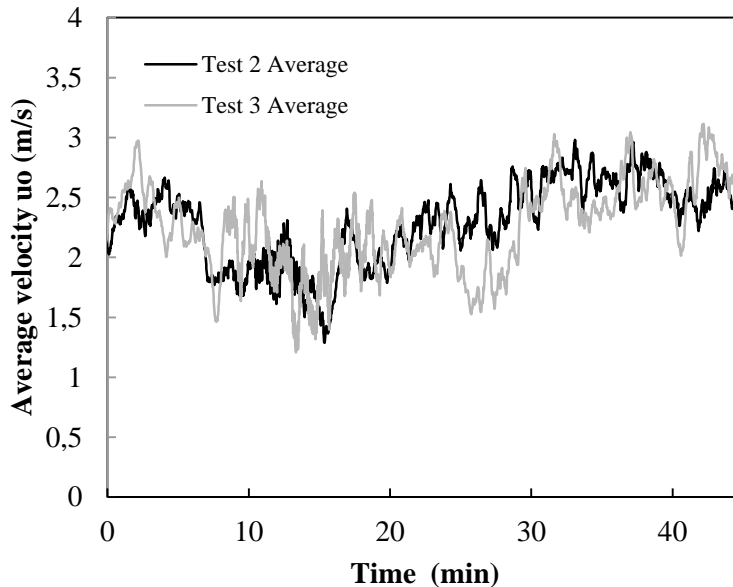


Figure 8.8. Comparison of average upstream velocities in test 2 and test 3 (30 s averaged values, modified time in test 3).

It is shown in Figure 8.8 that the average velocities follow a similar trend during the fire stage. The minimum velocity is approximately 1.3 m/s in both tests. It is known that the velocity decreases mainly due to the thermal expansion in a horizontal tunnel. This is proof of the similarity of the heat release rates in both tests.

8.3 Estimation of the HRR

Based on the method proposed in the chapter 5, the heat release rates in test 2 and test 3 were estimated.

8.3.1 Test 3

Figure 8.9 shows the heat release rate in test 3 using different methods. Note that the time index ranges from 100 min to 150 min after ignition. Oxygen consumption calorimetry is the most commonly used method to estimate the heat release rate (HRR). Therefore, it is considered as the reference in the comparison of different curves. Despite this, the fire curves based on other methods can be used to estimate the robustness of the oxygen method and further be used in the estimation of HRR in test 2 when the data of oxygen measurement at the measurement station are not available. In the following presentation, when a certain method is said to under- or overestimate HRR for a certain time period, this is in relation to the oxygen calorimetry method.

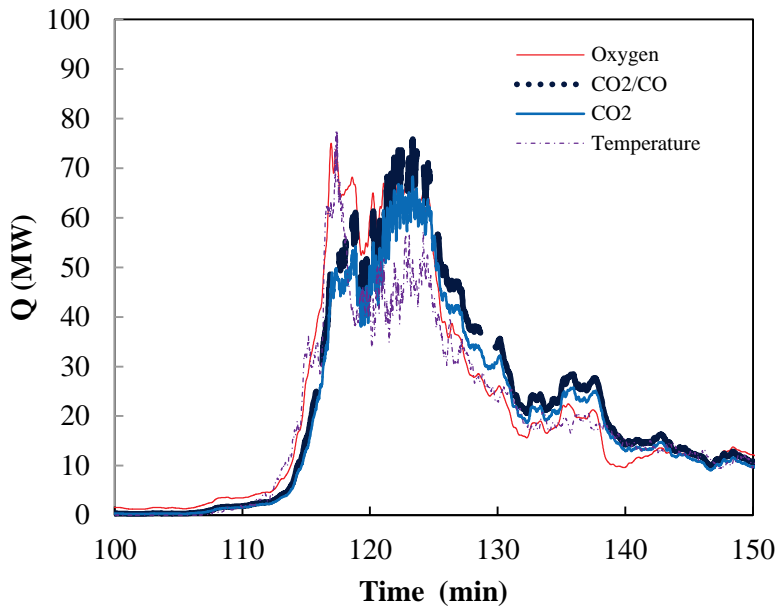


Figure 8.9. Heat release rate estimated based on different methods in test 3 (real time).

It is shown clearly that all the curves correlate with each other quite well. The maximum temperature method estimates the HRR quite well except for the second peak region. The reason will be discussed later. The CO_2/CO technique and CO_2 production method predict little lower HRR at the first peak. The maximum temperature method predicts this region quite well, but underestimates the HRR in the following fully developed region. The CO_2/CO technique and CO_2 production method overestimate the HRR somewhat in the decay period. The error is within 30 % in the analysis.

Theoretically, the heat release rate can be well estimated using the maximum ceiling gas temperature data. However, it might be so that the real maximum ceiling gas temperatures were not registered during part of the test due to the position of the flame in relation to the thermocouples. Thus the heat release rate is underestimated by the temperature method during a period after the peak time. In any case, the estimated HRR based on ceiling gas temperature measurement correlates well with the HRR curves estimated using oxygen consumption calorimetry, especially in the growth period and the decay period. It can also be concluded that the HRR curves should not be below the estimated HRR curve based on the maximum gas temperature near the ceiling.

Figure 8.10 shows the HRR in test 3. The curve obtained based on the oxygen consumption calorimetry is shown here since this is the most reliable method. The maximum heat release rate is about 77 MW in test 3. The fire starts to grow rapidly after approximately 112 min.

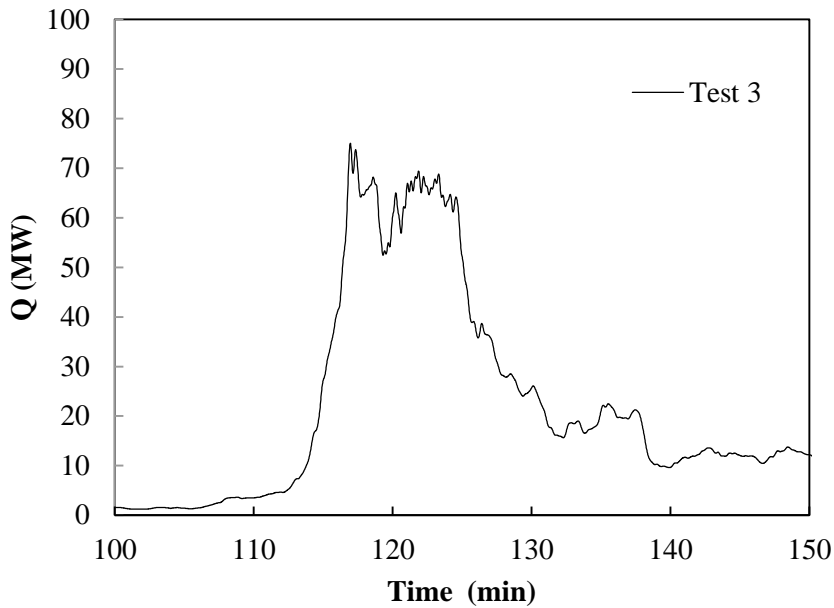


Figure 8.10. Estimated heat release rate based on oxygen calorimetry in test 3 (real time).

8.3.2 Test 2

During the test 2, no measurement data was obtained from the measurement station (+100 m) after 9.4 min because of cable failure due to the intense fire. The measured fresh air velocity in test 2 are comparable to the data in test 3, see Figure 8.8. Furthermore, the measured maximum ceiling gas temperature data in test 2 are compared to the data in test 3, see Figure 8.11. The heat release rates estimated based on the measured maximum ceiling gas temperature data in test 2 and in test 3 are compared in Figure 8.12.

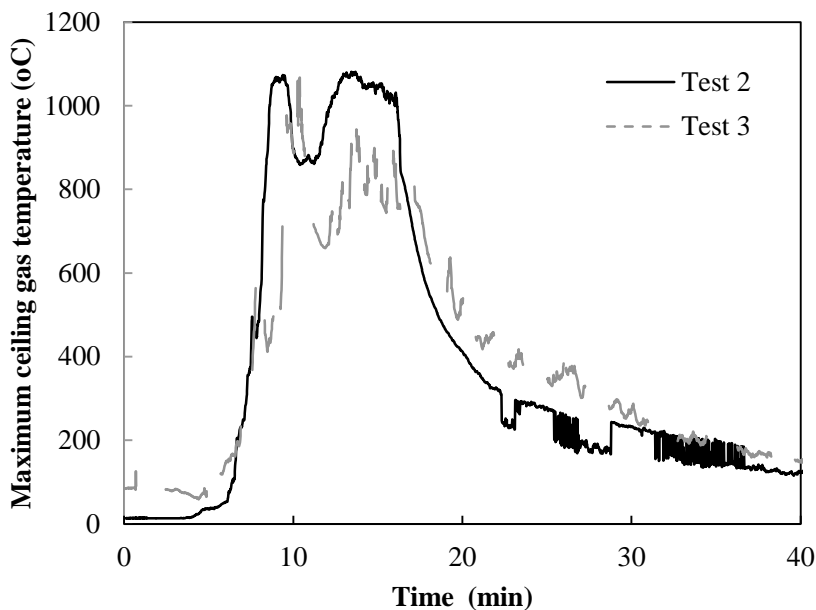


Figure 8.11. Comparison of measured maximum ceiling gas temperature in test 2 and test 3 (Modified time in test 3).

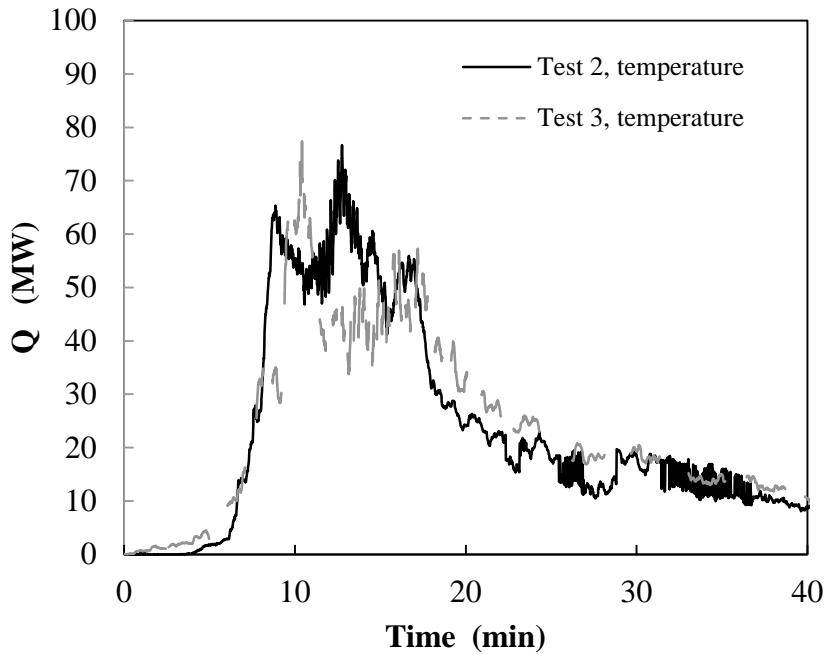


Figure 8.12. Comparison of estimated HRR based on maximum ceiling gas temperature in test 2 and test 3 (Modified time in test 3).

Figure 8.13 compares the heat release rate calculated from oxygen calorimetry in test 3 and the heat release rates estimated based on the measured maximum ceiling gas temperature data in test 2 and test 3. All the time indexes in test 3 are subtracted by 107 min for comparison with test 2.

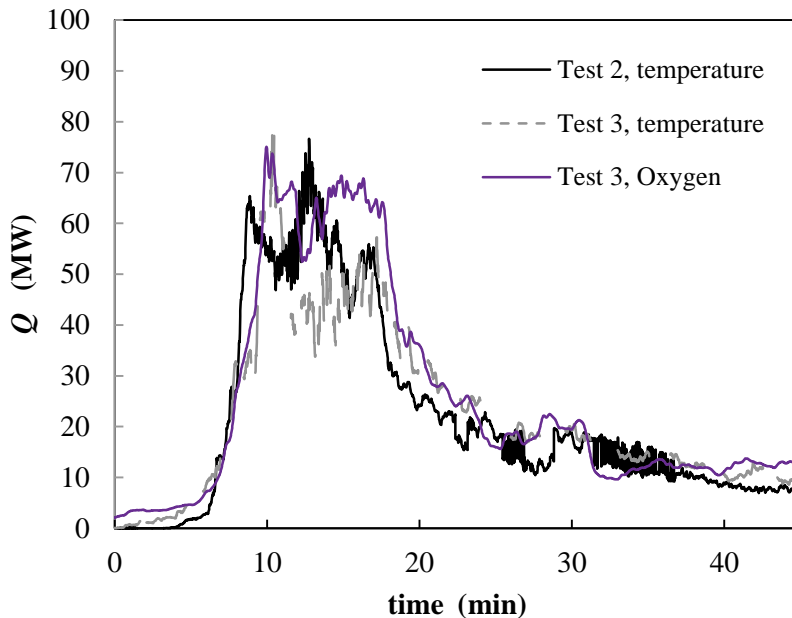


Figure 8.13. Comparison of estimated HRR (based either on gas temperature or consumption of oxygen) in test 2 and test 3 (modified time in test 3).

Both Figure 8.12 and Figure 8.13 show high similarity between the HRR curves in test 2 and test 3. Although the time to maximum HRR was delayed in test 3, the main fire curve was approximately the same as that in test 2. This phenomenon was also observed in

model scale tests. There are mainly two reasons for this. Firstly, the energy released before the rapid growth stage was quite small, about 10 % of the total energy released in test 3. Secondly, the fully developed metro carriage fires are quite similar since at this stage the fire in the carriage is ventilation controlled.

Note that the ventilation flow changed in the tests due to the thermal expansion of the fire. Thus the changes in velocities show the trend of the changes in HRR. As shown in Figure 8.8, the velocities in both tests in the fully developed stages approximately follow the same trend. This is also a proof showing the similarity between test 2 and test 3.

In a summary, the HRR curve in test 2 and in test 3 can be considered as essentially the same. Thus, the fire curves based on the maximum ceiling gas temperature as shown in Figure 8.12 can be used as a reference (lower limit). However, it should be pointed out that there is large difference in the time index, i.e. the rapid fire growth time in test 3 is delayed approximately 107 min, compared to test 2.

The estimated HRR curve in test 2 alone can be found in Figure 8.14. The fire grows rapidly after approximately 5 min.

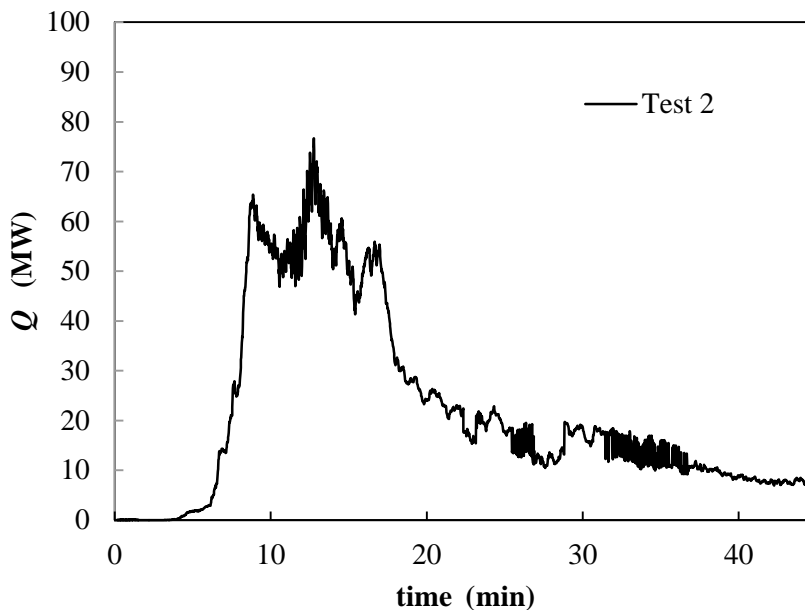


Figure 8.14. Estimated HRR in test 2 (real time).

The real-time comparison of the estimated heat release rate is shown in Figure 8.15. It can be seen clearly that the heat release rate curve in test 3 is delayed. This suggests that the surface covering plays an important role in the fire development.

The maximum HRR in test 2 was calculated to be 76.7 MW (12.7 min after ignition), while the corresponding value for test 3 was 77.4 MW (117.9 min after ignition), i.e. in both tests the maximum HRR was calculated to be approximately 77 MW, when calculated with the maximum temperature method. The corresponding value for maximum HRR in test 3 calculated with the oxygen consumption calorimetry method was approximately 75 MW. The value of 77 MW is used in the further discussion in the report since the HRR calculations based on the temperature measurements are available for both test 2 and test 3. The results of the HRR curves clearly show significant similarity between test 2 and test 3, although there is significant delay of HRR in test 3 due to incombustible wall surface linings.

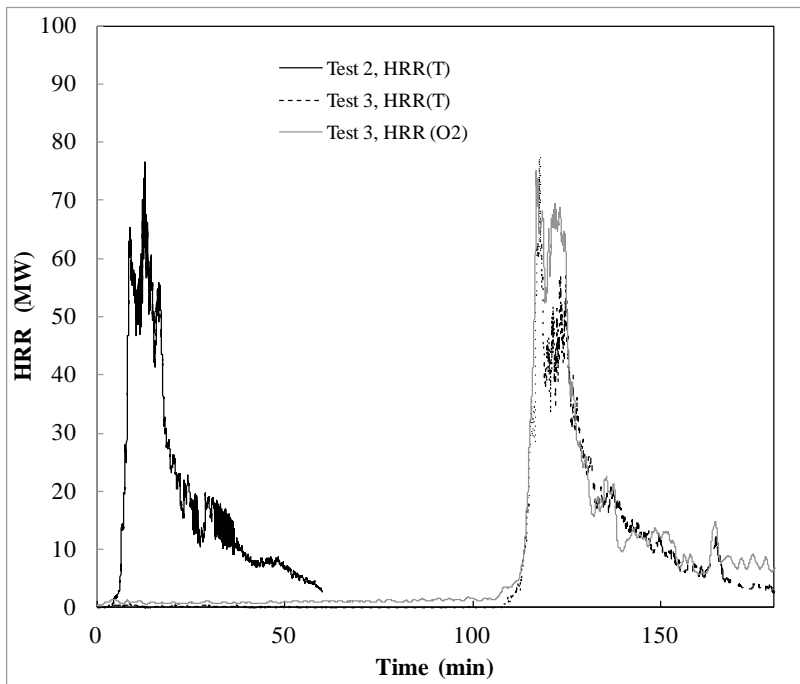


Figure 8.15. Estimated HRR in test 2 and test 3 (real time).

Different methods of estimating HRR were compared and good agreement obtained. The temperature method is quite robust, but is dependent on the correct measurement of the maximum gas temperature near the ceiling. CO₂/CO technology and CO₂ production method underestimate the HRR at the first peak and slightly overestimate the HRR in the decay period (in comparison to the O₂ consumption calorimetry), but predict the HRR quite well in the other periods.

8.4 Flashover of the carriage

To estimate the time for flashover of the carriage, the time when the gas temperature reached 600 °C in various positions and at different heights was evaluated. From this study the conclusion was drawn that the carriage was flashed over after 12 min in test 2 and after 119 min in test 3.

Based on the theory in Section 5.5 and the actual geometry of the carriage tested, the possible maximum heat release rate inside the carriage is estimated to be approximately 60.5 MW. Note that the total maximum heat release rate is 77 MW. Therefore, the fraction, ξ , corresponding to the fraction burning outside the carriage is approximately 20%. Compared to Ingason's model scale tests [17], the fraction is reasonable. In practice, this fraction is not necessarily the real fraction but approaches it depending on the local ventilation conditions and the flammability limit inside the compartment.

8.5 Gas temperatures

Temperatures in the tunnel and in the train carriage remained in general ambient or slightly higher during test 1. The only place where elevated temperatures were measured were close to the ignition source, the heptane pool fire, see Figure 8.16. An increase of the temperature in the floor, even after the extinguishment of the heptane pool, can also be noted. For temperatures in the rest of the tunnel and the train carriage see Appendix 2.

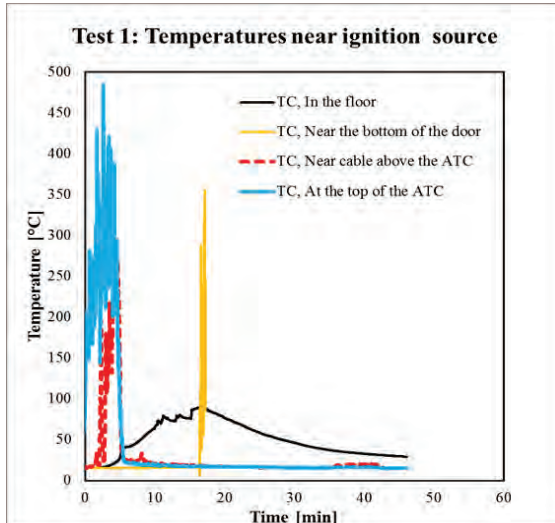


Figure 8.16 Temperatures close to the ignition source in test 1.

In comparison to test 1, there were significantly higher temperatures in test 2 and 3. Overall, the magnitude of the temperatures were rather similar in test 2 and 3, both in the train carriage itself and in the tunnel. However, some differences have been identified.

The ignition procedure was the same in test 2 and 3, a milk container of petrol was spilled over burning fire lighters (fibre board with added paraffin), see Chapter 7. As the petrol is spilled over the burnings fire lighter the temperature rapidly increases in this section of the train. In the Figure 8.17 the temperature above the ignition source is plotted for both test 2 and 3.

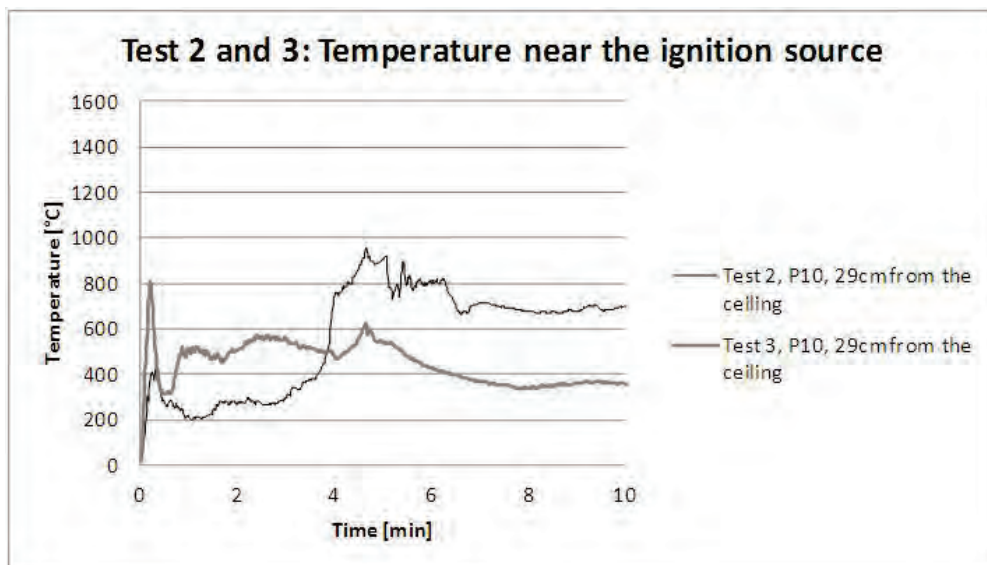


Figure 8.17 Ceiling temperature above the ignition source in test 2 and 3.

Interesting to see is that the temperatures differ between the tests. This might indicate that even though the ignition procedure was the same the actual course of the fire differed between the test. The petrol was spilled by pulling a string, this might have been done, unintentionally, with different strength in each test. The thermocouple at P10 might thereby been exposed to the hot gases in a different matter. Another possibility is that even though the luggage was similar and with the same mass, small differences in the material could have affected the initial fire spread. Whatever caused this difference between the tests it was of minor importance for the fully developed fire since it did not influence whether a flashover occurred or not and the temperature near the ignition source was higher in the test where the flashover was delayed, test 3.

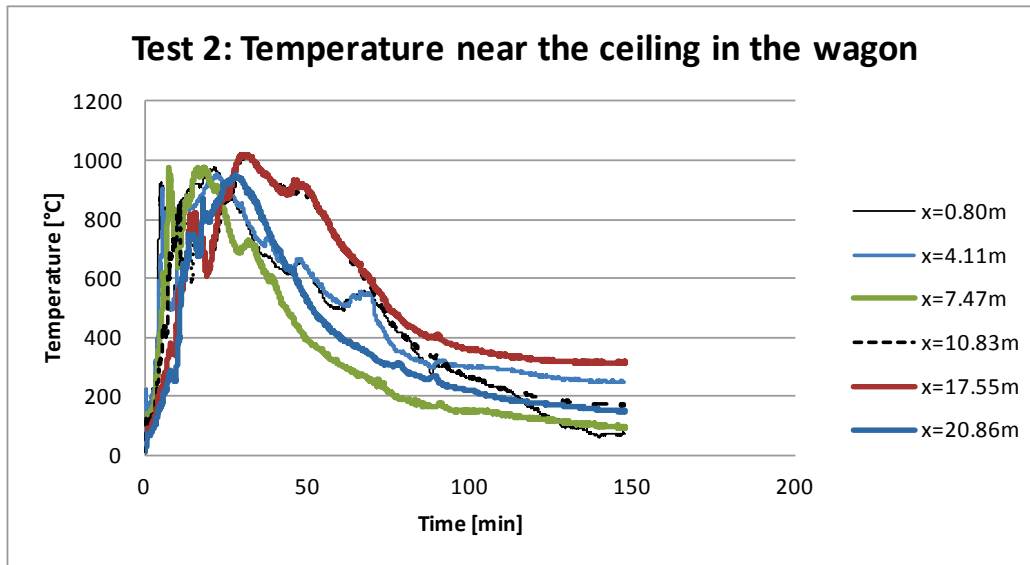


Figure 8.18 Gas temperature 29 cm from the ceiling in the carriage in test 2. The distance x is measured from the wall towards the driver's cabin.

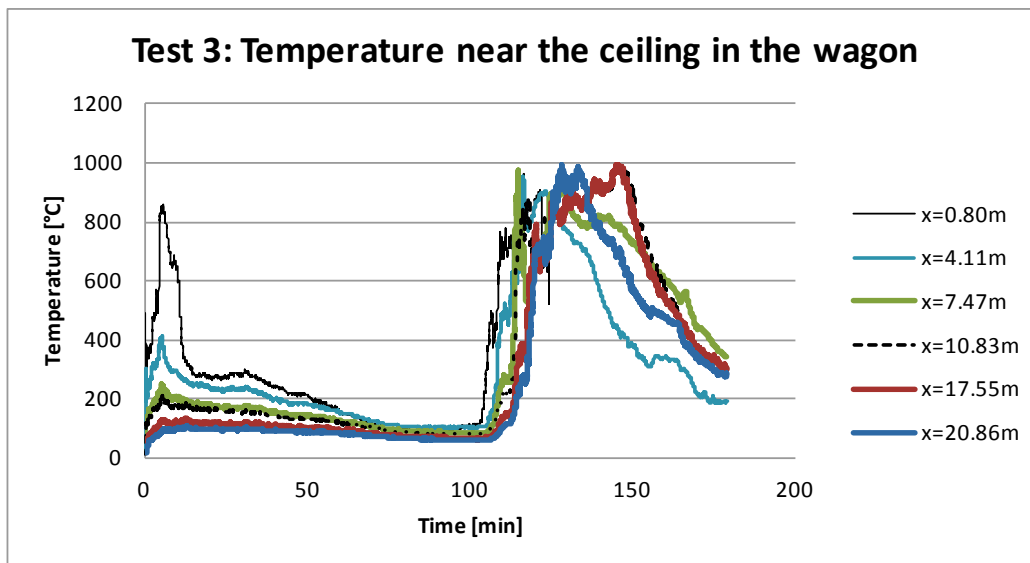


Figure 8.19 Gas temperature 29 cm from the ceiling in the carriage in test 3. The distance x is measured from the wall towards the driver's cabin.

The gas temperature inside the carriage reached approximately 1000 °C in both test 2 and test 3 (see Figure 8.18 and Figure 8.19) and although the large difference in fire development, as discussed above, the temperature development for the parts when the entire carriage becomes involved in the fire are similar to each other. In Figure 8.19 the period of initial fire spread in the beginning of test 3 is well illustrated showing a long period of low and relatively constant temperatures before the start of the fast fire spread.

The fast temperature increase (0.8 m from the driver's cabin; 0.29 m from the ceiling) started in test 3 approximately 103 min after ignition. At the time 108.4 min, the temperature in this position increased above 600 °C. At the time 103.8 min after ignition, the temperature was still higher in the driver's compartment than in the passenger compartment, but the flashover of the driver's compartment did not occur until the time

105 min, i.e. after the temperature has started to increase in the passenger compartment, but before the passenger compartment was fully involved in the fire. At the time 110 min after ignition, the temperature near the ceiling inside door 1 was approximately 500 °C.

As mentioned earlier the maximum temperature in the train carriage was rather similar in both test 2 and 3, as can be seen in Figure 8.20 below. The most significant difference is the time until maximum temperatures are registered. In Figure 8.20 it can also be seen that the time period of elevated temperatures is somewhat shorter in test 3. Both the time until maximum temperatures are registered and the shorter time period of elevated temperatures could be related to the fact that test 3 was performed with non-combustible lining.

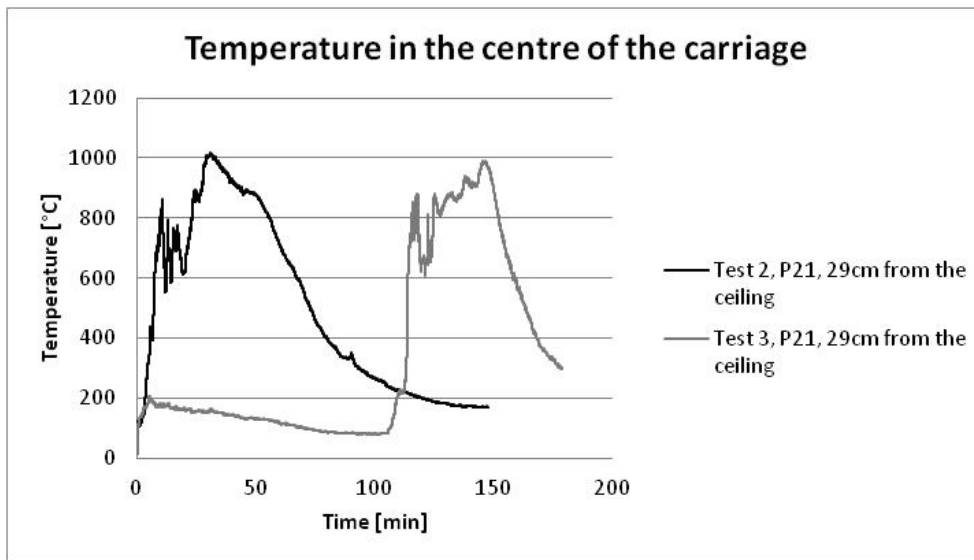


Figure 8.20 Temperature 29 cm from the ceiling in the train carriage. Measurement position P21 is in the middle of the carriage, see Figure 6.3.

To describe the temperature increase within the train carriage, the temperature will be plotted for each measurement point position. Figure 8.21 describes the temperature near the carriage ceiling at different times after ignition.

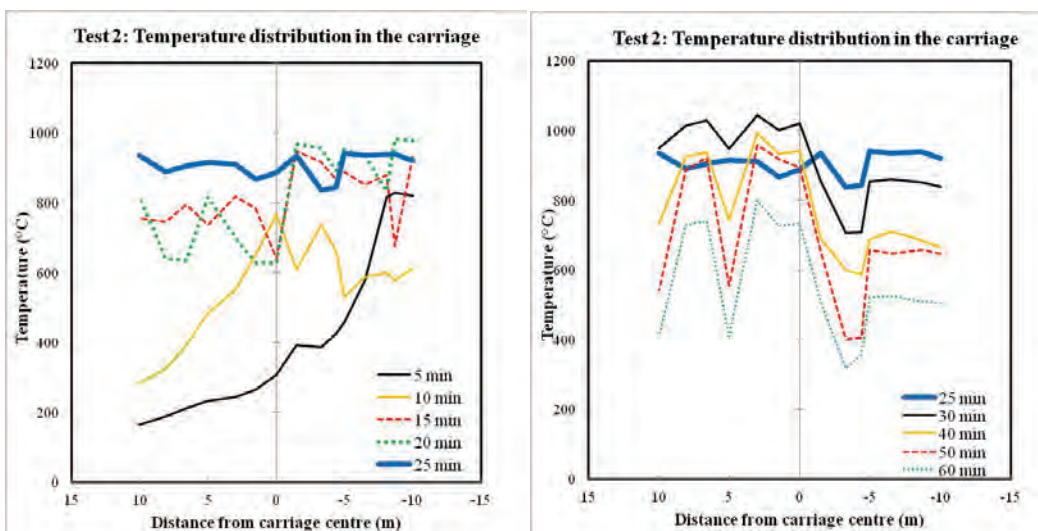


Figure 8.21. Centreline temperatures at approx. 29 cm from the ceiling. Measurement point P12 equals -10 m and measurement point P29 equals +10 m from the centre of the carriage. The plot is based on measurement points P12 – P15, P17 – P21, P23 – P26 and P28-P29 (see Figure 6.3).

The temperatures plotted in Figure 8.21 and 8.22 are average temperatures over 1 min. This means that the “5 min” line is average temperatures between 4 min 30 s and 5 min 30 s. In Figure 8.22 the temperature just above the carriage floor is plotted in the same way as in Figure 8.21, but less measurement points were used since the temperature near the floor was not measured in all positions.

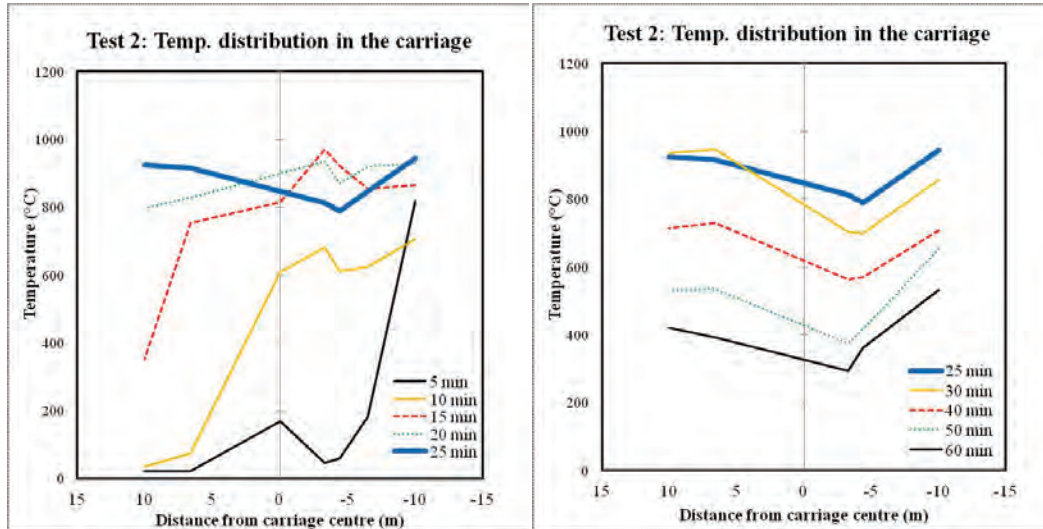


Figure 8.22 Centreline temperatures at approx. 211 cm from the ceiling. The plot is based on measurement points P12, P15, P18, P19, P21, P26 and P29.

From Figure 8.21 and Figure 8.22 it is possible to see a very strong temperature increase near the front of the carriage between 5 to 10 min after ignition. It is very likely that the fire grows from just involving the seats closest to the ignitions source to involving the entire front of the train (from the middle up to the drivers compartment). Fifteen to twenty minutes after ignition it appears as the entire train is involved in the fire and the temperature in the front of the train is at its highest during the test. In the rear section of the carriage, the temperature peaks approx. 30 min after ignition.

Figure 8.21 show that the temperature varies in the carriage from 30 min after ignition and forward. The temperature is lower at +5 m (P25) and -5 m (P17) than in the rest of the carriage. The most probable reason for this is that the most intense fire inside the carriage is near the doors.

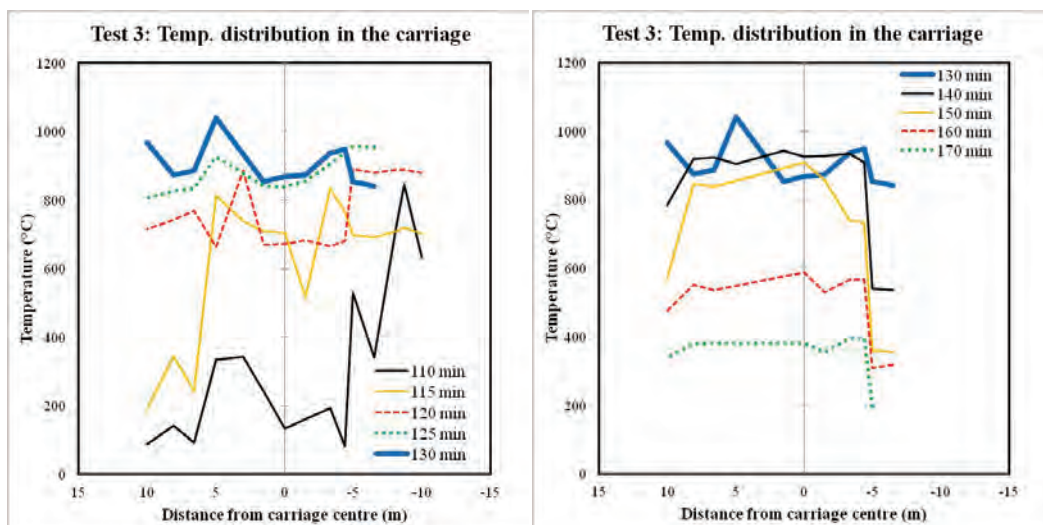


Figure 8.23 Centreline temperatures at approx. 29 cm from the ceiling. Measurement point P12 equals -10 m and measurement point P29 equals +10 m from the centre of the carriage. The plot is based on measurement points P12 – P15, P17 – P21, P23 – P26 and P28-P29 (see Figure 6.3).

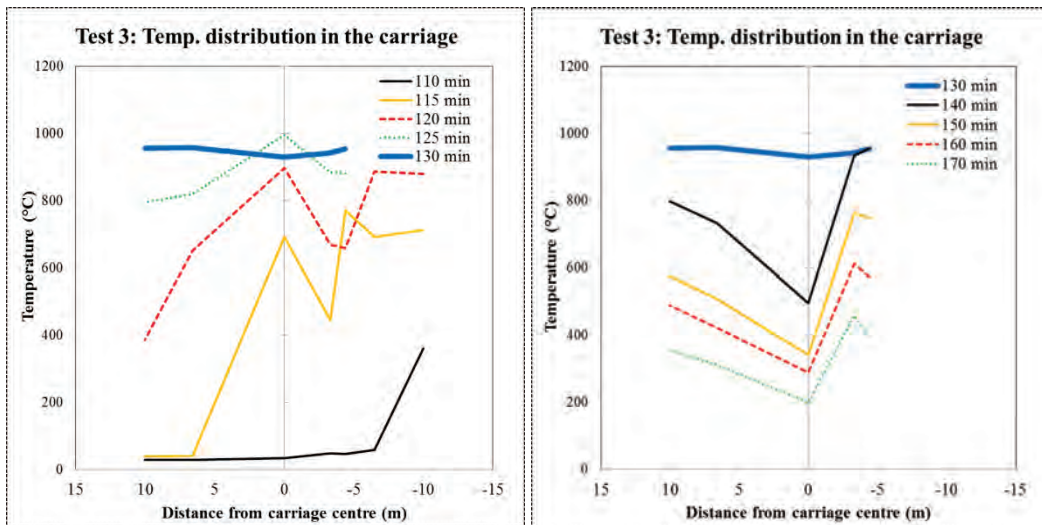


Figure 8.24 Centreline temperatures at approx. 211 cm from the ceiling. The plot is based on measurement points P12, P15, P18, P19, P21, P26 and P29.

From Figure 8.23 and Figure 8.24 it is possible to make assumptions regarding the fire growth in the train carriage. At 110 min after ignition, the section of the carriage where the fire was ignited is probably still burning. Five minutes later one can see a significant temperature increase which is very likely to correspond to a fire growth and fire spread over the entire front part of the carriage. Another 15 min later the entire carriage has an almost uniform temperature, which indicates that the entire carriage is involved in the fire and that the fire is fully developed. At this time, 130 min after ignition, the temperature reaches its peak value during the entire test 3.

By plotting the temperature in the driver compartment together with the temperature in the passenger compartment, a difference between test 2 and 3 can be identified. In test 2 the fire spread from the ignition source and backwards in the passenger cabin. After approx. 40 min when the passenger compartment was on fire it spread to the driver compartment. In test 3 the fire first spread from the ignition source to the driver compartment and then backwards in the carriage to the entire passenger compartment, see Figure 8.25. One difference is that the door to the passenger compartment was unintentionally left open in test 3 which explains the first peak in the driver compartment. The open door has initially spread fire gases to the driver compartment and might also have made the fire spread from the driver compartment to the passenger compartment easier later in the test. The conclusions drawn from the test series should, however, not be significantly affected by the open door. It should also be noted that smoke spread to the driver compartment relatively early also in test 2, even if it did not raise the temperature in the measurement points as much as in test 3. Another observation to be made is that the fast increase in temperature occurs at the same time in P12 (in the passenger compartment near the driver compartment) and in P31 (driver compartment).

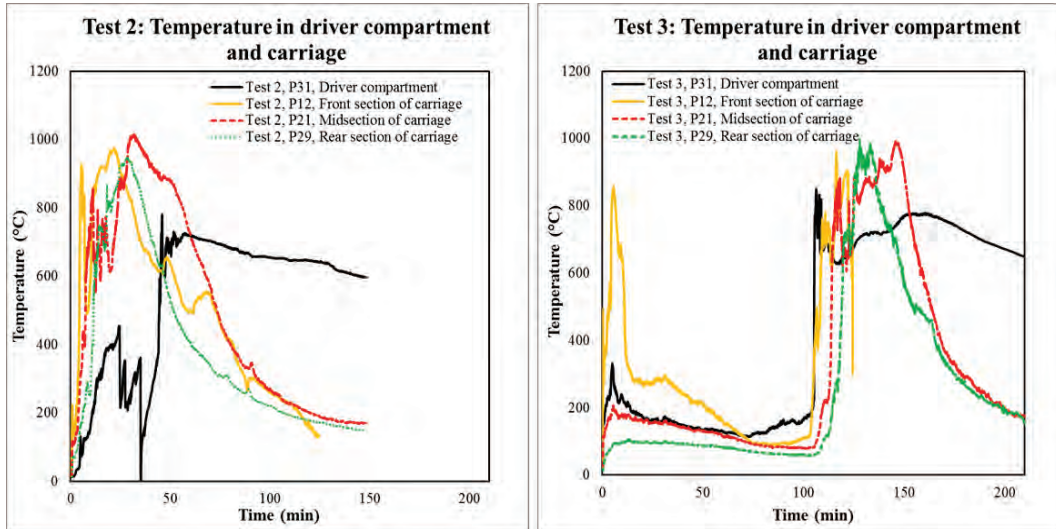


Figure 8.25 Temperatures 29 cm from the ceiling in test 2 (left) and 3 (right). By comparing the black line (P31) with the orange (P12), red (P21) and green (P29) line in each test it is possible to see that the fire spread differed between the tests.

In the tunnel, the maximum temperature measured near the tunnel ceiling was approximately 1100 °C both in test 2 and test 3. However, the maximum temperature was somewhat higher in test 3: approximately 1120 °C measured above the centre of the carriage, while the maximum temperature in test 2 was approximately 1080 °C, measured at the position +10 m. The time resolved temperature results are presented in Figure 8.26. The maximum temperatures in four positions above the carriage are summarized in Table 8.1. The gas temperatures near the ceiling in test 1 were not affected by the fire.

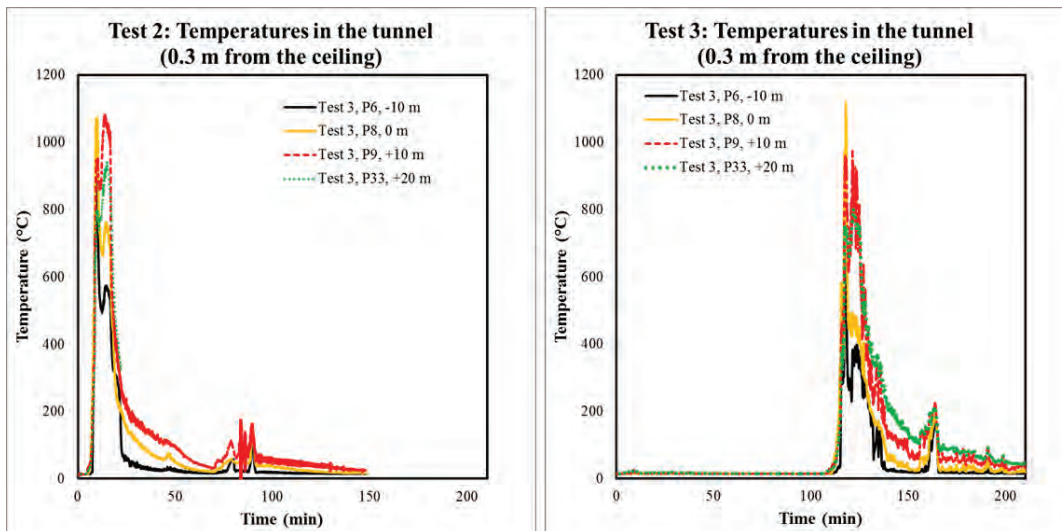


Figure 8.26 Temperature in the tunnel, just above and near the train carriage.

Table 8.1 The maximum gas temperature (and time for maximum) near the ceiling above the carriage in test 2 and test 3.

Test	Position -10 m		Position 0 m		Position +10 m		Position +20 m	
	(°C)	(min)	(°C)	(min)	(°C)	(min)	(°C)	(min)
2	911	9.03	1073	9.40	1081	13.44	944	14.50
3	702	117.86	1118	117.79	980	121.12	799	121.57

As with the temperature distribution in the train carriage, the temperature distribution in the tunnel is presented by plotting the temperature against the position of the measurement point. Measurement point P1, P2, P4, P6, P8, P9, P33, P35, P36, P37 and P38 (see Figure 6.1) have been used for all plots with temperature distribution in the tunnel.

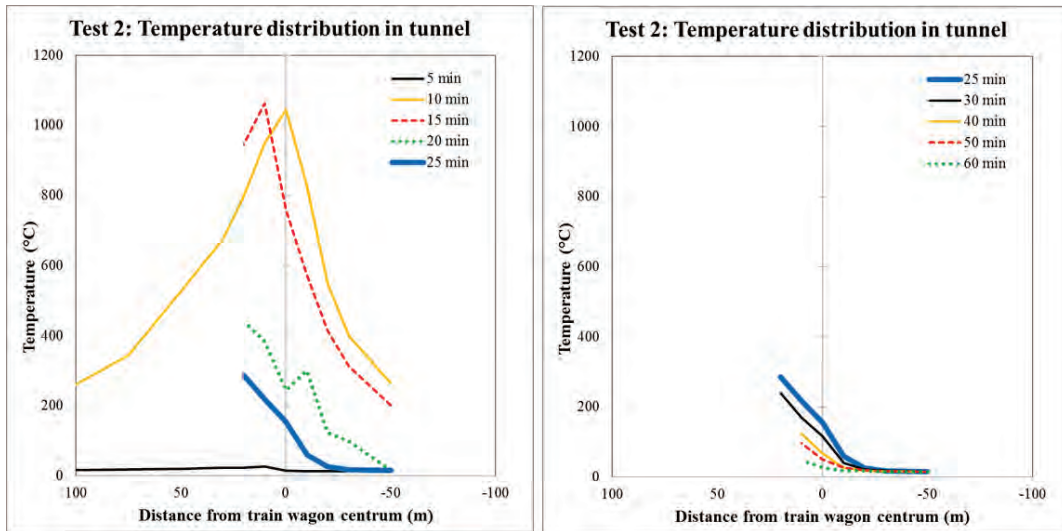


Figure 8.27 Centreline temperatures at 30 cm from the ceiling in the tunnel. Fifteen minutes after ignition a cable burnt resulting in void data from all measure point between P33 and P40.

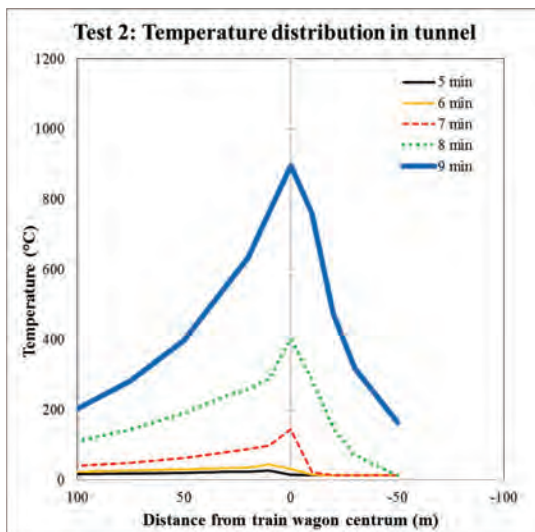


Figure 8.28. Centreline temperatures at approx. 29 cm from the ceiling in the tunnel. Temperature increase between 5 and 10 min after ignition in test 2.

In Figure 8.27 one can see a strong increase in temperature between 5 and 10 min after ignition. This increase appears not just behind the train but also in front of the train (front is at approx. -12 m), even though there was a fan at -96 m producing an airflow from east to west in the tunnel. This indicates transport of smoke in the upstream direction. This effect, called back-layering, was also observed during the test, approx. 7 min after ignition, see Appendix 1. Approximately 9 min after ignition it was not possible to see the front of the train because the back layering smoke descended to ground level. Note that the maximum temperature was reached at different times for different positions (see Table 8.1). The temperature increase between 5 and 10 min is plotted in more detail in Figure 8.28. The temperature decrease between 10 min – 25 min (see Figure 8.27) is

probably partly because the fan at -96 m is altered once after about 10 min and once more after about 16 min, see the test protocols in Appendix 1.

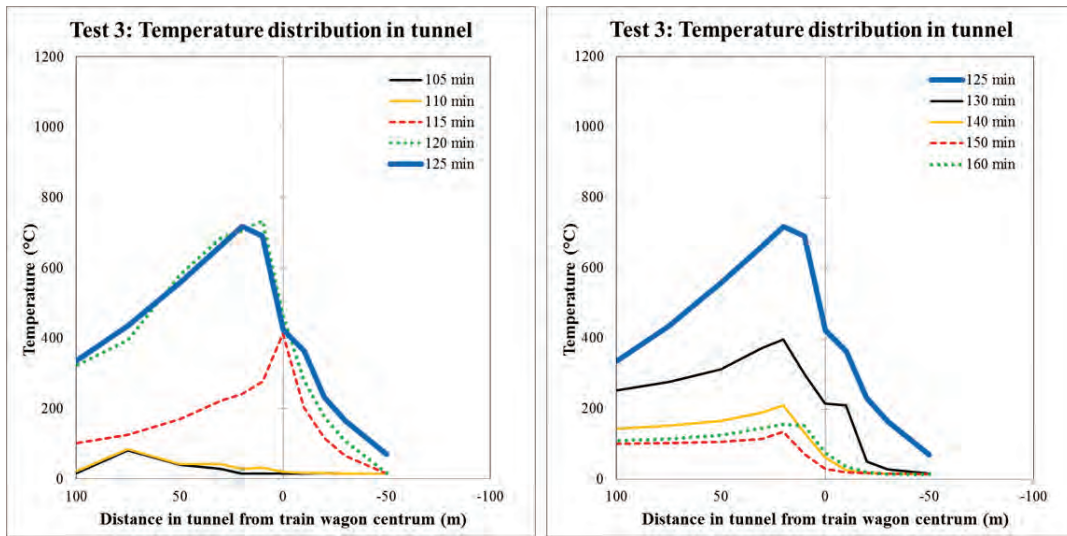


Figure 8.29 Centreline temperatures at 30 cm from the ceiling in the tunnel in test 3.

Figure 8.29 presents the temperature distribution in the tunnel in test 3. Between 110 and 115 minutes after ignition the temperature increases in the tunnel. The temperature increase in front of the train corresponds to the first observations of back layering after 115 min, see Appendix 1. The temperature in the tunnel appears to decrease after 125 min, which correspond with the observed decay. To visualize the peak temperature of test 3 and how the back layering was pushed back, the temperature is plotted between 115 and 120 min in Figure 8.30.

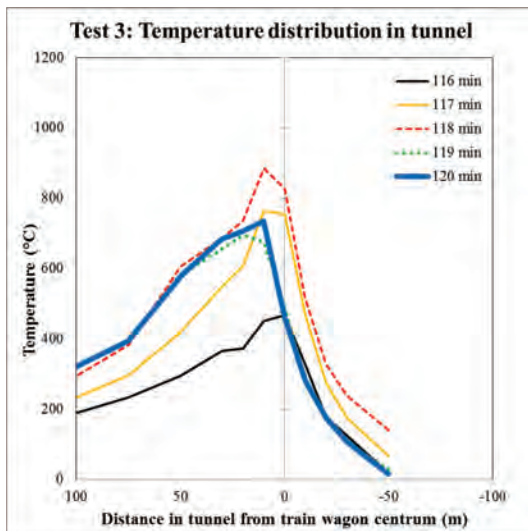


Figure 8.30 Centreline temperatures at 30 cm from the ceiling in the tunnel in test 3.

The observations (Appendix 1) from the test state that approximately 117 min after ignition the smoke in front of the train is lowering towards the ground. Between 117 and 118 min the power of the fan at -96 m is increased twice and between 119 min and 120 min the back layering is pushed back. All of this can be seen in the temperature profiles in Figure 8.30.

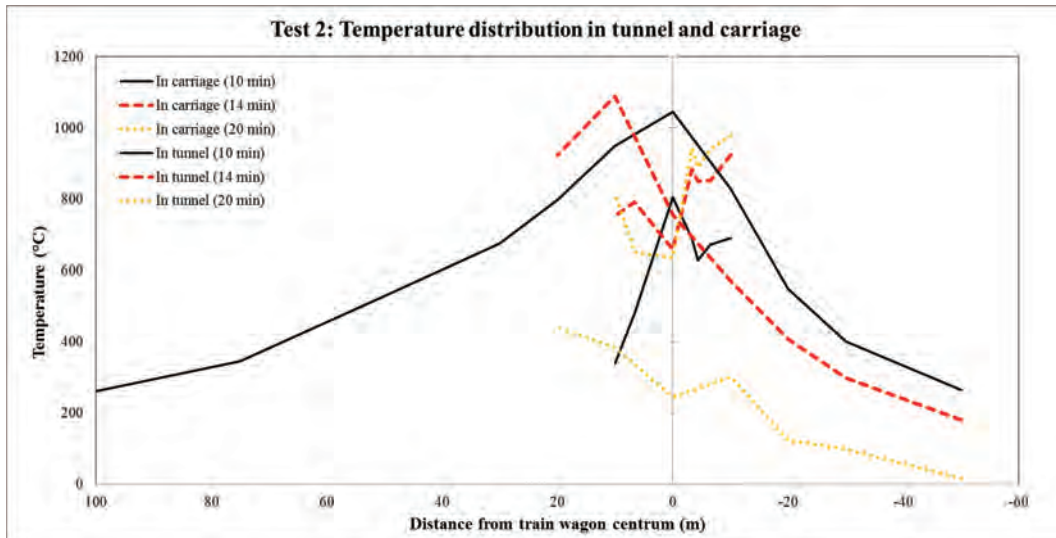


Figure 8.31 Centerline temperature at approximately 30 cm from the ceiling in both the tunnel and the train carriage. Also see Figure 8.21 and Figure 8.27.

In Figure 8.31 the temperature profile from the carriage and the tunnel is merged. What can be seen from this figure is that at 10 min after ignition, the temperature is higher in the tunnel than in the train carriage. The reason for this is probably the development of the fire where the fire starts at one end of the passenger compartment to spread to the rest of the compartment. When the fire intensity increases the ventilation opening (doors and windows) affect the burning and much of the combustion probably takes place near or outside the openings. These ventilation conditions were also altered during the tests when windows broke and doors fell out. Sometime between 10 and 20 min after ignition this stage changes and the temperature becomes significantly higher in the train carriage. If the same comparison between train carriage and tunnel is performed for test 3, this difference cannot be seen to the same extent, see Figure 8.32. The temperature is almost always higher in the carriage compared to in the tunnel. It is important to note that the temperature condition varied relatively rapidly, especially in the tunnel and, therefore, the selection of measurement positions and time to use for the comparisons affect the results. This is of course the case for both tests.

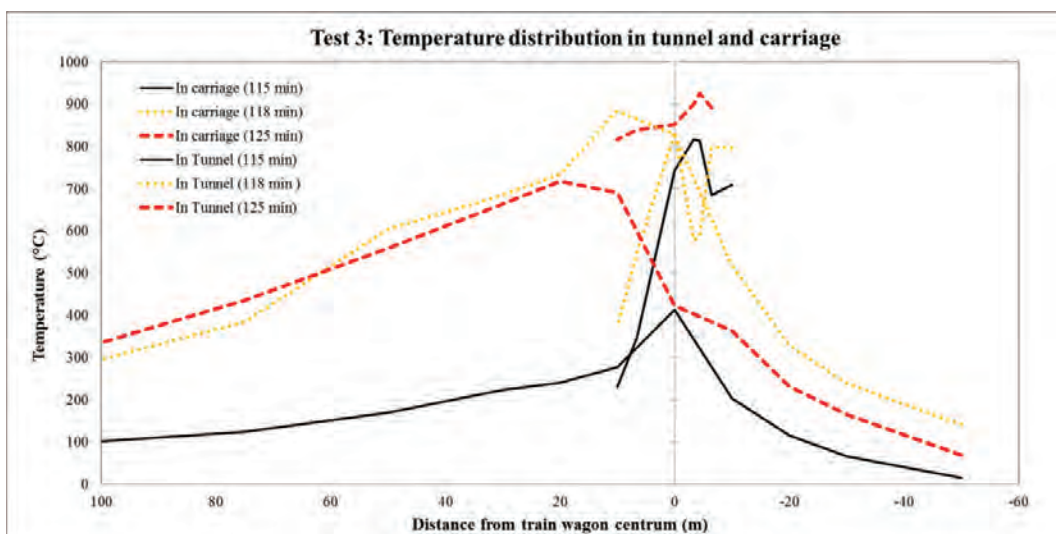


Figure 8.32 Centerline temperature at approx. 29 cm from the ceiling in both the tunnel and the train carriage. Also see Figure 8.23 and Figure 8.29.

8.6 Gas concentrations

The gas concentrations in the train carriage, including CO₂, CO and O₂, were measured in position P19, at 0.29 m, 1.20 m and 2.11 m from the ceiling.

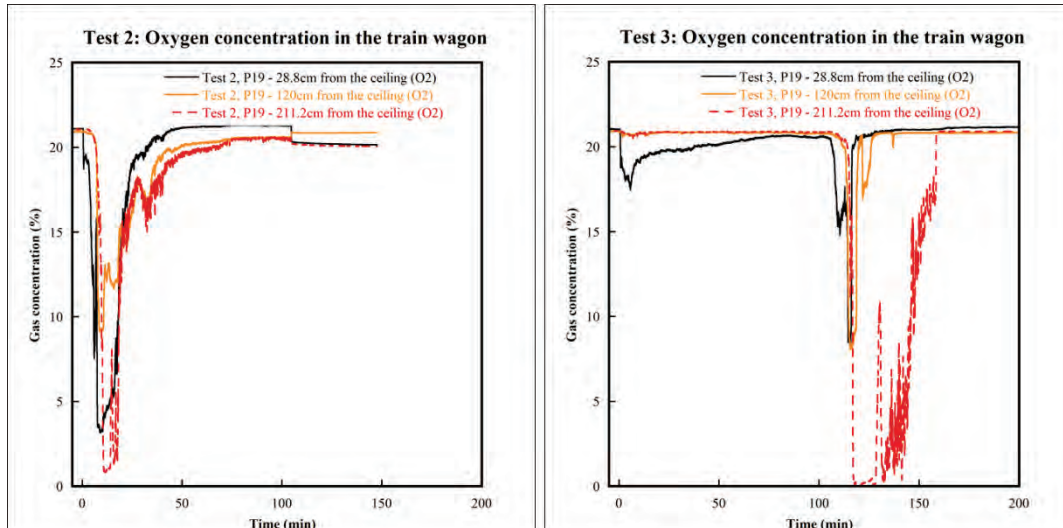


Figure 8.33 Oxygen concentration (vol-%) in the train carriage, test 2 (left) and test 3 (right). Measurements were made at approx. -3.4 m from the centre of the carriage.

The most significant differences between the tests are the difference in oxygen concentration in the ceiling and close to the floor. In test 2 the oxygen concentration is several percentages lower in the ceiling compared to test 3 but close to the floor the oxygen concentration is lower for a longer time period in test 3 compared to test 2. This difference is probably due to the fact that the fire development before the fast increase was very different in the two tests. In test 3 there was a long period of slow burning. This together with possible differences in the ventilation openings (breakage of windows and doors) might have created differences in the local ventilation conditions.

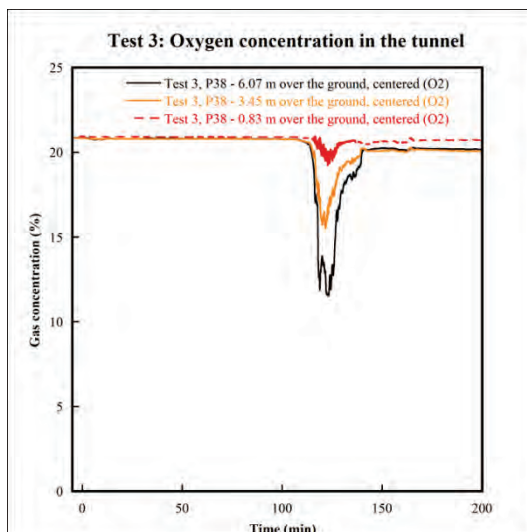


Figure 8.34 Oxygen concentration (vol-%) in the tunnel, measured at the measurement station (+100 m).

The oxygen concentrations in the tunnel (see Figure 8.34) were measured at three different heights (0.83 m, 3.45 m and 6.07 m from the ceiling in the tunnel) at +100 m from train carriage centre, marked as *measurement station*, see Appendix 3. Unfortunately, the burnt cable in test 2 lost the data at the measurement station for most of the test. Comparison between test 2 and test 3 can, therefore, not be made for this position. Gas concentrations in the tunnel will, therefore, only be reported for test 3.

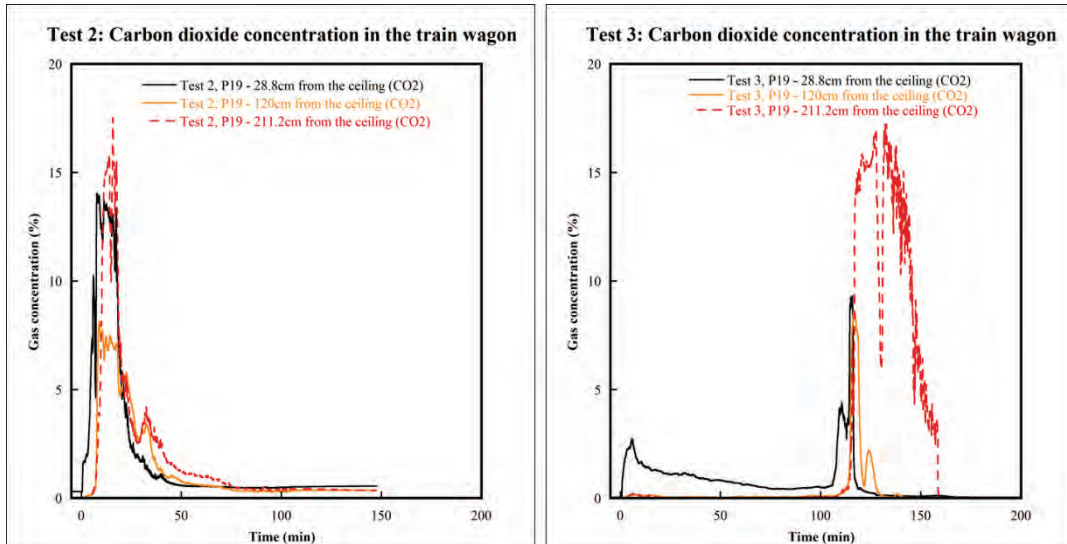


Figure 8.35. Carbon dioxide concentration (vol-%) in the train carriage, test 2 (left) and test 3 (right). Measurements were made at approx. -3.4 m from the centre of the carriage.

Not unexpectedly the differences in CO₂ concentrations between test 2 and 3 correspond with the differences in oxygen concentration. For all the gas concentrations in the carriage (see Figure 8.33, Figure 8.35 and Figure 8.37), there is a longer time period of low O₂ concentration and high CO₂ and CO concentrations. Since there is no information concerning the timing of the breakage of most of the windows and the rupture of the closed doors, the variation in ventilation conditions cannot be temporally specified in detail. However, the differences between test 2 and test 3 can probably be related both to the difference in fire development (the long period of a slowly burning fire in test 3 before a fast increase in fire intensity) and the ventilation condition inside the carriage. The importance of the local ventilation conditions were seen in tests with a scale model of the carriage [22].

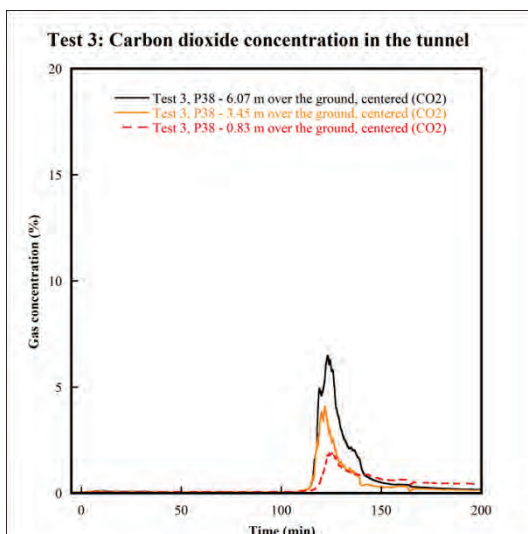


Figure 8.36 Carbon dioxide (vol-%) concentration in the tunnel, measured at the measurement station (+100 m).

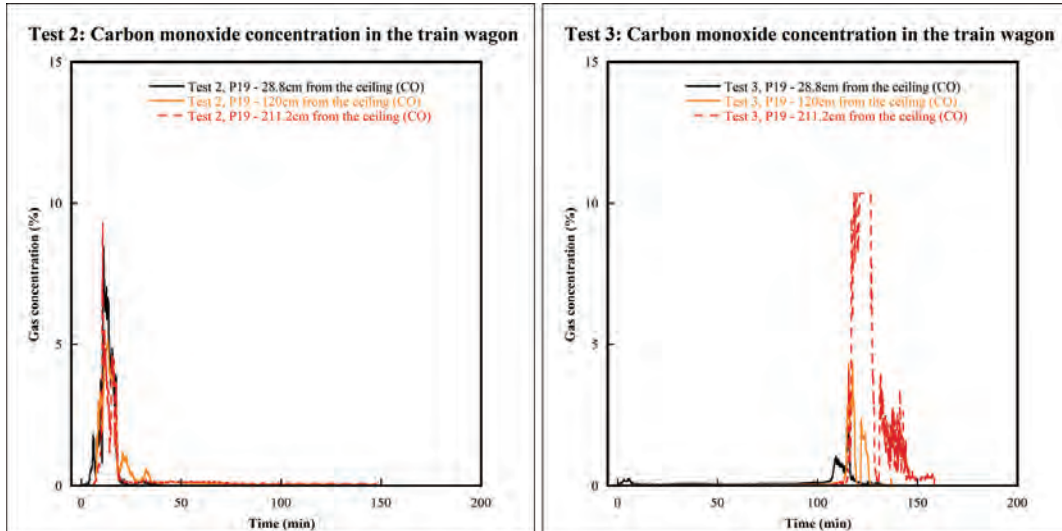


Figure 8.37 Carbon monoxide concentration (vol-%) in the train carriage, test 2 (left) and test 3 (right) Measurements were made at approx. -3.4 m from the centre of the carriage.

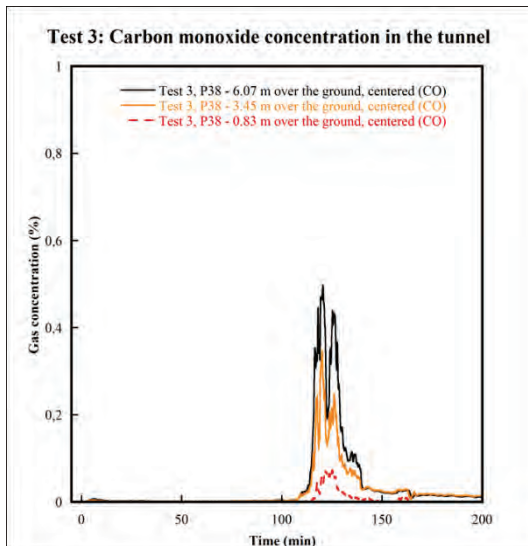


Figure 8.38 Carbon monoxide concentration (vol-%) in the tunnel, measured at the measurement station (+ 100 m).

8.7 Radiant heat Flux

Heat fluxes were measured using plate thermometers. Three plate thermometers were placed upstream of the carriage, three on the tunnel wall, 1.5 m from the carriage and three downstream of the carriage. The plate thermometer registers a temperature and the incident heat flux is calculated according to equation 6.1, see section 6.2. The following figures only present the calculated incident heat flux, the registered temperatures are presented in Appendix 2.

The plate thermometers did not register any elevated temperatures in test 1.

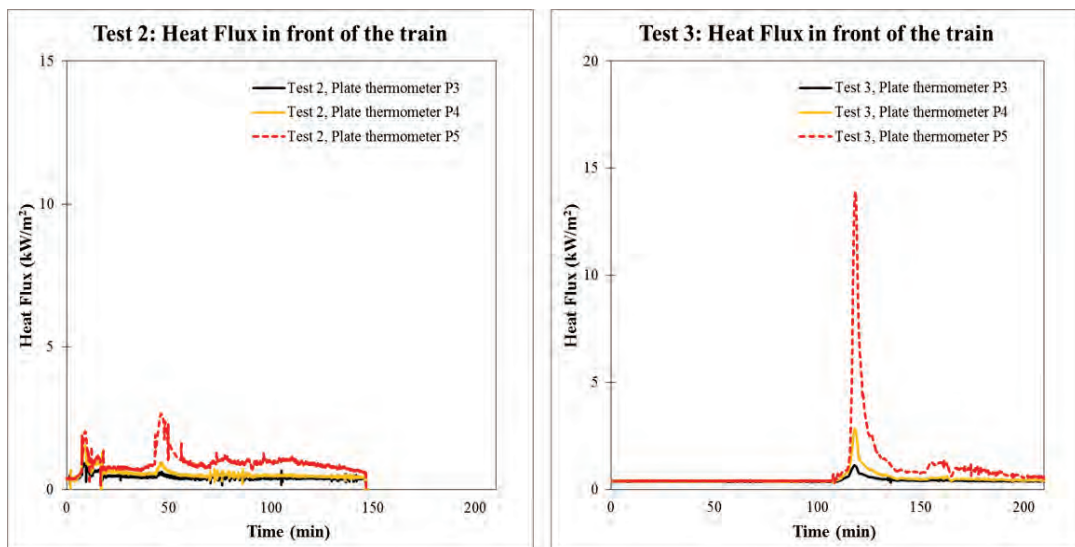


Figure 8.39 Heat flux towards plate thermometers in front of the train. Plate thermometer P3 is placed at -25 m, P4 at -20 m and P5 at -15 m.

The heat fluxes registered in front of the train are significantly higher in test 3. Possibly this could be due to the fact that the fire spread to the driver compartment in the early stage of the fire in test 3 and later in the fire in test 2.

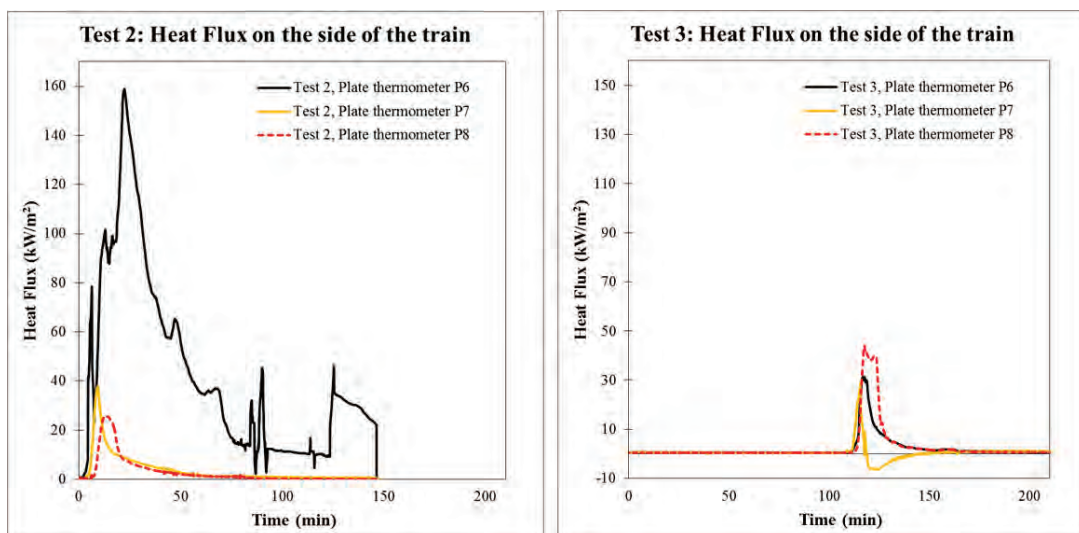


Figure 8.40 Heat flux towards plate thermometers on the side of the train. Plate thermometer P6 is placed at -10 m, P7 at -6.5 m and P5 at -15 m.

The high values of the calculated heat flux in P6 in test 2 (see Figure 8.40) can probably be explained by that the plate thermometer was exposed to the flames through the

window. The readings in the later part of the test seems to be unrealistic which indicates that something has happened with the plate thermometer during the test.

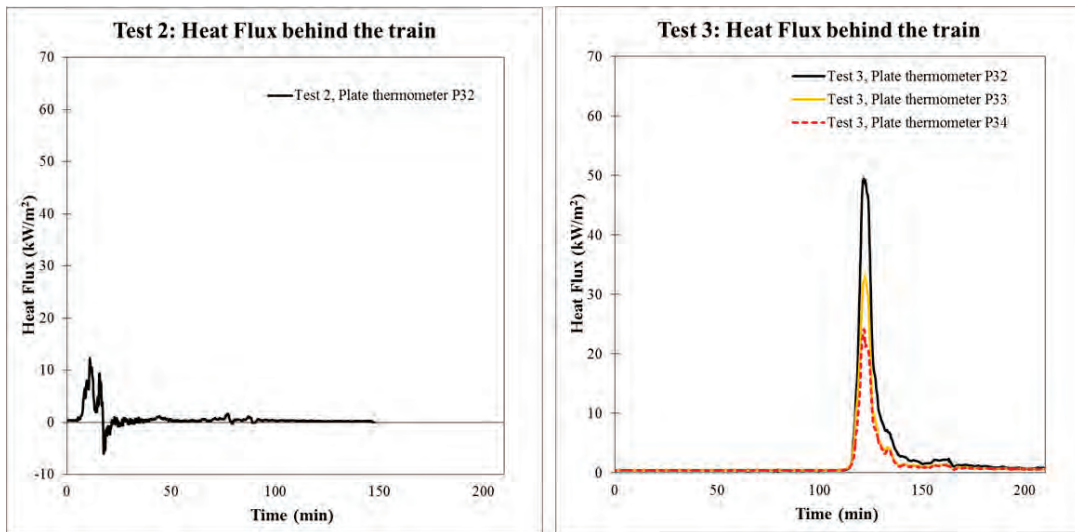


Figure 8.41 Heat flux towards plate thermometers downstream of the carriage. Plate thermometer P32 is placed at +15 m, P33 at +20 m and P34 at +25 m. Measure point P33 and P34 are not plotted for test 2 since they reported void data after the cable burnt.

In Figure 8.40 and Figure 8.41 negative values have been plotted for measurement point P7 (test 3) and measurement point P32 (test 2), respectively. The incident heat flux towards the plate thermometers cannot be negative (it is defined as always being positive) and the negative values are considered void data. When the heat flux is calculated, the temperatures registered by the PTC is compared to the surrounding temperature registered by a thermocouple placed in the vicinity of the plate thermometer. This means that if either the PTC or the thermocouple malfunction or temporarily is exposed for very extreme conditions, this will result in inaccurate heat fluxes.

8.8 Extinction coefficient

The smoke density was measured inside the train carriage, measurement point P18 (-4.5 m) and in the tunnel at the measurement station, measurement point P38 (+100 m). The measurements were made at 28.8 cm, 120 cm and 211.2 cm from the ceiling in the train carriage and 3.45 m over the railway sleepers in the tunnel. The measuring device records a laser beam between a transmitter and a receiver. The attenuation in the smoke is described by the extinction coefficient, calculated with equation 5.20, see section 5.8.

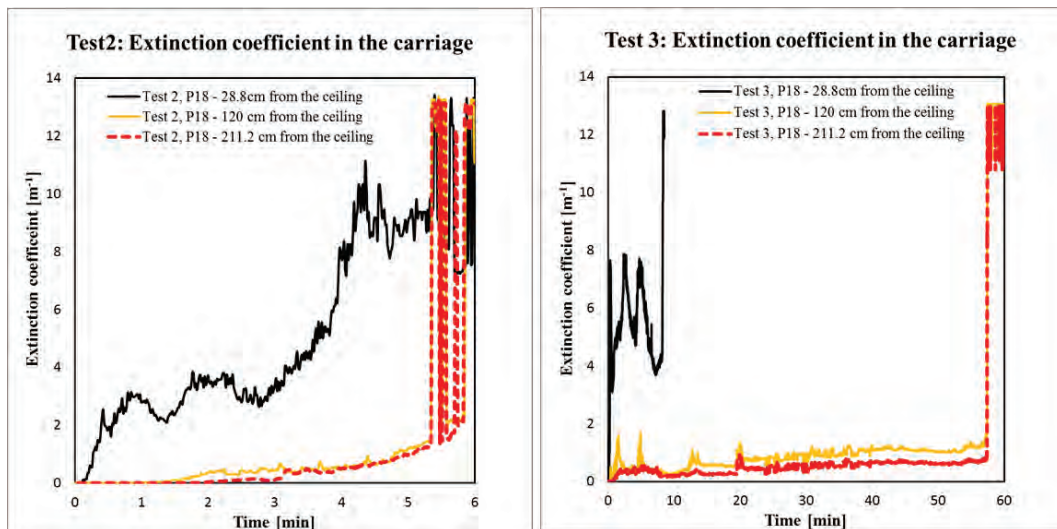


Figure 8.42 Extinction coefficient for test 2 (left) and test 3 (right). Measurements were only available up to approx. 5.5 min in test 2 and up to 57 min in test 3 (8 min for measurements in the ceiling) due to void data.

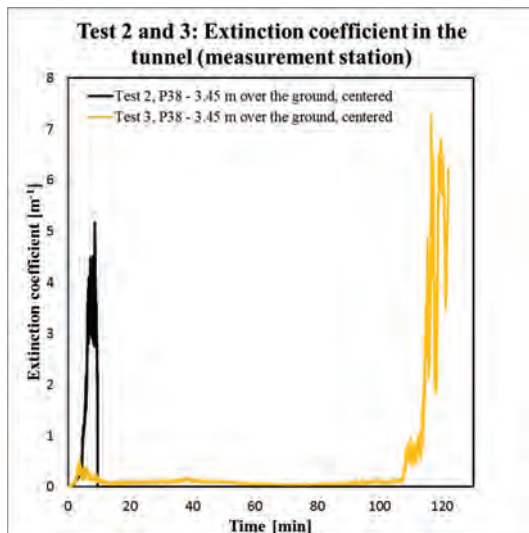


Figure 8.43 Extinction coefficient in the tunnel (at measure station) for test 2 and 3. Measurements were only available up to approx. 10 min in test 2 because of a burnt cable and up to 122 min in test 3 because of void data.

8.9 Pulsations

During the periods of most intense fire in test 2 and test 3, pulsations in the tunnel were observed. The pulsations could be seen (e.g. swaying trees, in phase with the pulsations, outside the tunnel portal), felt and heard (variation in the work of the fan) also outside the tunnel. Pulsations have been observed previously during large-scale tests performed in 2003 in the Runehamar tunnel in Norway [16, 23, 24]. The pulsations were identified as thermoacoustic instabilities.

The measured pressure (for the velocity calculations) was not logged fast enough to fully resolve the frequency of the oscillation even if the time period of fast and regular variations is easily identified in Figure 8.5 and Figure 8.6. Using the videos from the tests, the oscillation period was determined to be approximately 1.6 s both in test 2 and test 3. If the acoustic theory is used [24], the period of the first (fundamental) mode for the tunnel was calculated to be 1.64 s, i.e. close to the observed oscillation period.

9 Conclusions

Three fire tests were performed under and inside commuter train carriages in a tunnel. Both tests initiated inside the carriage developed to fully flashover conditions. In the test conducted with the original seats and linings ignited inside the carriage, the maximum heat release rate (HRR) was 76.7 MW and occurred 12.7 min after ignition. In the test conducted on the refurbished carriage (with more modern seats and non-combustible aluminium wall and ceiling lining) ignited inside the carriage, the maximum HRR occurred after almost 118 min and was approximately 77.4 MW. This means that the maximum heat release rate was approximately the same in both tests, but the time to reach maximum HRR differed significantly. For these HRR calculations, the maximum gas temperature near the tunnel ceiling was used. The corresponding HRR calculated with oxygen consumption calorimetry was approximately 75 MW in test 3.

The main reason for the difference in fire growth rate between these two tests was due to the involvement of the combustible wall and ceiling lining in the test conducted in the originally fitted X1 carriage. This proves the importance of the lining material where a high performance material can increase the time available for evacuation. It should, however, be noted that the lining material in the original X1 were of relative good performance (HL2 according to CEN/TS 45545-2:2009).

The maximum HRR calculated from the experimental results are significantly higher than those obtained in other documented test series. The luggage in, under or between different seats is assumed to increase the fire spread significantly in both cases. Clearly, it is necessary for train owners to consider this transient load when conducting risk assessments and designing response tactics.

Different methods of estimating HRR are compared and good agreement was obtained. The temperature method is quite robust, but dependent on the correct measurement of the maximum ceiling temperature. The CO₂/CO technology and CO₂ production method underestimate the HRR at the first peak and slightly overestimate the HRR in the decay period (in comparison to the O₂ consumption calorimetry), but predict quite well in the other periods.

To estimate the time to flashover of the carriage, the time when the gas temperature reached 600 °C in various positions and at different heights was evaluated. From this study the conclusion was drawn that the carriage was flashed over after 12 min in test 2 and after 119 min in test 3.

The gas temperature inside the carriage reached approximately 1000 °C in both test 2 and test 3 and although the large difference in fire development, as discussed above, the temperature development for the parts of the tests when the entire carriage became involved in the fire were similar to each other

In the tunnel, the maximum temperature measured near the tunnel ceiling was approximately 1100 °C both in test 2 and test 3. However, the maximum temperature was somewhat higher in test 3: approximately 1120 °C measured above the centre of the carriage, while the maximum temperature in test 2 was approximately 1080 °C, measured at the position +10m (10 m downstream the centre of the carriage).

During the periods of most intense fire in test 2 and test 3, pulsations in the tunnel were observed. The pulsations could be seen, felt and heard also outside the tunnel. The pulsations were identified as thermoacoustic instabilities.

10 References

1. Rohlén, P., and Wahlström, B., "Tunnelbaneolyckan i Baku, Azerbadjan 28 oktober 1995", Räddningsverket, P22-133/96, Karlstad, Sweden (in Swedish), 1996.
2. Burns, D., and Gillard, J., "External Observations of the Daegu Metro Fire Disaster 18 February 2003", Proceedings of the Fifth International Conference on Safety in Road and Rail Tunnels, pp 13-26, Marseille, France, 6-10 October, 2003.
3. "Fires in Transport Tunnels: Report on Full-Scale Tests", edited by Studiengesellschaft Stahlanwendung e. V., EUREKA-Project EU499:FIRETUN, Düsseldorf, Germany, 1995.
4. Ingason, H., Gustavsson, S., and Dahlberg, M., "Heat Release Rate Measurements in Tunnel Fires", SP Swedish National Testing and Research Institute, SP Report 1994:08, Borås, Sweden, 1994.
5. Ingason, H., and Lönnemark, A., "Heat Release Rates in Tunnel Fires : A Summary". In *In The Handbook of Tunnel Fire Safety, 2nd edition* (A. Beard and R. Carvel, Eds.), ICE Publishing, London, 2012.
6. "X1", <http://www.jarnvag.net/index.php/vagnguide/utgangna-motorvagnar/x1> (accessed 2012-11-29; in Swedish), 2011.
7. Lönnemark, A., Ingason, H., Claesson, A., Lindström, J., Li, Y. Z., and Kumm, M., "Laboratory fire experiments with a 1/3 train carriage mockup", SP Technical Research Institute of Sweden, SP Report 2012:06, Borås, Sweden, 2012.
8. Larsson, S., "The Tunnel Blaze in Kaprun, Austria", Swedish National Defence College, CRISMART studier N:o 1, Stockholm, Sweden, 2004.
9. Bergqvist, A., "Rapport från besöket vid brandplatsen i Kaprun, Österrike", The Greater Stockholm Fire Brigade, Stockholm, Sweden (in Swedish), 2001.
10. Kumm, M., "Carried Fire Load in Mass Transport Systems - a study of occurrence, allocation and fire behavior of bags and luggage in metro and commuter trains in Stockholm", Mälardalen University, SiST 2010:04, Västerås, Sweden, 2010.
11. Kumm, M., Lönnemark, A., and Palmkvist, K., "Användande av mobila fläktar vid bränder i tunnlar - En sammanställning av försök och erfarenheter 2002 till 2013", Mälardalen University Press, Research Report MDH SiST 2013:01, Västerås, Sweden (in Swedish), 2013.
12. Janssens, M., and Parker, W. J., "Oxygen Consumption Calorimetry". In *Heat Release in Fires* (V. Babrauskas and T. J. Grayson, Eds.), E & FN Spon, 31-59, London, UK, 1995.
13. Ingason, H., "Fire Dynamics in Tunnels". In *In The Handbook of Tunnel Fire Safety, 2nd Edition* (A. N. Beard and R. O. Carvel, Eds.), ICE Publishing, 273-304, London, 2012.
14. Tewarson, A., "Experimental Evaluation of Flammability Parameters of Polymeric Materials". In *Flame Retardant Polymeric Materials* (M. Lewin, S. M. Atlas, and E. M. Pearce, Eds.), Plenum Press, 97-153, New York, 1982.
15. Grant, G. B., and Drysdale, D., "Estimating Heat Release Rates from Large-scale Tunnel Fires", Fire Safety Science - Proceedings of the Fifth International Symposium, 1213-1224, Melbourne, 1995.
16. Ingason, H., Lönnemark, A., and Li, Y. Z., "Runehammar Tunnel Fire Tests", SP Technical Research Institute, SP Report 2011:55, 2011.
17. Ingason, H., "Model Scale Railcar Fire Tests", SP Swedish National Testing and Research Institute, SP REPORT 2005:48, Borås, 2005.

18. McCaffrey, B. J., and Heskestad, G., "Brief Communications: A Robust Bidirectional Low-Velocity Probe for Flame and Fire Application", *Combustion and Flame*, **26**, 125-127, 1976.
19. Wickström, U., "The Plate Thermometer - A simple Instrument for Reaching Harmonized Fire Resistance Tests", SP Swedish National Testing and Research Institute, SP REPORT 1989:03, Borås, Sweden, 1989.
20. Häggkvist, A., "The Plate Thermometer as a Mean of Calculating Incident Heat Radiation - A practical and theoretical study", Luleå University of Technology, 2009.
21. Drysdale, D., *An Introduction to Fire Dynamics*, 2nd Edition ed., John Wiley & Sons, 1999.
22. Lönnermark, A., Lindström, J., and Li, Y. Z., "Model-scale metro car fire tests", SP Technical research Institute of Sweden, SP Report 2011:33, Borås, Sweden, 2011.
23. Lönnermark, A., Persson, B., and Ingason, H., "Pulsations during Large-Scale Fire Tests in the Runehammar Tunnel", *Fire Safety Journal*, **41**, 5, 377-389, 2006.
24. Lönnermark, A., and Ingason, H., "Acoustic Considerations Regarding Pulsations during Large-Scale Fire Tests in a Tunnel", Proceeding of the 8th International Symposium on Fire Safety Science, pp 1473-1484, Beijing, China, 18-23 September, 2005.

Appendix 1 - Test Protocols

Test 1

Comments and test Conditions

Fire placement: Under the ATC receiver beneath the carriage

Fire source: Heptane pool (350 mm × 350 mm × 35 mm) with 3.2 L of heptane

Open doors: 0

Fan placement: 4 m into the tunnel from the eastern tunnel opening

Notes before test start

Before the fan was started, the air velocity in the tunnel was 0-0.1 m/s. When the fan was running the velocity above the fuel pan (under the train) was 2-3 m/s and next to the carriage 4.5 – 5 m/s.

Observations

Time [h:min:ss]	Time ign [h:min:ss]	Observation and description
0:10	0:00	Ignition
3:20	3:10	Flames “sweeps” around a pressure vessels (not pressurized)
5:06	4:56	A cable above the ATC ignites
		Sparks can be seen
5:30	5:20	The fire has decreased, but one can see sparks from the shield downstream och the ATC.
5:58	5:48	The cable self-extinguished
6:11	6:01	The pool fire self-extinguished (the fuel was consumed)
10:07	9:57	The door closest to the fire was opened
11:10	11:00	Material ATC shield fell down and continued to burn on the ground
14:00	13:50	Only small flames left
15:00	14:50	The fire on the ground self-extinguish
		Only smoke can be seen, but is still produced
19:43	19:33	All flames seems to be extinguished

Test 2

Comments and test Conditions

Ignition source: 1 L of petrol and three small pieces of fibre board igniters (23 mm × 30 mm × 15 mm) with added paraffin

Ignition source placement: The container with petrol was placed on a seat in one of the corners closest to the driver's cabin. One piece of fibre board was placed on the seat and two on the floor in front of the same seat.

Ignition source amount: 1 L of petrol

Temperature in tunnel: 14-15 °C

Air pressure: 980 mbar

Notes before test start

The three doors on the left side of the carriage were open already at the time of the ignition.

Before the fan was started the air velocity in the tunnel was 0.4-0.5 m/s from east to west.

When the fan (2250 rpm) was running before ignition the air velocity at -30 m (height 2.5 – 3 m) was 1.5 – 2.5 m/s

Observations

Time ign [h:min:ss]	Description
0:00	Ignition
0:19	Smoke layer in the carriage level descends, in height with personnel heads
0:36	Backpack (A52) on fire
0:37	Smoke starts to escape through the door closest to the ignition source
0:50	Trunk (A2) on fire
0:53	Gas layer in height with the yellow horizontal bar close to each door
1:05	Most of the petrol probably burnt
1:30	Gray smoke in the driver compartment
2:53	Increased smoke flow through door or ventilation above door closest to the ignition source
3:27	Further increase in flow of black smoke escapes from the door closest to the ignition source
3:45	Driver compartment filled with smoke, as far as can be seen through the front windows.
4:00	Window above ignition source on the right side breaks
4:15	Flames through window above ignition source on the right side of the train
4:30	Black and gray smoke from window on the right side
4:49	Window on the left side of the train, closest to the front, breaks. Black smoke from window.
5:04	Flames through the broken window
5:22	Flames coming out from the top of the door closest to the ignition source
5:27	Window on the left side of the train breaks. Window is located just left of the window broken after 4:49
5:34	Burning object falling from window on the right side
5:40	Only black smoke coming out of the train
5:45	Flames through the right window reaches over the roof of the train
6:07	Heavy burning from broken window on the left side of the train
6:10	Flames through the left window reaches over the roof of the train
6:37	Flames coming out from the entire door closest to the ignition source.

Time ign [h:min:ss]	Description
6:40	Train is now burning heavily. Isolation on the right side of the tunnel wall is on fire. Flames from the train reach the wall on the right side.
6:54	Backlayering in the tunnel appears
7:00	Flames from the train reach the tunnel wall on the left side
7:37	Weak pulsation starts
7:54	Backlayering several meters upstream of the train. Smoke lowering, still above train roof.
8:00	Smoke layer in the tunnel just above train roof. Weak pulsation started.
8:24	Smoke layer ahead of train in height with heads of personnel on the left side of the tunnel. Approx. 1 m above personnel heads on the right side.
8:27	Pulsation increases
8:49	Smoke upstream of the train at ground level
8:52	Heavy pulsation
9:35	The speed of fan is increased
11:07	Pulsation have increased further
15:37	Pulsation have decreased somewhat
16:17	The speed of fan is increased again.
17:07	Small increase in pulsation from the window on the left side closest to the front of the train
18:30	Pulsation decreasing
19:30	Pulsation stopped, fire is limited to the inside of the train
20:07	Downstream of the fire the smoke layer was 1 m above the ground
23:07	No pulsation, but increased fire in the front of the train. Flames coming out of the window on the left side closest to the front of the train.
27:30	Burning objects are falling from the floor of the train on to the rails
29:00	The headlight to the right close to the roof of the train on fire
33:00	Flames coming out of the left headlight
34:00	Burning object falling from underneath the train on to the rails. This time further back in the train.
37:00	A small fire underneath the train, probably fallen materials from the train burning.
38:34	Fire under train increases somewhat
41:14	Fire beneath the train decreases
42:47	Small flames from the window in the door to the driver compartment
43:27	Fire from the window in the door to the driver compartment intensifies. Driver compartment is burning.
43:40	Front left window in the driver compartment breaks.
44:00	Heavy burning in the driver compartment
44:17	Heavy burning around the window in the door to the driver compartment. Wall next to the driver compartment door is on fire.
46:00	Right front window breaks
47:02	Still burning in the driver compartment
48:00	Fire in the driver compartment decreases
57:00	Fire in the driver compartment almost extinct; still some burning up front by the broken windows.
1:06:32	Smoke has decreased somewhat on the western side
1:12:41	The speed of the fan is decreased
1:17:00	Still small flames by the broken windows in the driver compartment. Otherwise no visible flames from the train.

The sleepers were affected approximately 1 m beyond +20 m, especially the part of the sleepers that are outside the rails.

All armatures on the left wall of the tunnel melted during the test, but for the two closest to the western opening, which means that armature approximately 50 m from the opening were melted while the one approximately 30 m from the opening was not.

Test 3

Comments and test Conditions

Ignition source: 1 L of petrol and three small pieces of fibre board igniters (23 mm × 30 mm × 15 mm) with added paraffin

Ignition source placement: The container with petrol was placed on a seat in one of the corners closest to the driver's cabin. One piece of fibre board was placed on the seat and two on the floor in front of the same seat.

Ignition source mass: 1 L of petrol

Temperature in tunnel: 16 °C

Notes before test start

The three doors on the left side of the carriage were open already at the time of the ignition.

Before the fan was started the air velocity in the tunnel was 1-1.6 m/s from east to west. When the fan was running before ignition the air velocity at -50 m (height 3.45 m) was 2.5-3.5 m/s. The air velocity on the left side of the carriage, in front of the doors, was 2.5-3 m/s.

Observations

Time ign [h:min:ss]	Observation and description
-5:00	Measurement start
-2:00	1 L petrol was poured into the 1 L milk container
-0:40	The three small igniters were ignited
0:00	Ignition by letting the petrol pour out and be ignited by the small igniters
0:15	Smoke layer in the driver compartment is below the lower part of the front windows. Backpack B48 and large sport bag B2 next to the ignition source are on fire.
0:32	Smoke layer is approx. 1.5 – 2m above floor in the carriage
1:00	Smoke layer level is in height the top of the seats in the carriage
1:13	Some smoke from door closest to the ignitions source
2:45	Heavy smoke from doors closest to the ignitions source
3:48	Carriage filled with black smoke
5:00	No visible flames
5:30	Window above the ignition source breaks, orange smoke from window.
5:40	Burning through window above ignition source
6:40	Some flames through the broken window
7:48	Smoke layer in carriage rises. Layer height above train seats (backrest top).
13:48	Smoke layer lowers, in height with the seats (backrest top)
15:48	Smoke layer rises again approx. 0.5 m above the seats (backrest top)
14:40	Flames on the right side of the carriage
17:15	Smoke comes out of the ceiling; heavy orange smoke from the window on the

Time ign [h:min:ss]	Observation and description
	right side.
17:48	Non or few signs of fire spread backwards in the train
21:00	Flames at and around the ignitions source are approximately 1 m above the seats.
26:00	Smoke layer approx. 0.5 m above the roof
27:00	Still no fire spread. Smoke from the doors is somewhat whiter than previously.
30:00	Four seats are on fire. Smoke layer in the carriage is approx. 0.5 m from the ceiling.
34:48	Flames in the front part of the carriage have decreased
45:48	Still no signs of fire spread backwards in the train. Still a distinct smoke layering approx. 0.5 - 1 m above seats (backrest top)
48:00	The fire has burnt through the floor at the place of ignition
61:48	The fire is still limited to the front of the train
69:48	Mostly gray smoke in the gas layer.
1:47:20	Flames visible in the driver compartment
1:47:33	Flames through a window on the right side
1:48:00	It is burning in the driver compartment
1:48:18	Flames from the window on the right side almost in height with train roof
1:49:33	Flames from window on the right side in height with train roof
1:50:00	The cabin bag B28 in position 21 was ignited manually (with the aid of 2 L of Diesel). At the same time the fire fighter observed flames spreading along the ceiling and he exited the carriage.
1:52:03	Flames from window on the right side have increased further, over the train roof and half way to the tunnel wall
1:52:33	Flames have spread on the right train wall beneath the broken window on the right side
1:53:03	Flames from a broken window on the left side
1:53:33	Flames on the right side now reaches approx. 1 m over the train roof and flames on the right side reaches up to the roof
1:54:03	Flames reach the tunnel wall on the right side
1:54:48	Flames reach the tunnel wall also on the left side
1:55:03	Backlayering of smoke begins
1:55:33	Heavy fire around the front of the train carriage. Smoke starts to spread ahead of the train. Smoke layer in the tunnel approx. 1 m above the train roof.
1:56:03	Heavy pulsation
1:56:33	Pulsation has increased further and flames collides with the tunnel walls.
1:57:28	Right front window breaks
1:57:33	Smoke layer upstream of the train and the lowering towards the ground. Smoke layer height at approx. train roof. Flame pulsation through the broken (right) front window.
1:57:48	The speed of the fan is increased to 2500 rpm).
1:58:18	Left front window breaks. Flame pulsation from both front windows.
1:58:19	The speed of the fan is increased again (to 3000 rpm).
1:58:33	Fire seams more intense than in test 2. Might be because of the flame pulsation through the front windows.
1:59:30	The smoke (backlayering) was pushed back
1:59:33	Pulsation has decreased somewhat.
2:00:45	Blue flames were observed
2:02:33	Further decrease in pulsation
2:02:55	The speed of the fan is decreased to 2500 rpm.
2:04:33	Further decrease in pulsation
2:08:33	Pulsation almost gone

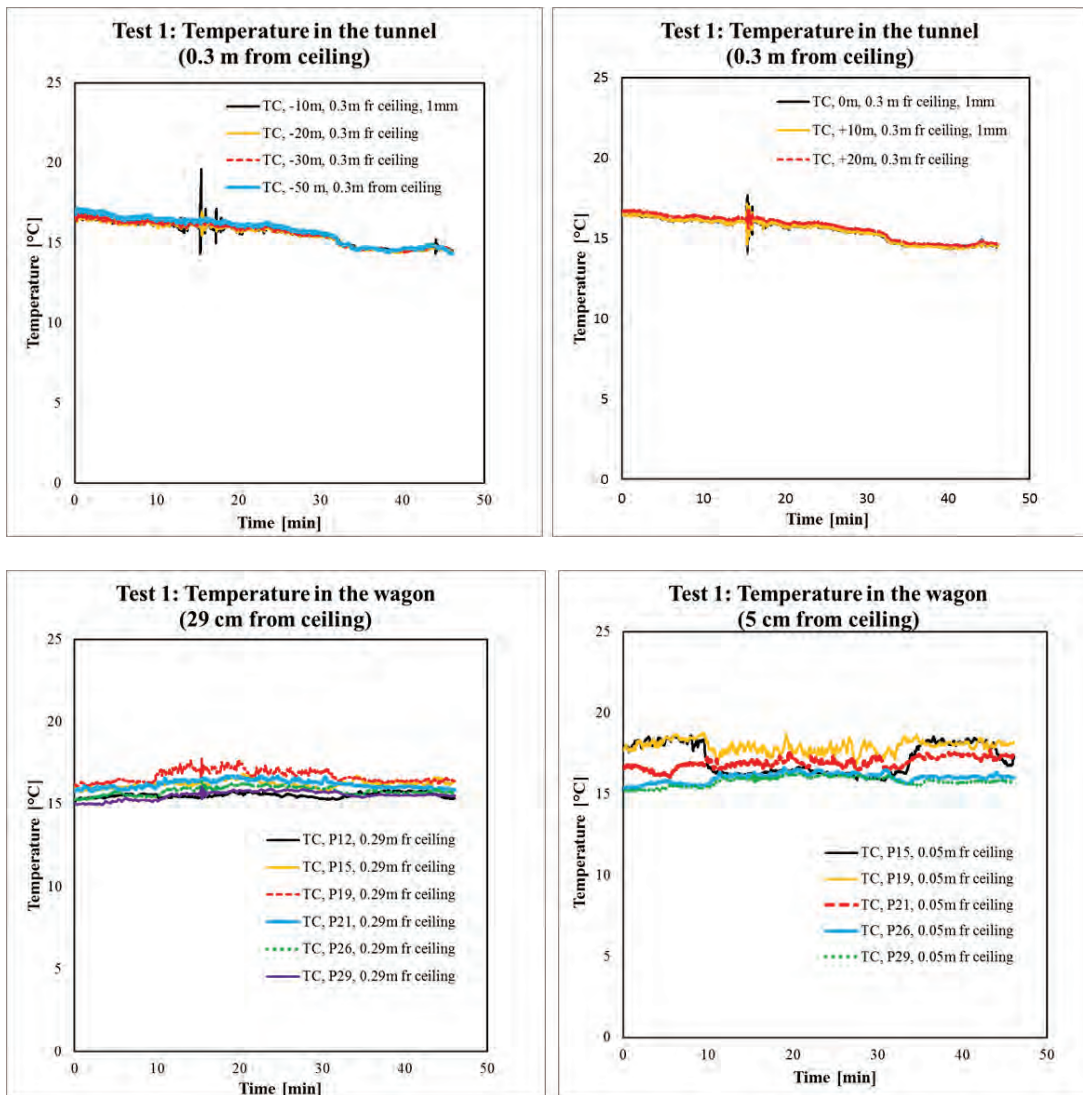
Time ign [h:min:ss]	Observation and description
2:09:33	The fire still have some tendencies to pulsate, but very weak.
2:09:40	The smoke is at the carriage
2:10:05	The smoke is behind the carriage
2:10:33	Pulsation stopped
2:12:25	The speed of the fan was decreased (to 2000 rpm).
2:13:38	The speed of the fan was increased (to 2250 rpm).
2:15:00	It is burning to the left of the carriage
2:35:15	The speed of the fan was decreased (to 1000 rpm).
	It is burning in a tube in front of (coming from) the carriage
2:41:00	The fan was stopped
2:44:25	The fan was turned on again

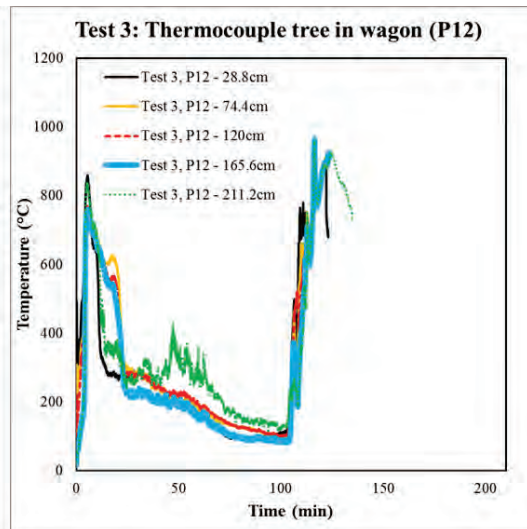
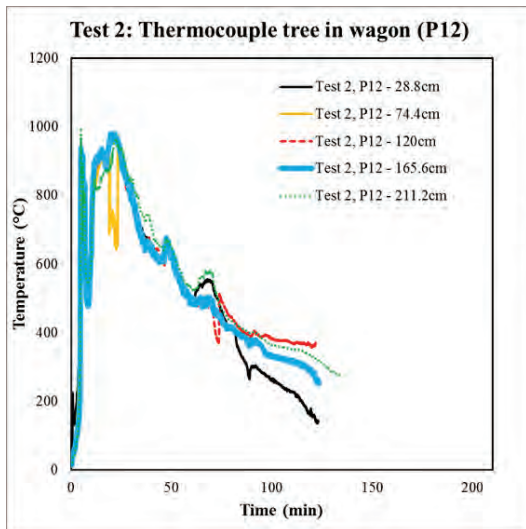
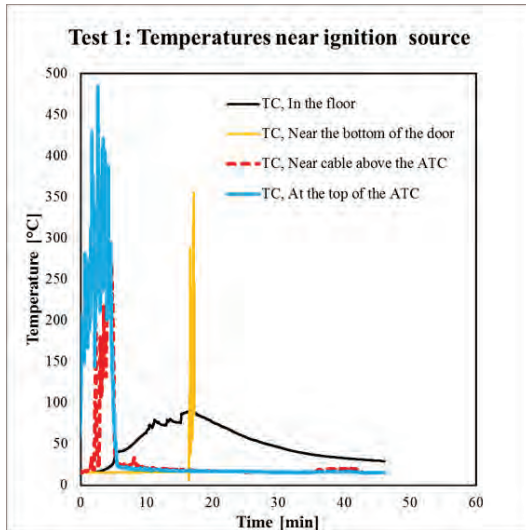
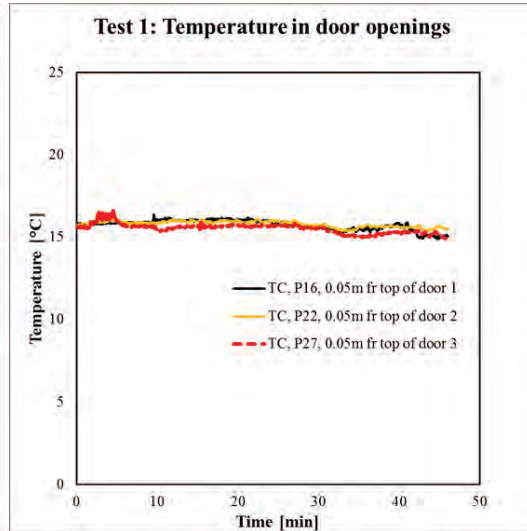
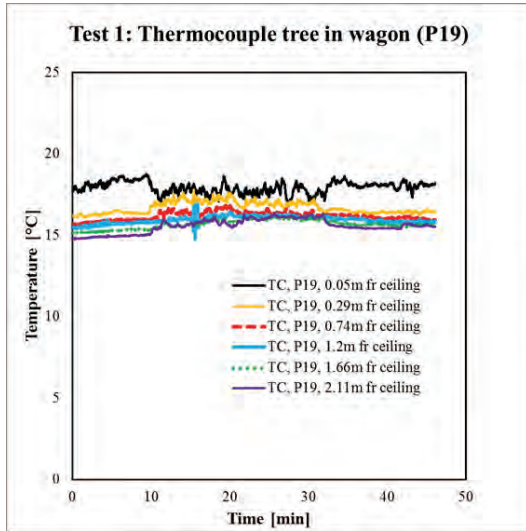
Next morning it was still burning in some of the wooden cross-tie downstream of the carriage.

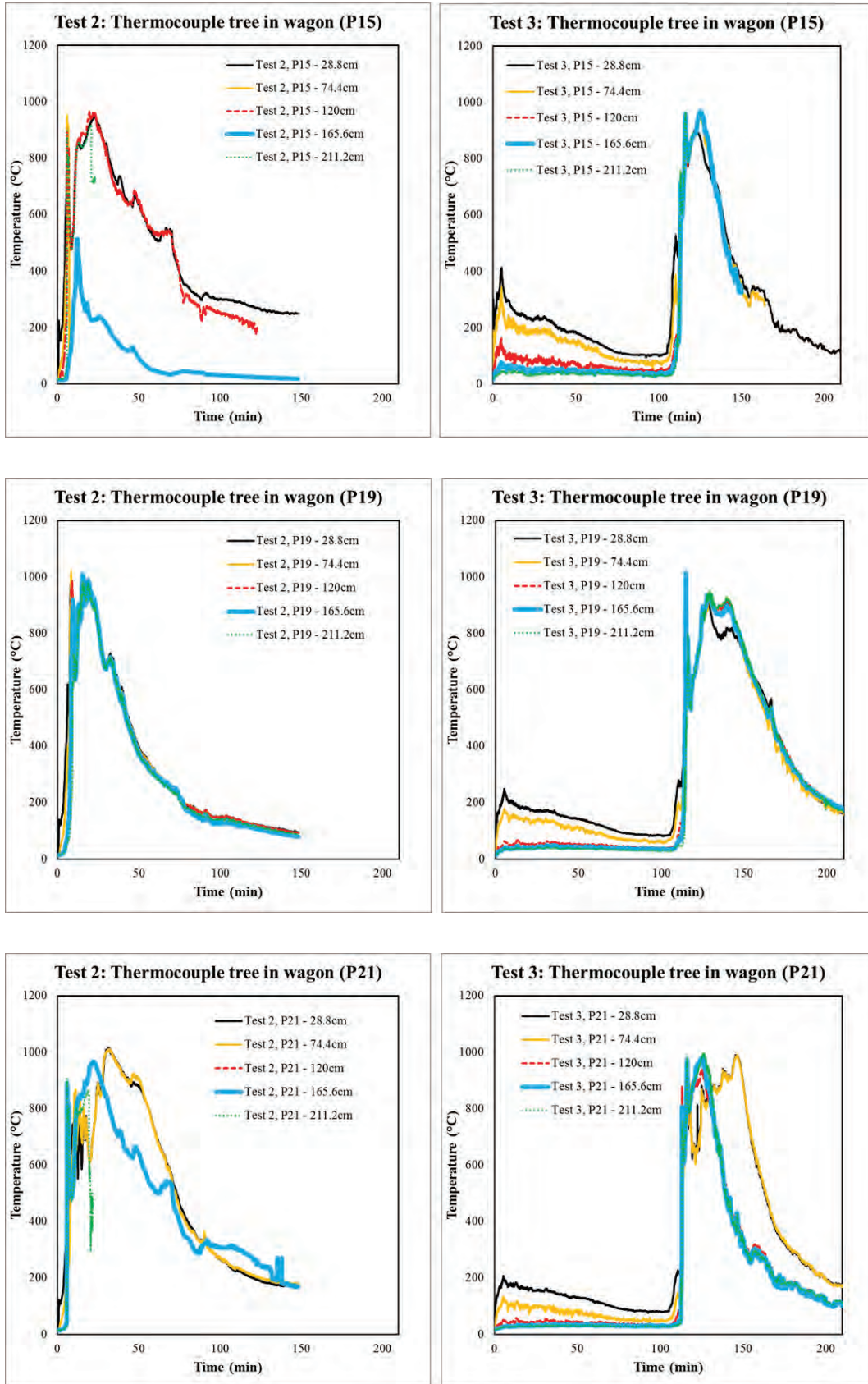
Appendix 2 – Test Results

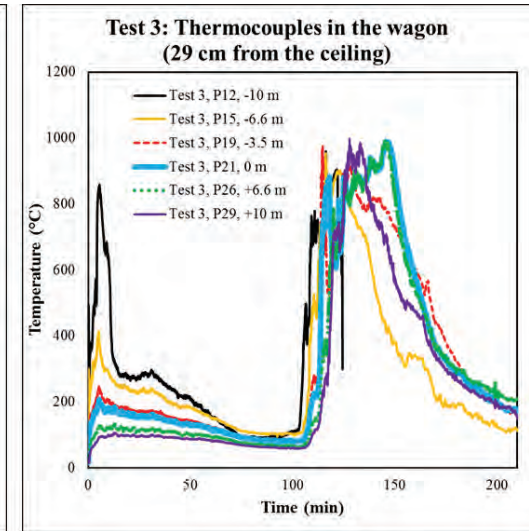
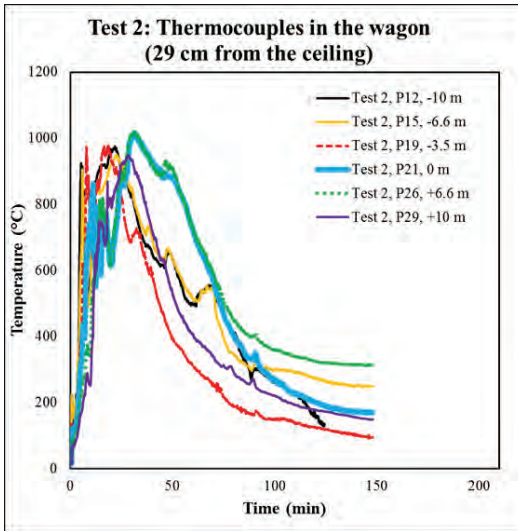
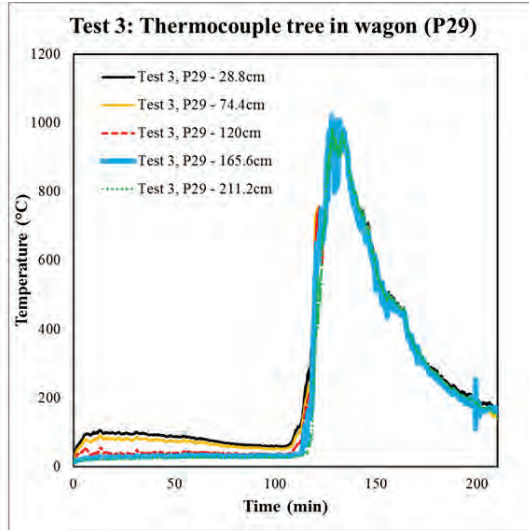
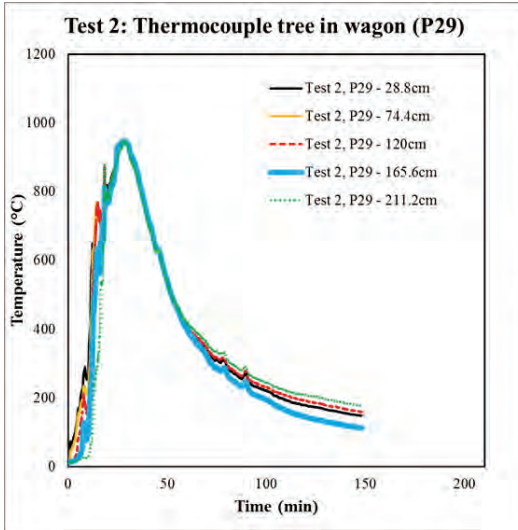
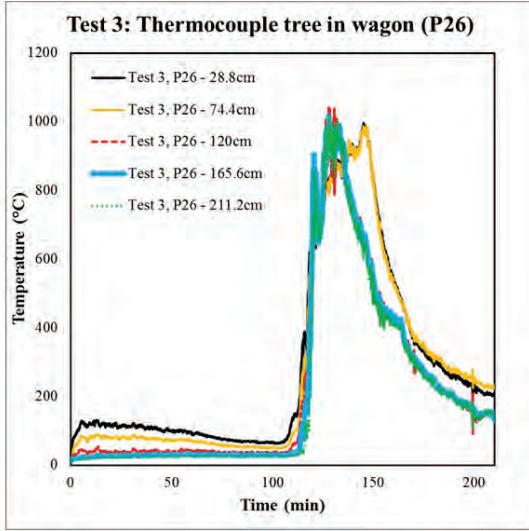
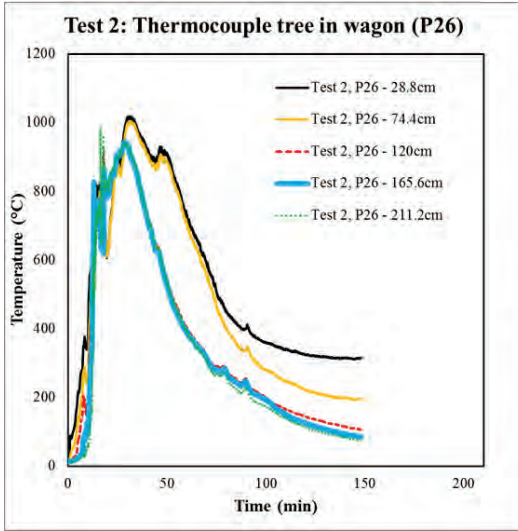
Measurement data have been logged for approx. 150 min in test 2 and 220 min in test 3. However, several measurement points have reported void data. This means that some of the results presented below are only from parts of the test period. The graphs are presented one parameter (gas temperatures, plate thermometer temperatures, gas concentrations and air velocities) at a time. In test 1, only four temperature measurements are of particular interest and they are presented first. Then follows a comparison between test 2 and test 3 for each position and each parameter.

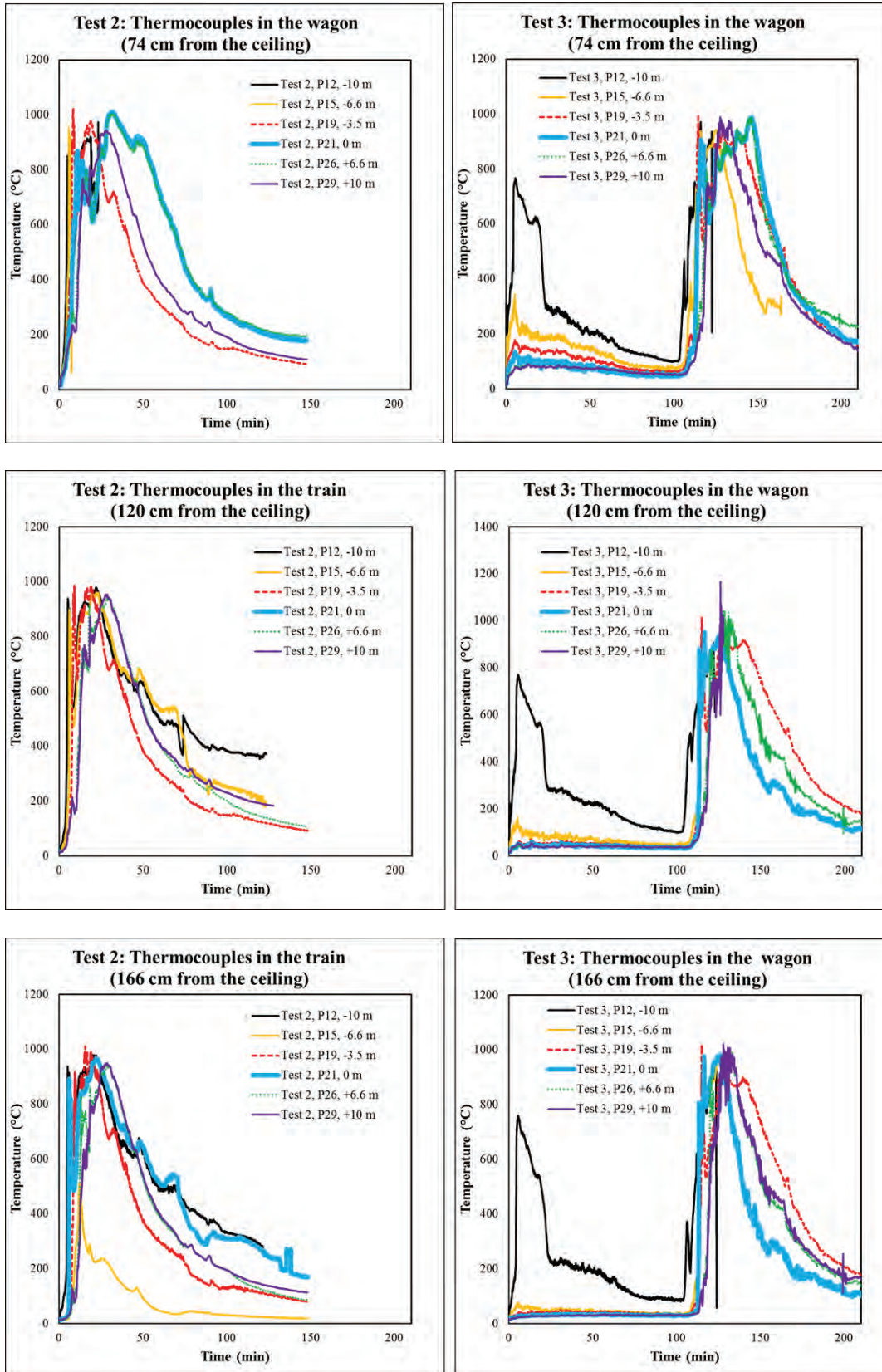
Temperature

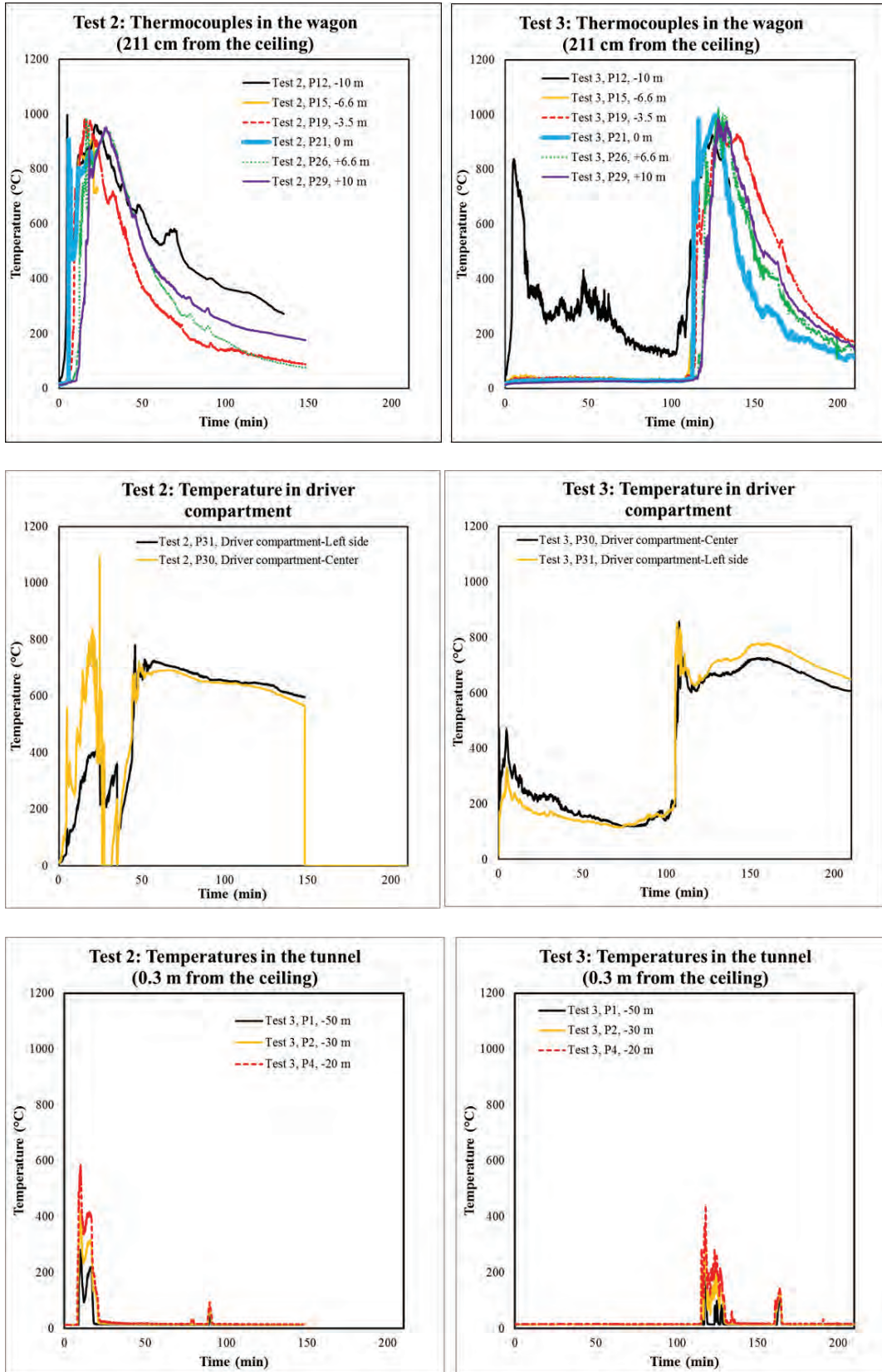


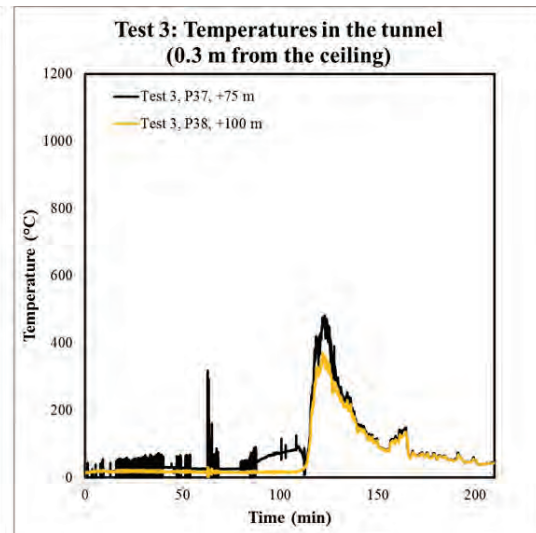
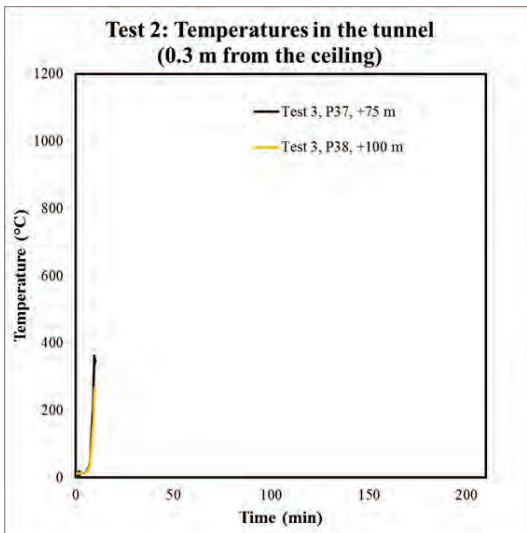
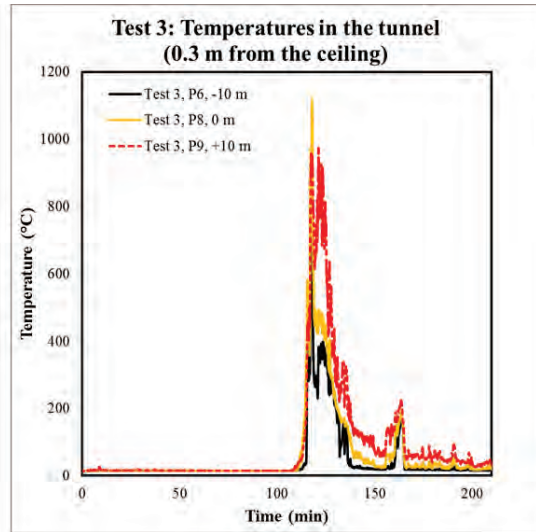
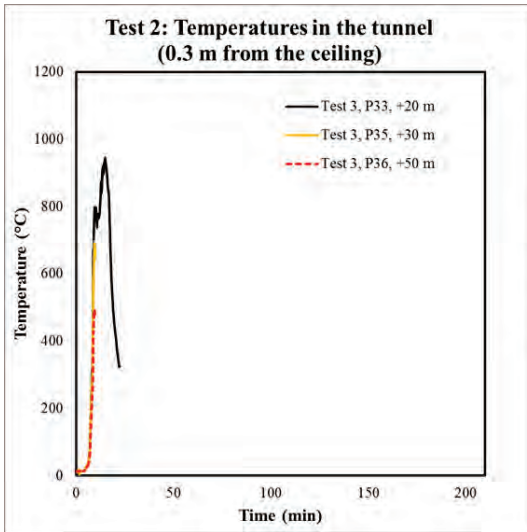
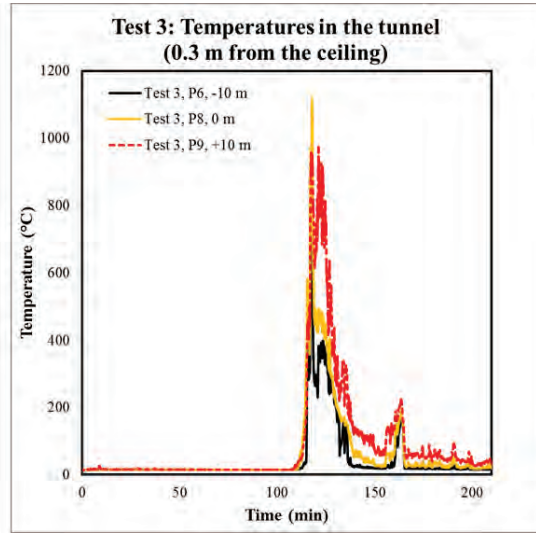
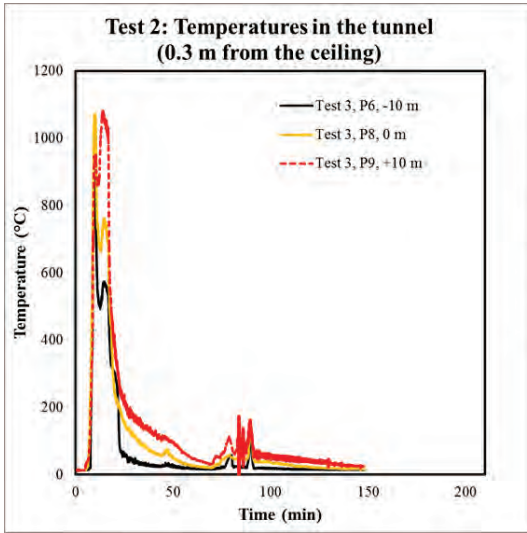


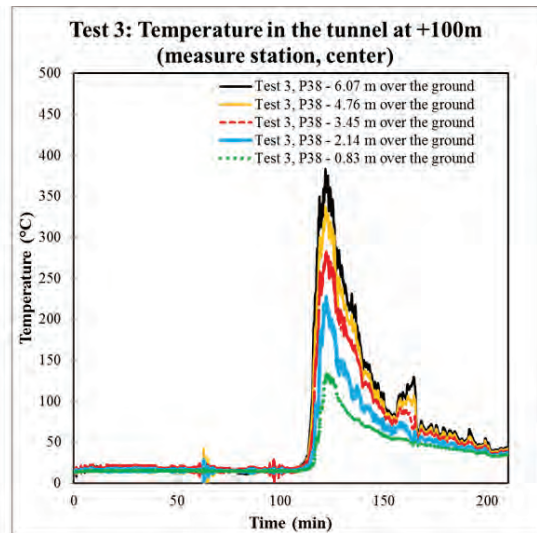
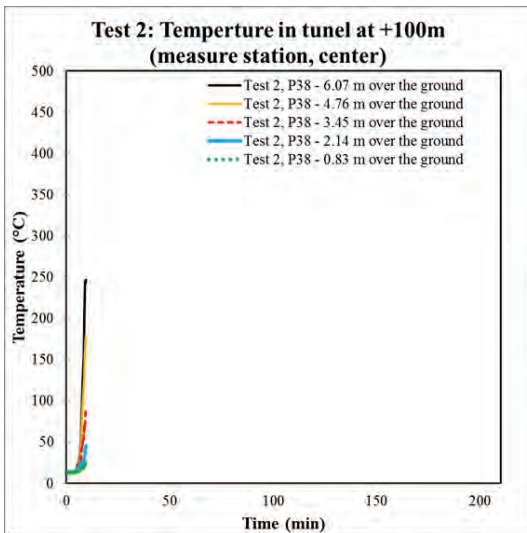
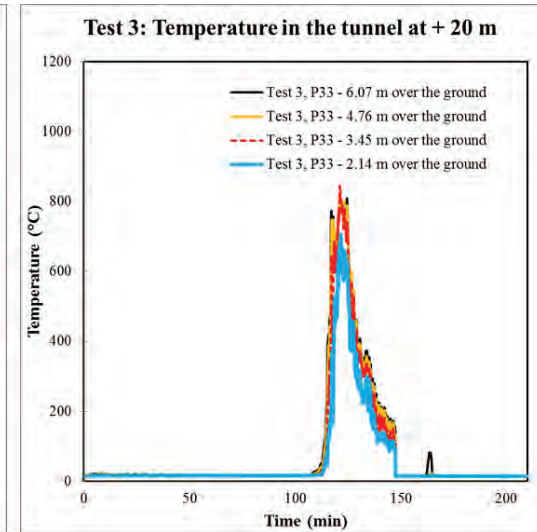
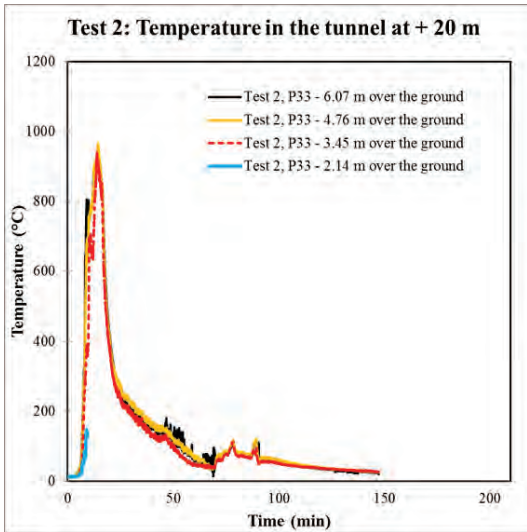
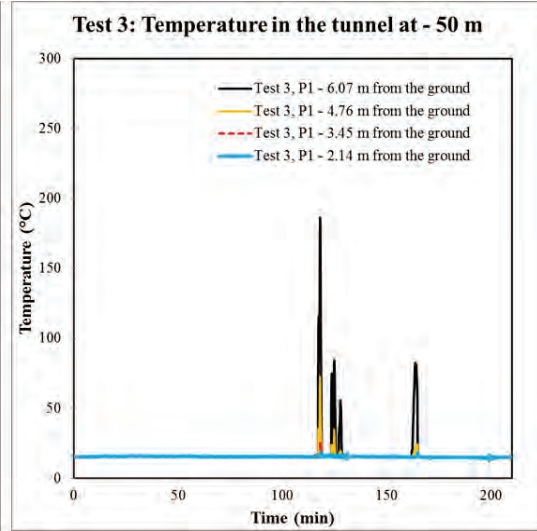
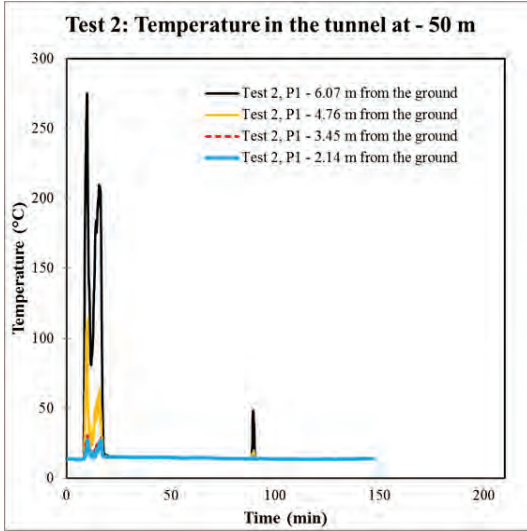












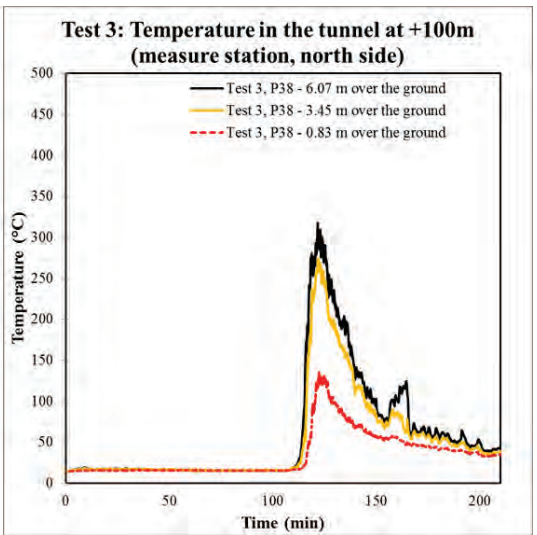
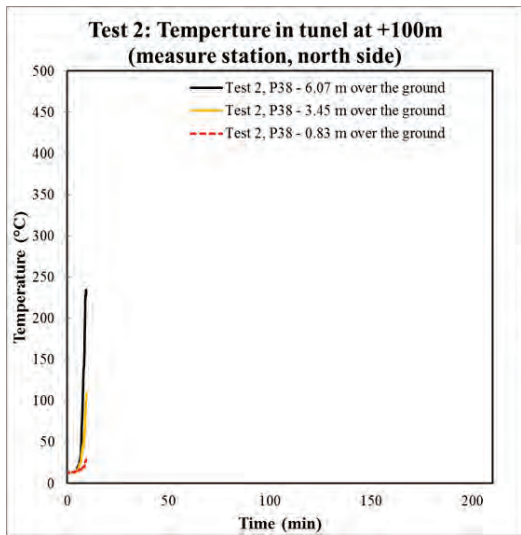
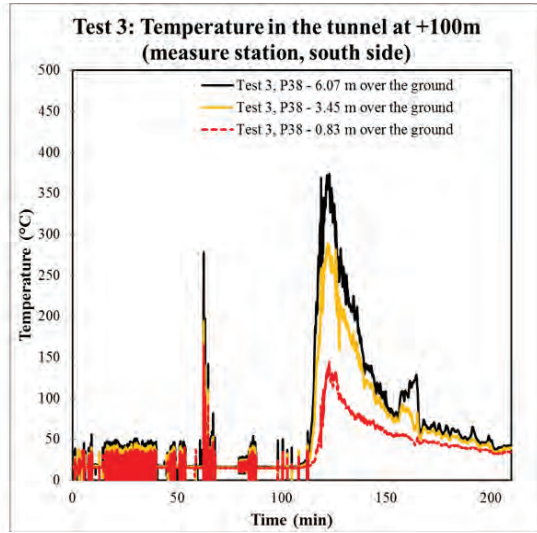
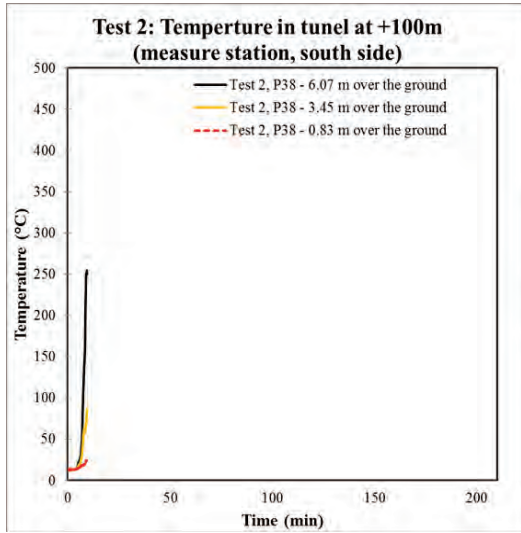
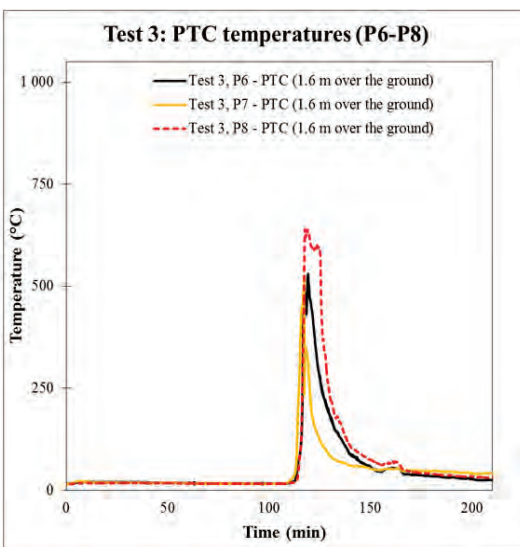
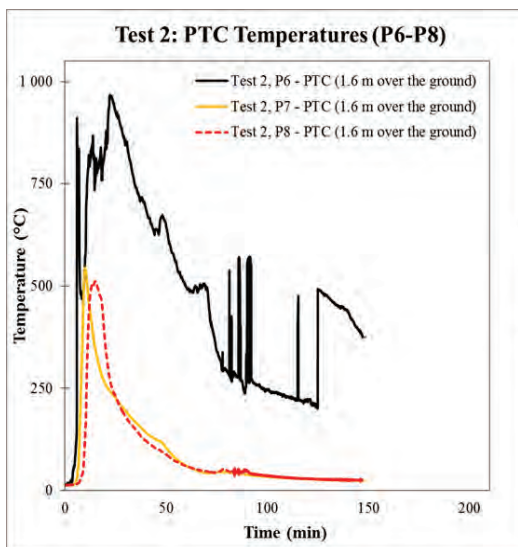
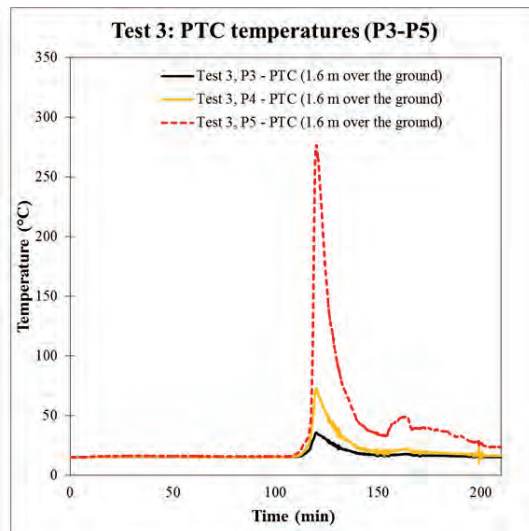
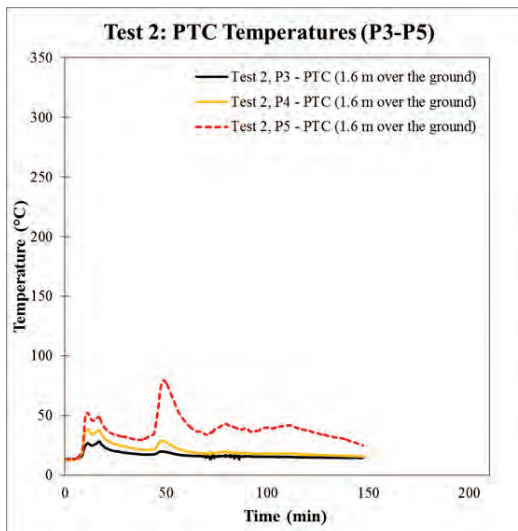
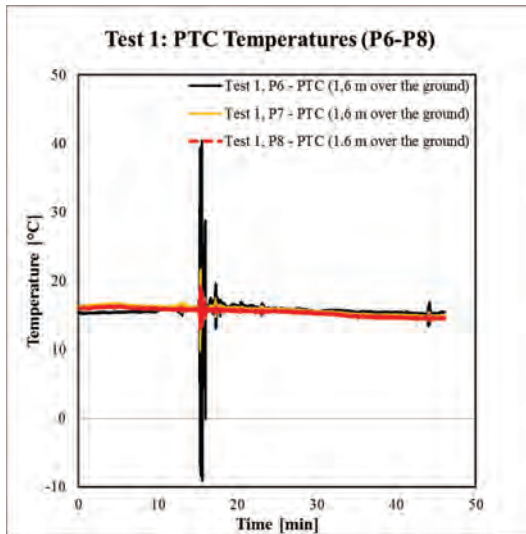
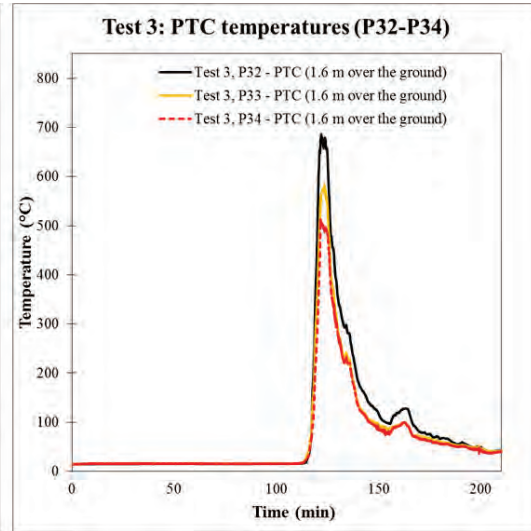
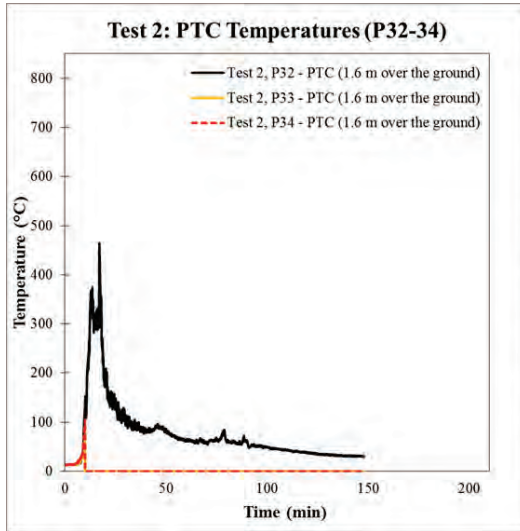
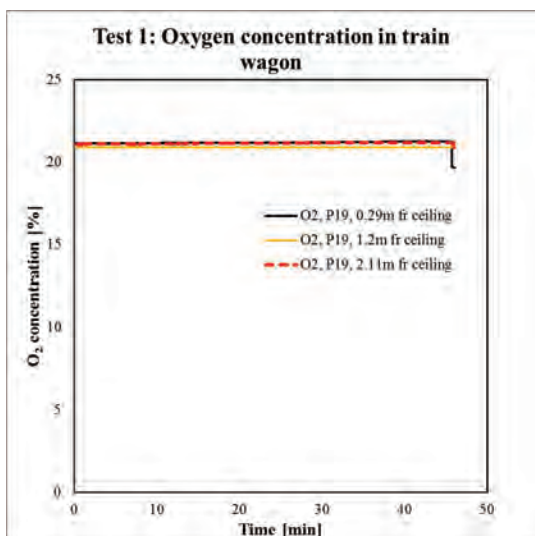
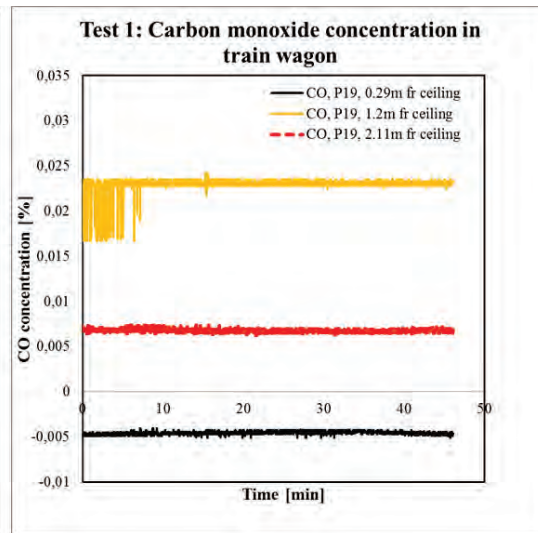
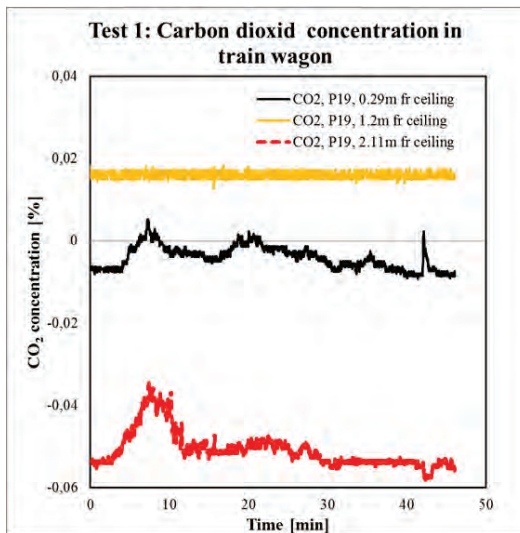


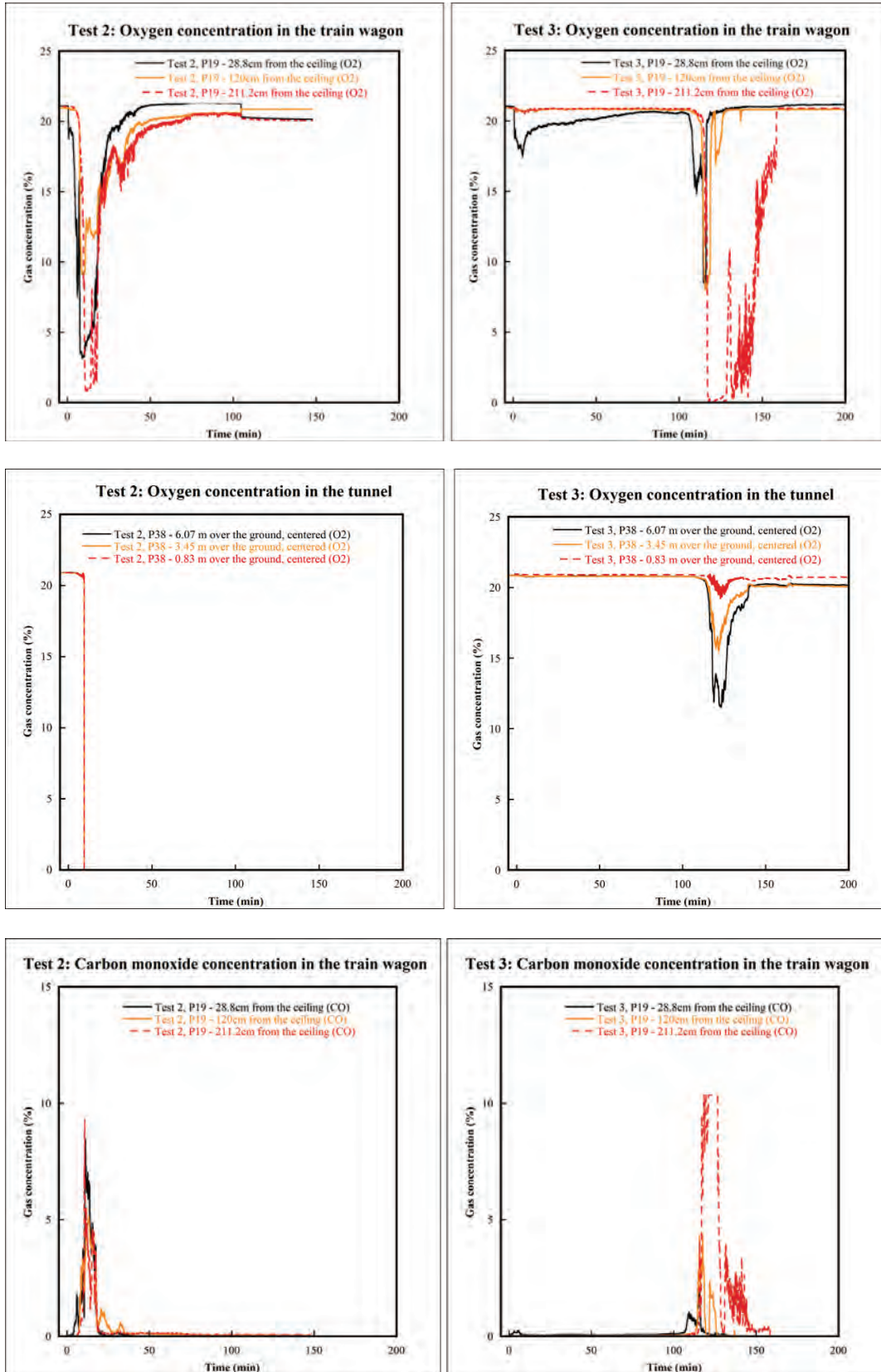
Plate thermometers

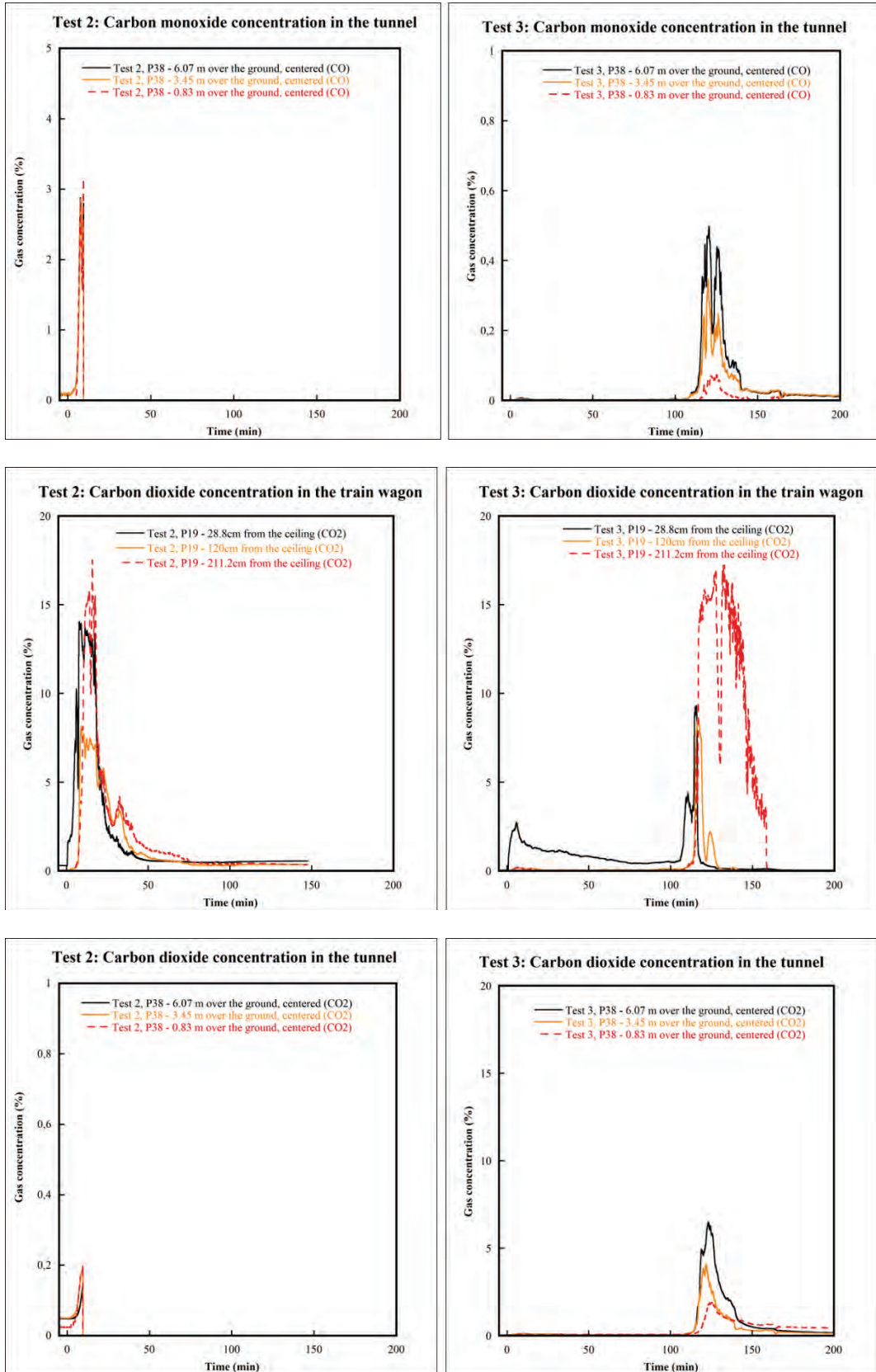




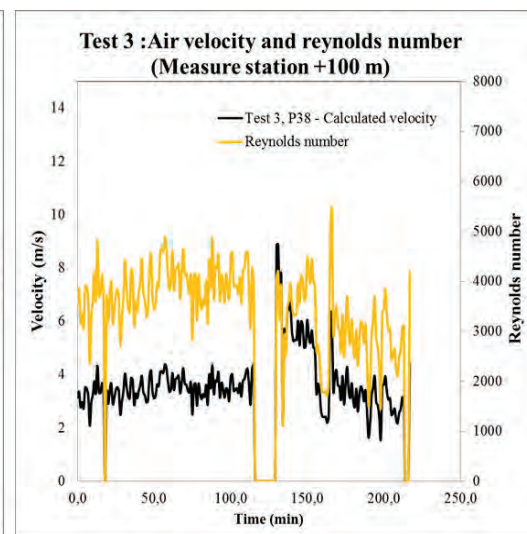
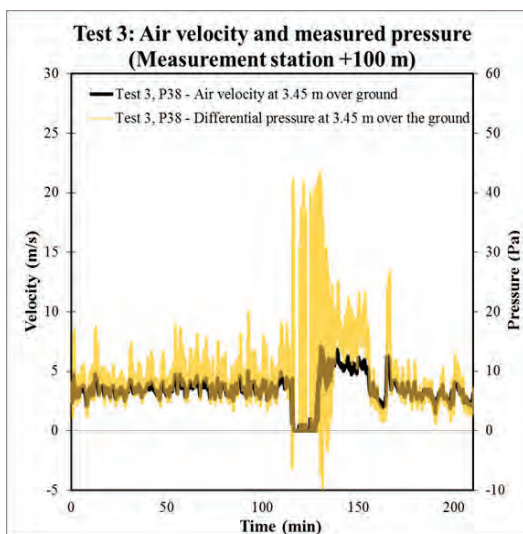
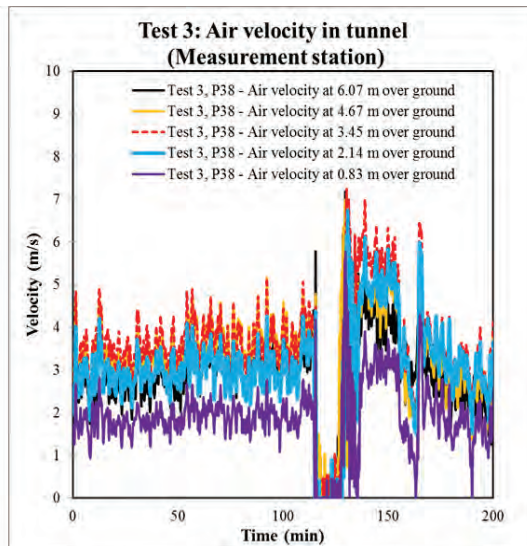
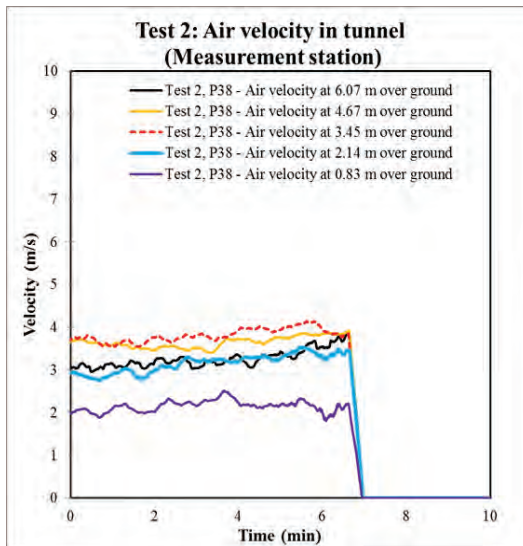
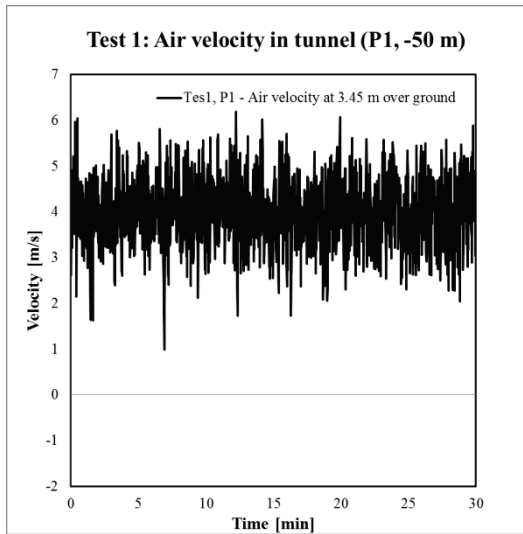
Gas concentrations

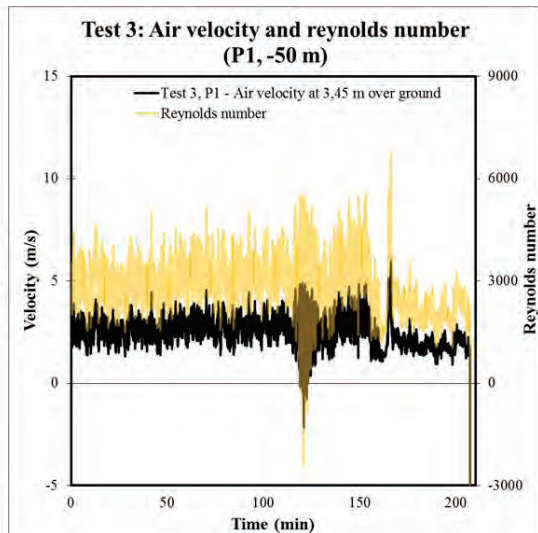
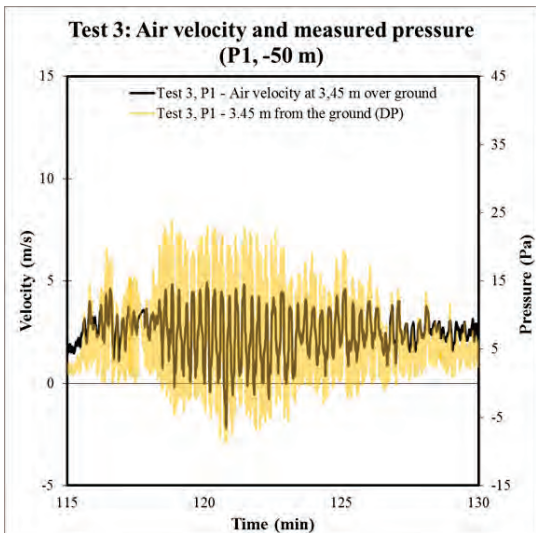
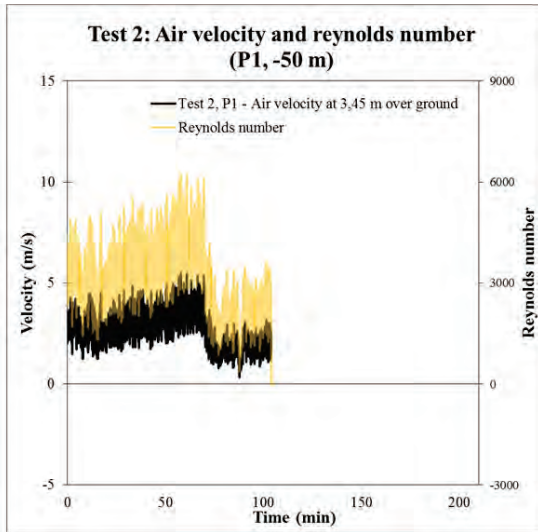
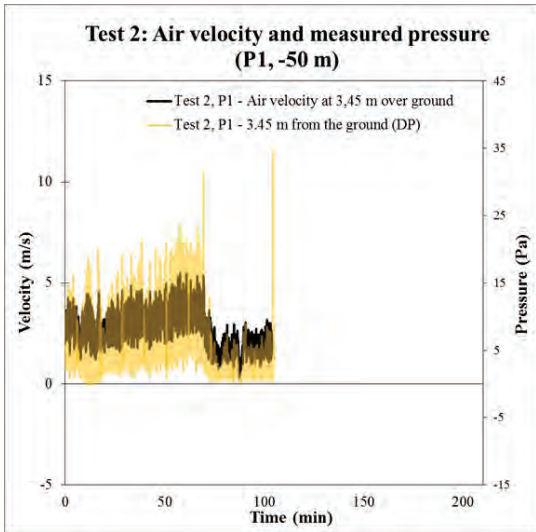
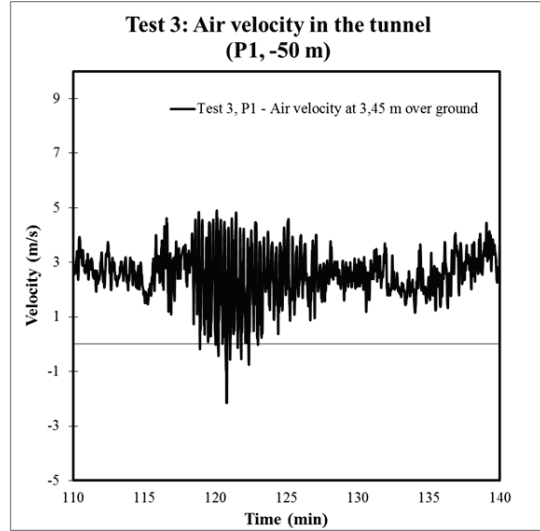
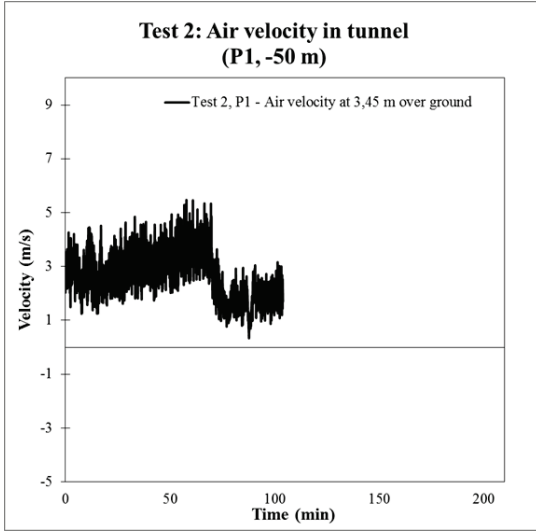






Air velocity in the tunnel





Appendix 3 – Drawings

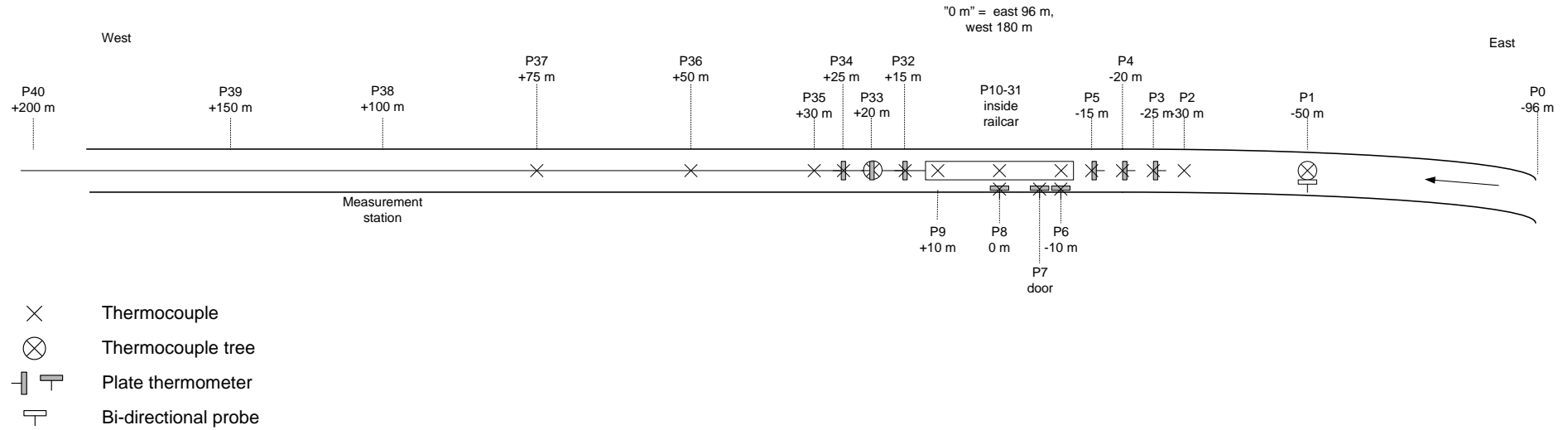


Figure A3.1 Measurement positions and types of measurements used during the tests. Detailed drawings of the measurements at the measurements station and inside the carriage are shown in Figure A3.2 and A3.3, respectively.

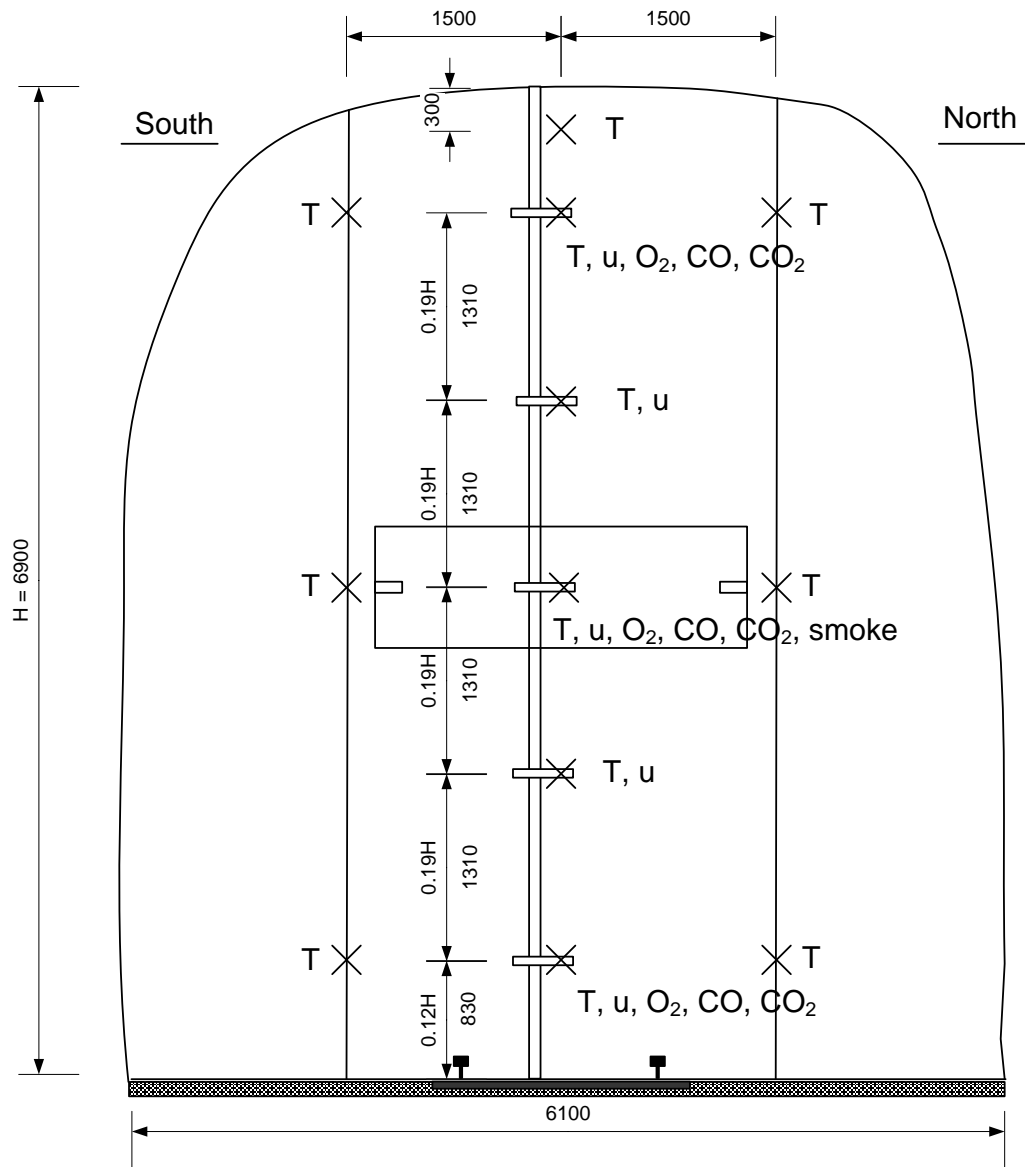


Figure A3.2 Instrumentation at the measurement station 100 m downstream of the fire, P38.

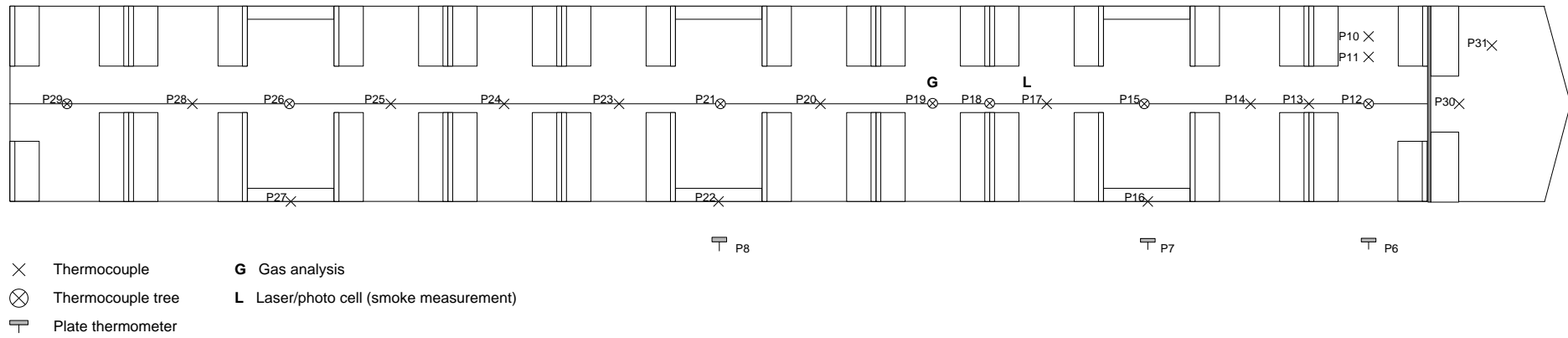


Figure A3.3 Instrumentation of the railway carriage.

Appendix 4 – Photos from the tests

Test 1



Figure A4.1 Flames from the heptane pool shortly after ignition in test 1.(Photo: Per Rohlén)



Figure A4.2 Flames from the heptane pool a few minutes after ignition in test 1.(Photo: Anders Lönnermark)



FigureA4.3 Flames from the ATC receiver and after the heptane was burnt in test 1
(Photo: Anders Lönnermark)

Test 2



Figure A4.4 The ignition set up in test 2. The milk cartridge was filled with one liter of petrol and the three small fiber board pieces was lit. The petrol was ignited by pulling the string (Photo: Per Rohlén)



Figure A4.5 Flames shortly after ignition in test 2. (Photo: Per Rohlén)



Figure A4.6 Flames from the windows on the right side of the carriage approx. 4 min after ignition.
(Photo: Per Rohlén)



Figure A4.7 Left picture: Flames from the windows on the left side of the carriage approx. 4 min after ignition. (Photo: Per Rohlén)
 Right picture: Flames form the carriage approx. 7 min after ignition. The backlayering can be seen in the ceiling of the tunnel. (Photo: Per Rohlén)



Figure A4.8 Flames from the carriage approx. 20 min after ignition. Most of the carriage is now on fire but the driver compartment is still intact. (Photo: Per Rohlén)



Figure A4.9 Flames from the carriage approx. 45 min after ignition, the driver compartment is now on fire and the right window is broken. (Photo: Per Rohlén)



Figure A4.10 The flames from the carriage in the beginning of the decay period. The picture is taken approx. 50 min after ignition. (Photo: Per Rohlén)



Figure A4.11 The remains of the carriage after test 2. (Photo: Per Rohlén)



Figure A4.12 The remains of the carriage after test 2. (Photo: Per Rohlén)

Test 3



Figure A4.13 Left picture: Picture form inside the carriage shortly after ignition. (Photo: Per Rohlén)
Right picture: The fire has started to spread from the ignition source to the surrounding bags, picture is taken approx. 1 – 2 min after ignition. (Photo: Per Rohlén)



Figure A4.14 There was a long fire growth period in test 3. This picture is taken approx. 40 min after ignition and the fire has still not spread any further than between the seats were it was lit. (Photo: Per Rohlén)



Figure A4.15 This picture shows the first flames outside of the carriage, the picture is taken approx. 1 h 50 min after ignition. In contrast to test 2 the first flames exit from the driver compartment. (Photo: Per Rohlén)



Figure A4.16 Flames from the carriage approx. 1h 55 min after ignition (Photo: Per Rohlén)



Figure A4.17 Flames from the carriage approx. 1h 57 min after ignition. The fire is now growing rapidly. From the picture it is also possible to see the emerging backlayering. (Photo: Per Rohlén)



Figure A4.18 This picture shows the flame pulsations from the carriage, the picture is taken approx. 2 h after ignition. (Photo: Per Rohlén)



Figure A4.19 This picture is from the beginning of the decay period approx. 2 h 5 min after ignition. (Photo: Per Rohlén)



Figure A4.20 The remains of the carriage after test 3. (Photo: Per Rohlén)



Figure A4.21 The remains of the carriage after test 3. (Photo: Per Rohlén)

Luggage

Below examples of the different types of bag used in the tests are presented.

Test 2



Figure A4.22 Examples of large duffel bags and suitcases used in test 2, each with a total mass of 14 kg.



Figure A4.23 Examples of middle sized bags used in test 2, each with a total mass of 10 kg.



Figure A4.24 Examples cabin bags used in test 2, each with a total mass of 5.3 kg.



Figure A4.25 Examples of sports/shoulder bags and backpacks used in test 2, each with a total mass of 3 kg.

Test 3



Figure A4.26 Examples of large duffel bags and suitcases used in test 3, each with a total mass of 14 kg.



Figure A4.27 Examples of middle sized bags used in test 3, each with a total mass of 10 kg.



Figure A4.28 Examples cabin bags used in test 3, each with a total mass of 5.3 kg.



Figure A4.29 Examples of sports/shoulder bags and backpacks used in test 2, each with a total mass of 3 kg.

Appendix 5 – Results from material tests

Selected pieces of material from the interior and furniture of the carriages were tested with small scale methods in order to compare the results to the classification according to the technical specification CEN/TS 45545-2:2009. The description of the experiments and the results were described in a separate test report which is included in this Appendix.

CEN/TS 45545-2:2009 Railway applications - Fire protection on railway vehicles - Part 2: Requirements for fire behavior of materials and components

(6 appendices)

Introduction

A series of full scale fire tests on train have been conducted in the project "METRO" and in connection to this it is of interest to know what classification the interior and furniture of the trains tested would achieve according to technical specification CEN/TS 45545-2:2009. In order to estimate the classification a number of materials from the trains have been tested using small scale fire test methods; ISO 5658-2, ISO 5659-2, ISO 5660-1 and ISO 9239-1. Fire behaviour of passenger seats in full scale was evaluated according to CEN/TS 45545-2:2009, Annex B.

Procedure for classification

References in parenthesis, e.g. (table 4) refer to clauses in CEN/TS 45545-2:2009. In order to classify the interior and furniture of a train according to CEN/TS 45545-2:2009, the interior and furniture products are divided into different product groups called "product number", e.g. "IN1", "F1A". The product numbers are each connected to different requirement sets, e.g. "R1", "R2" (table 4). Each requirement set stipulates test methods and test parameters for fire testing and also what classification criteria need to be achieved (table 7). Classification criteria are divided into three Hazard Levels; HL1, HL2 and HL3. The three Hazard Levels have been determined using a product of the relation between operation categories and design categories, defined in CEN/TS 45545-1:2009. Operation categories and design categories are defined by type of train and operation conditions for the train, definitions are reproduced in appendix no 6.

Table 1 - Hazard Levels versus Operation Categories and Design Categories

	Design Category			
Operation Category	N: Standard vehicles	A: Automatic vehicles having no emergency trained staff on board	D: Double decked vehicle	S: Sleeping and couchette cars double decked or single deck
1	HL1	HL1	HL1	HL2
2	HL2	HL2	HL2	HL2
3	HL2	HL2	HL2	HL3
4	HL3	HL3	HL3	HL3

SP Technical Research Institute of Sweden

Postal address
SP
Box 857
SE-501 15 BORÅS
Sweden

Office location
Västerås
Brinellgatan 4
SE-504 62 BORÅS

Phone / Fax / E-mail
+46 10 516 50 00
+46 33 13 55 02
info@sp.se

Laboratories are accredited by the Swedish Board for Accreditation and Conformity Assessment (SWEDAC) under the terms of Swedish legislation. This report may not be reproduced other than in full, except with the prior written approval of the issuing laboratory.

Tested material

Two types of trains were involved in the METRO-project, train type "X1" and a combination of train types "C20" and "X10", in this report referred to as "C20/X10". The "C20/X10" corresponds to interior material, except for the floor, from train type "C20" with ceiling and walls covered with an aluminium layer, passenger seats are from train type "X10". Materials tested in this study were wall linings, floor from "X1" and passenger seats from both train types. Ceiling lining was not tested because of lack of material.



Photo 1 - Interior of "X1"



Photo 2 - Interior of "C20/X10"

Classification “X1”

Test results regarding the furniture and interior of the train called “X1” indicates Hazard Level HL2 for wall lining and Hazard Level HL3/HL1 for passenger seats. The floor did not achieve any Hazard Level due to too high values for CIT_G.

Table 2 - Indicated Hazard Levels

“X1”	Product Number	Requirement Set	Hazard Level
Wall lining	IN1	R1	HL2
Complete passenger seat	F1	R17	HL3
Passenger seat, upholstery	F1A	R20	HL1
Floor	IN16	R9	Not Classified

Classification “C20/X10”

Test results regarding the furniture and interior of the train called “C20/X10” indicates Hazard Level HL3 for wall lining and Hazard Level HL3/HL1 for passenger seats.

Table 3 - Indicated Hazard Levels

“C20/X10”	Product Number	Requirement Set	Hazard Level
Wall lining + Aluminium sheet	IN1	R1	HL3
Complete passenger seat	F1	R17	HL3
Passenger seat, upholstery and back shell	F1A	R20	HL1
Floor	Not tested because of lack of material.		

On the following pages conducted tests and compilation of test results are reported. Detailed test results are reported in the appendices of this document.

Conducted tests and compilation of test results - wall lining, “X1”

Wall lining consisting of, nearest to the cabin, 3 mm laminate with 36 mm insulation layer behind.

Conducted tests indicate that classification according to CEN/TS 45545-2:2009 would be HL2.



Photo 3 - "X1", wall lining

Table 4 - Test methods, parameters, classification criteria and test results

Test method	Parameter	Classification Criteria			Test results			Average (of two)
		HL1	HL2	HL3	Test 1	Test 2	Test 3	
ISO 5658-2	CFE, min	20	20	<u>20</u>	>51 ¹⁾	39 ¹⁾	50 ²⁾	-
EN ISO 5659-2: 50 kW/m ² without pilot flame	D _S (4), max	600	<u>300</u>	150	167	174	-*	171
	VOF4, max	1200	<u>600</u>	300	340	384	-*	362
	CIT _G 4, max	1.2	0.9	<u>0.75</u>	0.11	0.16	-*	0.14
	CIT _G 8, max	1.2	0.9	<u>0.75</u>	0.33	0.41	-*	0.37
ISO 5660-1: 50 kW/m ²	MARHE, max	-	90	<u>60</u>	40	31	-*	36

¹⁾ Because of limited access to test material, test was conducted with laminate layer only.

²⁾ Test conducted with laminate layer and insulation layer.

* Test not conducted.

Conducted tests and compilation of test results - passenger seat, "X1"

The seat consisted of, from the top; fabric 3 mm, foam for seat 60 mm, foam for backrest 12-25 mm, cork wood 9 mm and painted wooden board 4 mm. Downwards facing surfaces and also vertical surfaces where covered with steel sheet why only the upwards facing surface need to be tested.

Conducted tests indicate that classification according to CEN/TS 45545-2:2009 would be HL1.



Photo 4 - "X1", passenger seat



Photo 5 - "X1", material composition of passenger seat

Table 5 - Test methods, parameters, classification criteria and test results

Test method	Parameter	Classification Criteria			Test results			Average (of two)
		HL1	HL2	HL3	Test 1	Test 2	Test 3	
Full scale passenger seat: CEN/TS 45545-2:2009, Annex B: 7 kW								
	MARHE, max	75	50	<u>20</u>	8	-*	-*	-
Upholstery: EN ISO 5659-2: 25 kW/m ² with pilot flame								
	D _s , max	600	<u>300</u>	150	289	299	-*	294
	CIT _G 4, max	1.2	0.9	<u>0.75</u>	0.32	0.10	-*	0.21
	CIT _G 8, max	1.2	0.9	<u>0.75</u>	0.72	0.25	-*	0.49
ISO 5660-1: 25 kW/m ²								
	MARHE, max	<u>75</u>	50	50	62	58	-*	60

* Test not conducted.

Conducted tests and compilation of test results - wall lining, "C20/X10"

Wall lining consisting of, nearest to the cabin, 1 mm aluminium sheet on a 3 mm laminate with 36 mm insulation layer behind.

Testing according to ISO 5658-2 "Surface Spread of Flame" has not been conducted since the aluminium surface obviously would not maintain any flame spread. Testing according to EN ISO 5659-2 and ISO 5660 was conducted with one single test per method, only to confirm the assumption that a metallic cover would protect the material for the test time 20 minutes and there would be small, barely detectable reactions of the materials included in the tests.

Conducted tests indicate that classification according to CEN/TS 45545-2:2009 would be HL3.

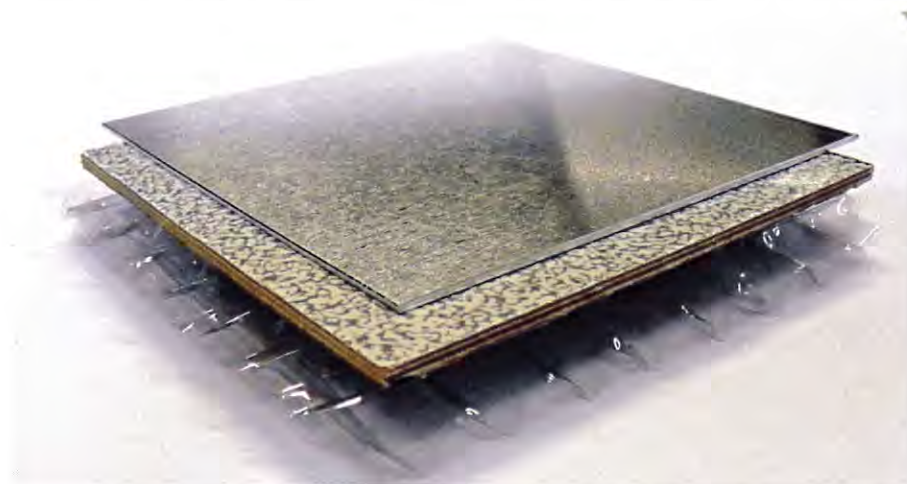


Photo 6 - "C20/X10", wall lining + 1 mm aluminium sheet.

Table 6 - Test methods, parameters, classification criteria and test results

Test method	Parameter	Classification Criteria			Test results			Average
		HL1	HL2	HL3	Test 1	Test 2	Test 3	
ISO 5658-2	CFE, min	20	20	20	-*	-*	-*	-
EN ISO 5659-2: 50 kW/m ² without pilot flame	D _S (4), max	600	300	<u>150</u>	0.4	-*	-*	-
	VOF4, max	1200	600	<u>300</u>	1.1	-*	-*	-
	CIT _G 4, max	1.2	0.9	<u>0.75</u>	0	-*	-*	-
	CIT _G 8, max	1.2	0.9	<u>0.75</u>	0	-*	-*	-
ISO 5660-1: 50 kW/m ²	MARHE, max	-	90	<u>60</u>	0.5	-*	-*	-

* Test not conducted

Conducted tests and compilation of test results - passenger seat, "C20/X10"

The material composition of the seat consisted of, from the top; fabric 4 mm, foam for seat 75-120 mm, foam for backrest 30-40 mm and corrugated plastic board 3 mm.

Conducted tests indicate that classification according to CEN/TS 45545-2:2009 would be HL1.



Photo 7 - "C20/X10", passenger seat



Photo 8 – “C20/X10”, Upholstery, material composition of passenger seat*



Photo 9 - "C20/X10", back shell, material composition of passenger seat*

* Picture showing principle of specimen, the foam in the specimens tested had overall the same thickness.

Table 7 - Test methods, parameters, classification criteria and test results

Test method	Parameter	Classification Criteria			Test results			Average (of two)
		HL1	HL2	HL3	Test 1	Test 2	Test 3	
Full scale passenger seat: CEN/TS 45545-2:2009, Annex B: 7 kW	MARHE, max	75	50	<u>20</u>	16	-*	-*	-
Upholstery: EN ISO 5659-2: 25 kW/m ² with pilot flame	D _S , max	600	<u>300</u>	150	156	168	-*	162
	CIT _G 4, max	1.2	0.9	<u>0.75</u>	0.17	0.19	-*	0.18
	CIT _G 8, max	1.2	0.9	<u>0.75</u>	0.26	0.31	-*	0.29
ISO 5660-1: 25 kW/m ²	MARHE, max	75	50	<u>50</u>	45	42	-*	44
Backshell: EN ISO 5659-2: 50 kW/m ² without pilot flame	D _S (4), max	<u>600</u>	300	150	301	321	-*	311
	VOF4, max	1200	<u>600</u>	300	336	373	-*	355
	CIT _G 4, max	1.2	0.9	<u>0.75</u>	0.02	0.02	-*	0.02
	CIT _G 8, max	1.2	0.9	<u>0.75</u>	0.04	0.08	-*	0.06
ISO 5660-1: 50 kW/m ²	MARHE, max	-	90	60	89	100	-*	95

* Test not conducted.

Conducted tests and compilation of test results - floor, "X1"

Floor consisting of, nearest to the cabin, 2.5 mm PVC carpet glued onto 11 mm plywood. Under the plywood, insulation consisting of approx. 40 mm Styrofoam.

Conducted tests indicate that the floor would not achieve any classification due to too high CIT_G.

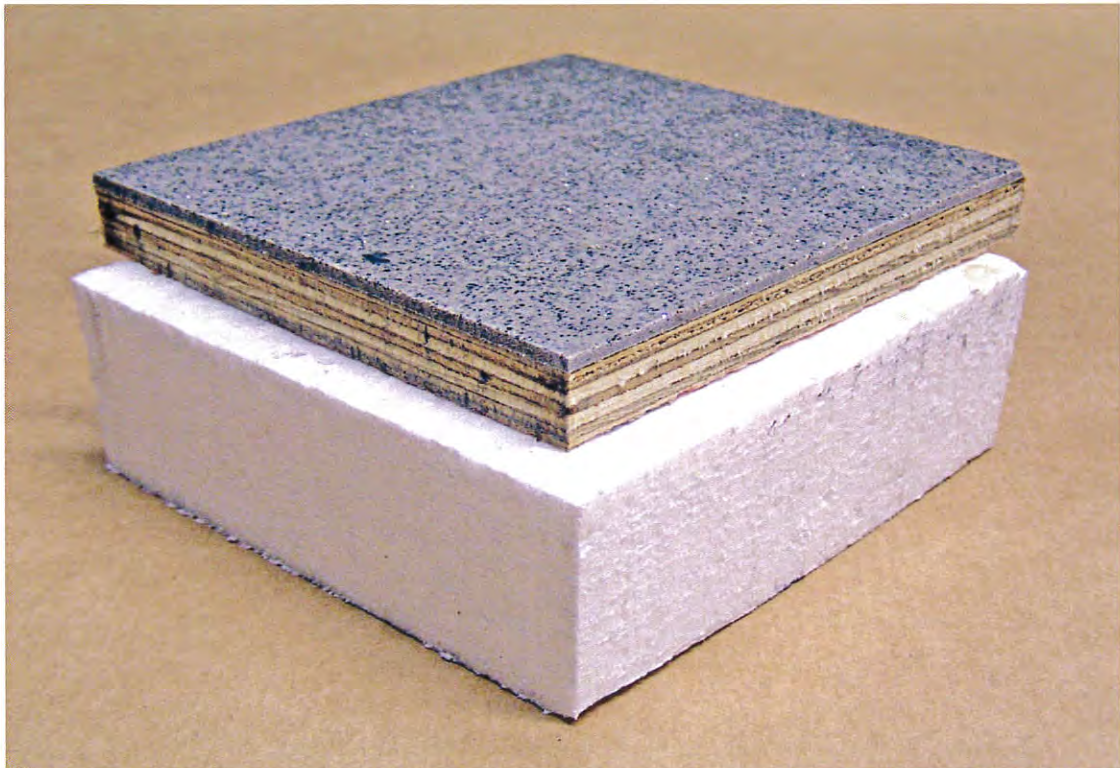


Photo 10 - "X1", floor

Table 8 - Test methods, parameters, classification criteria and test results

Test method	Parameter	Classification Criteria			Test results			Average (of two)
		HL1	HL2	HL3	Test 1	Test 2	Test 3	
EN ISO 5659-2: 50 kW/m ² without pilot flame	D _s , max	<u>600</u>	300	150	404	421	-*	413
	CIT _G 4, max	1.2	0.9	0.75	4.63	5.97	-*	5.30
	CIT _G 8, max	1.2	0.9	0.75	5.67	7.17	-*	6.42
ISO 5660-1: 50 kW/m ²	MARHE, max	-	50	50	61	61	-*	61
EN ISO 9239-1	CHF, min	4.5	6	<u>8</u>	11	10	-*	11

* Test not conducted.

Notes

It is not known to SP Fire Technology if the materials tested are representative of the mean production characteristics.

The test results relate only to the behaviour of the materials under the particular conditions of the test and they are not intended to be the sole criterion for assessing the potential fire hazard of the product in use.

All material tested where before testing pre-conditioned according to EN 13238:2010 at temperature (23 ± 2) °C and relative humidity (50 ± 5) %.

During all testing the edges of the test specimens where protected with a steel retainer frame.

Because of a limited access to test material, for each material tested, only one or two tests were conducted instead of the three stipulated by the standard.

The accreditation referred to is valid for ISO 5658-2, ISO 5659-2, ISO 5660-1 and ISO 9239-1.

The document CEN/TS 45545-2:2009 “Railway applications – Fire protection on railway vehicles – Part 2: Requirements for fire behaviour of materials and components” is a technical specification that may be changed before it is published as the final standard.

SP Technical Research Institute of Sweden Fire Technology - Fire Dynamics

Performed by



Kerstin Borgerud

Examined by



Per Thureson

Appendices

1. Test results, ISO 5658-2 Surface spread of Flame
2. Test results, ISO 5659-2 Smoke Box with additional FTIR-analysis
3. Test results, ISO 5660-1 Cone Calorimeter
4. Test results, ISO 9239-1 Reaction to fire tests for floorings
5. Rate of heat release of upholstered furniture
6. Definitions of “Operation Category” and “Design Category”

Appendix 1

ISO 5658-2:2006, Reaction to fire tests – Spread of flame – Part 2: Lateral spread on building products in vertical configuration

The test method consists of exposing a specimen placed in a vertical position adjacent to a gas-fired radiant panel where the surface of the specimen is exposed to a well-defined field of radiant heat flux. Time to ignition, lateral spread of flame and time to flame extinguishment is measured.

The results are expressed in terms of flame spread distance versus time, flame front velocity versus heat flux, the critical heat flux at extinguishment and the average heat for sustained burning.

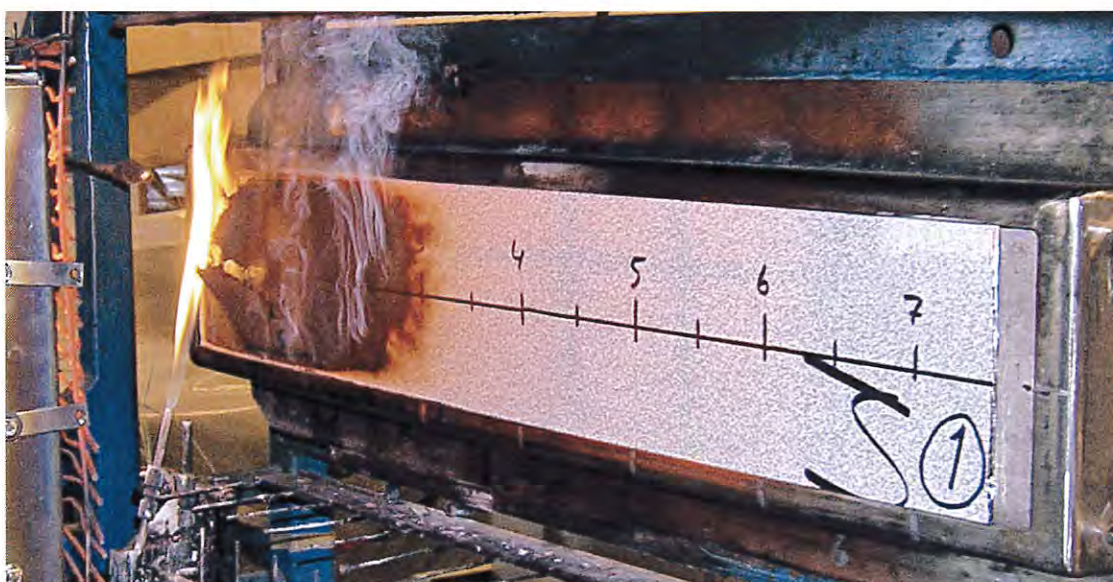


Photo 11 - Fire test according to ISO 5658-2 "Surface spread of Flame"

Application

Test specimen is, as stipulated by the standard, wrapped with aluminium foil which is cut away from the front side of the specimen. The specimen is loosely placed in front of a 3 mm steel plate and then in front of a backing of a non-combustible board, type "Promatect H" with a nominal density of 800 kg/m³.

Specimens

The test specimens consisted of, from the exposed side, 3 mm laminate with a 27 mm insulation layer behind.

Because of limited access to test material, only the laminate layer (without insulation layer behind) was tested in test number one and two. In test number three the laminate layer was tested with the insulation layer mounted behind it.

Test procedure

Propane gas was used in the pilot flame, the pilot flame was used in an impinging mode.

Appendix 1

Table 9 - Observations made during fire test

Test no	1		2		3	
The flame front reached, mm	Time, min:s	Heat for sustained burning, MJ/m ²	Time, min:s	Heat for sustained burning, MJ/m ²	Time, min:s	Heat for sustained burning, MJ/m ²
50	NI*	NI*	1:43	5.2	1:25	4.3
100	-	-	2:03	6.0	-	-
150	-	-	2:03	5.7	-	-
200	-	-	2:35	6.6	-	-
Flames at flame front went out:	NI*		2:55 at 230 mm		2:00 at 55 mm	
Burning droplets:	none		none		none	

* NI = No ignition.

Note

For all three specimens the surface cracked during the test, see photo no 12.

Table 10 - Derived fire characteristics

Test no	1	2	3
Heat for ignition, MJ/m ²	NI*	5.7	4.3
Average heat for sustained burning, Q _{sb} , MJ/m ²	NI*	6.1	**
Critical flux at extinguishment, CFE, kW/m ²	>50.5	39.1	50.1
Total heat release, Q _t , MJ	NI*	<0.1	<0.1
Peak heat release rate, Q _p , kW	NI*	0.5	0.6

* NI = No ignition.

** This value is unknown since the flame front did not reach 150 mm.

Appendix 1

Figure 1- Heat release rate, graph

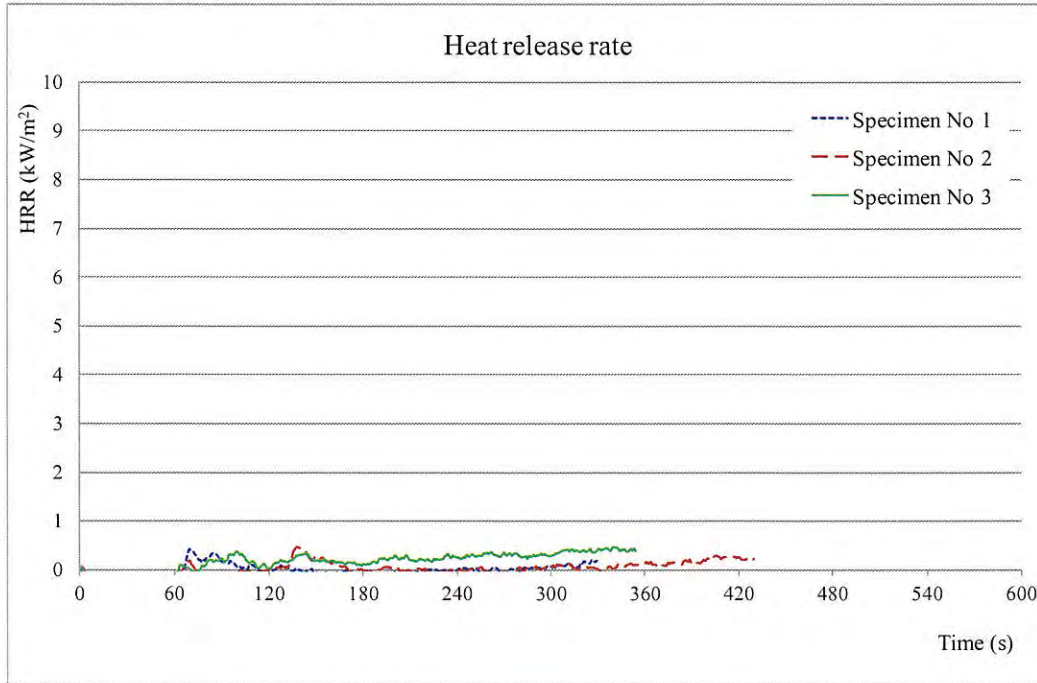


Photo 12 - All three of the tested specimens, no difference detected between specimens with or without insulation layer behind the laminate layer.

Table 11 - Measured data

Test no	Specimen	Layer	Thickness (mm)	Area weight (kg/m ²)
1 & 2	Wall lining, "X1"	laminate	3.03	4.72
3	Wall lining, "X1"	laminate insulation	2.95 17.10	4.54 0.25

Date of test

February 7, 2012.

Appendix 2

ISO 5659-2:2006, Plastics - Smoke generation - Part 2: Determination of optical density by a single-chamber test with additional FTIR analysis according to CEN/TS 45545-2:2009

A specimen is mounted horizontally within a closed chamber and exposed to a constant irradiance, irradiance level is 25 or 50 kW/m². The test is conducted with resp. without a pilot flame. The smoke evolved is collected in the chamber and measured using a photometric equipment. The results are reported in terms of specific optical density.

In accordance with CEN/TS 45545-2:2009, Annex C, “Method 1”, the smoke additionally is analysed using FTIR. The method consists of a sampling procedure and analysis of gases present in the fire effluents using spectroscopy in the Fourier transform infrared technique (FTIR). Eight compounds are quantified: CO₂, CO, HF, HCl, HBr, HCN, NO_x and SO₂, the ratios of emission levels and a reference level for each compound are used to calculate “Conventional Index of Toxicity” (CIT_G, where “G” stands for “General products”, see CEN/TS 45545-2:2009, paragraph C.16.2).

Application

The test specimen is wrapped with aluminium foil which is cut away from the front side of the specimen as stipulated by the standard CEN/TS 45545-2, appendix D. The test specimens “Wall and ceiling liner, X1” was placed on a substrate of steel sheet. The test specimen then is loosely placed on to a layer of low-density (nominally 65 kg/m³) refractory-fibre blanket so that the total thickness of the test specimen is 50 mm.

During all tests a retainer frame was used. No other backing than the non-combustible required in the standard was used.

Table 12 - Specimens

Test specimens	Test no	Irradiance, kW/m ²	Pilot flame
Wall lining, “X1”	1, 2	50	without
Passenger seat, upholstery “X1”	3, 4	25	with
Wall lining with surface layer of 1 mm Al. sheet, “C20/X10”	5	50	without
Passenger seat, upholstery “C20/X10”	6, 7	25	with
Passenger seat, back shell “C20/X10”	8, 9	50	without
Floor, “X1”	10, 11	25	with

Appendix 2

Figure 2- Light Transmission, "X1"

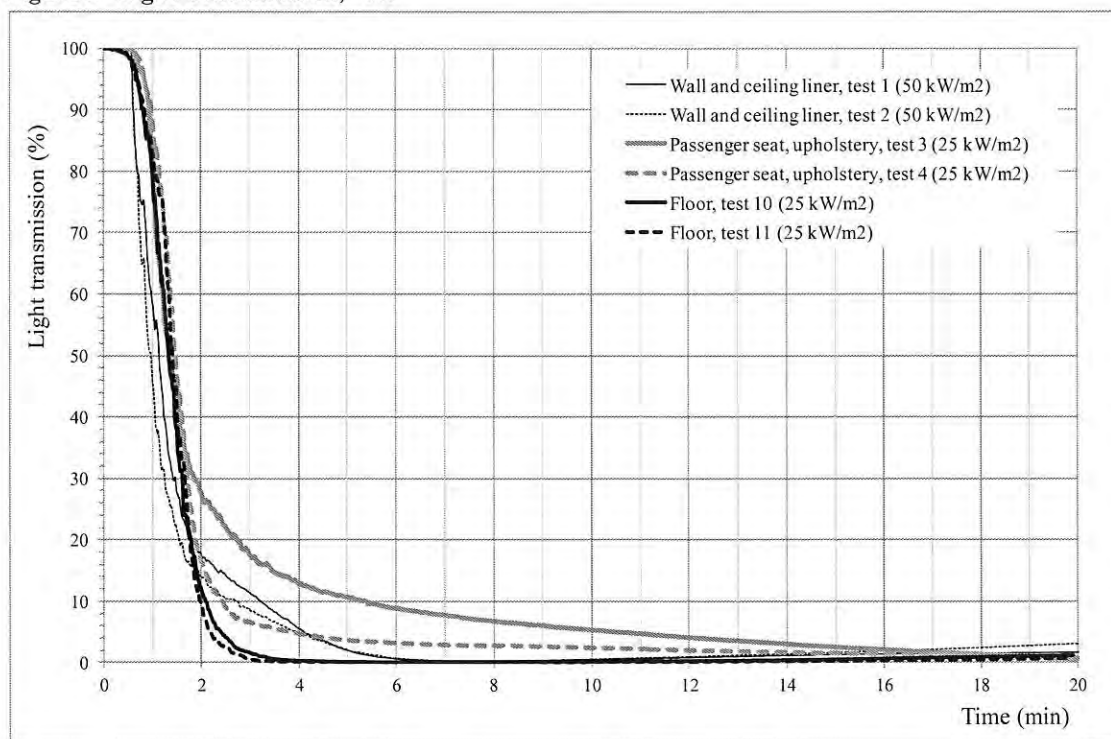


Table 13 - Test results, "X1"

Variable*	Wall lining		Passenger seat, upholstery		Floor	
	Test 1	Test 2	Test 3	Test 4	Test 10	Test 11
$D_{S, max}$	362	342	289	299	404	421
$D_{S,4}$	167	174	118	173	324	384
$D_{S,10}$	315	299	170	214	362	419
D_c	31	29	22	0	59	62
VOF4	340	384	242	351	530	617
$CIT_G 4$	0.11	0.16	0.32	0.10	4.63	5.97
$CIT_G 8$	0.33	0.41	0.72	0.25	5.67	7.17
Duration of test, s	1200	1200	1200	1200	1200	1200

* Variable explanation given in Table 14.

Appendix 2

Figure 3- Light Transmission, “C20/X10”

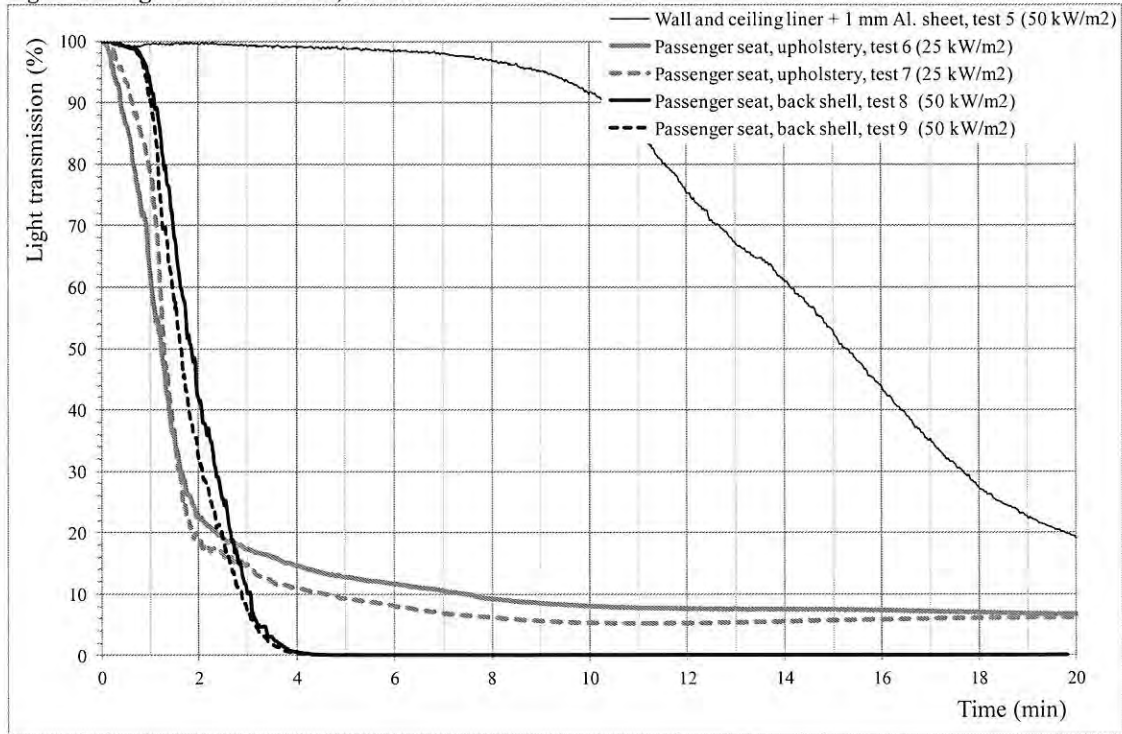


Table 14 - Test results, “C20/X10”

Variable	Wall and ceiling lining (+ 1 mm Al. sheet)	Passenger seat, upholstery		Passenger seat, back shell	
	Test 5	Test 6	Test 7	Test 8	Test 9
$D_{S, max}$	97	156	168	898	748
$D_{S,4}$	0.4	111	127	301	321
$D_{S,10}$	5	145	167	807	659
D_c	7	26	30	179	157
VOF4	1	268	281	336	373
$CIT_G 4$	0	0.17	0.19	0.02	0.02
$CIT_G 8$	0	0.26	0.31	0.04	0.08
Duration of test, s	1200	1200	1200	1200	1200

* Variable explanation given in Table 14.

Appendix 2

Table 15 - Table of signs

D_s	Specific optical density, calculated as follows: $D_s = 132 \log \frac{100}{T}$ where T = percent light transmittance.
$D_{s,max}$	Maximum specific optical density.
D_{s4}	Specific optical density at 4 minutes.
D_{s10}	Specific optical density at 10 minutes.
D_c	Specific optical density correction factor for the smoke absorbed on the glass windows of the optical system.
VOF4	Cumulative value of specific optical density of smoke in the first 4 minutes of the test calculated as follows: $D_s(1) + D_s(2) + D_s(3) + \frac{D_s(4)}{2}$
$CIT_G 4$	Conventional Index of Toxicity, general products, at 4 minutes.
$CIT_G 8$	Conventional Index of Toxicity, general products, at 8 minutes.

Notes

None of the specimens tested in test no 1, 2 or 5 ignited.
 In test no 3 the sample ignited at 44 seconds and extinguished at 90 seconds.
 In test no 4 the sample ignited at 121 seconds and extinguished at 209 seconds.
 In test no 6 the sample ignited at 53 seconds and extinguished at 1200 seconds.
 In test no 7 the sample ignited at 65 seconds and extinguished at 1200 seconds.
 In test no 8 the sample ignited at 244 seconds but it was not possible to establish when it extinguished.
 In test no 9 the sample ignited at 233 seconds but it was not possible to establish when it extinguished.
 In test no 10 the sample ignited at 83 seconds and extinguished at 747 seconds.
 In test no 11 the sample ignited at 70 seconds and extinguished at 730 seconds.

Appendix 2

Gas analysis

The gas concentrations given in table 1 and 2 were measured in the test chamber. The gas samples were taken from 300 mm below the ceiling of the test chamber. The concentrations of the different gas species were measured with FTIR gas analysis. The gas concentrations at the 4 and 8 minutes sampling points are evaluated and reported as the Conventional Index of Toxicity (General products), CIT_G, according to CEN/TS 45545-2:2009, table 8, ref. T11.01.

Table 16 - Measured concentration at 4 min.

Gas species	Test 1 ppm/mg/m ³	Test 2 ppm/mg/m ³	Test 3 ppm/mg/m ³	Test 4 ppm/mg/m ³	Test 5 ppm/mg/m ³	Test 6 ppm/mg/m ³
CO ₂	1567 / 2523	1693 / 2691	5224 / 8536	3398 / 5529	<300 / 0	4905 / 8059
CO	547 / 561	613 / 620	268 / 279	187 / 194	<20 / 0	123 / 128
HF	<5 / 0	<5 / 0	<5 / 0	<5 / 0	<5 / 0	<5 / 0
HCl	<5 / 0	<5 / 0	100 / 134	21 / 28	<5 / 0	27 / 36
HBr	<10 / 0	<10 / 0	<10 / 0	<10 / 0	<10 / 0	<10 / 0
HCN	55 / 54	87 / 85	24 / 24	16 / 16	<2 / 0	20 / 21
NO _x	<15 / 0	<15 / 0	24 / 31	<15 / 0	<15 / 0	19 / 21
SO ₂	<10 / 0	<10 / 0	63 / 149	38 / 89	<10 / 0	55 / 132
CIT_G at 4 min	0.11	0.16	0.32	0.10	0	0.17

* For gas species not detected a zero value is used in the CIT equation.

Table 17 - Measured concentration at 4 min, continued.

Gas species	Test 7 ppm/mg/m ³	Test 8 ppm/mg/m ³	Test 9 ppm/mg/m ³	Test 10 ppm/mg/m ³	Test 11 ppm/mg/m ³
CO ₂	4556 / 7423	4575 / 7169	2236 / 3540	5957 / 9669	6658 / 10684
CO	180 / 187	181 / 180	306 / 308	720 / 743	800 / 817
HF	<5 / 0	<5 / 0	<5 / 0	<5 / 0	12 / 9
HCl	30 / 39	<5 / 0	<5 / 0	3196 / 4243	4114 / 5401
HBr	<10 / 0	<10 / 0	<10 / 0	<10 / 0	20 / 59
HCN	30 / 30	<2 / 0	<2 / 0	12 / 12	8 / 7
NO _x	18 / 20	<15 / 0	<15 / 0	<15 / 0	<15 / 0
SO ₂	56 / 133	<10 / 0	<10 / 0	<10 / 0	13 / 31
CIT_G at 4 min	0.19	0.02	0.02	4.63	5.97

* For gas species not detected a zero value is used in the CIT equation.

Appendix 2

Table 18 - Measured concentration at 8 min, continued.

Gas species	Test 1 ppm/mg/m ³	Test 2 ppm/mg/m ³	Test 3 ppm/mg/m ³	Test 4 ppm/mg/m ³	Test 5 ppm/mg/m ³	Test 6 ppm/mg/m ³
CO ₂	2733 / 4342	3005 / 4731	7596/12263	5320 / 8531	<300 / 0	8005 / 13002
CO	2033 / 2055	2143 / 2146	502 / 516	336 / 343	<20 / 0	255 / 263
HF	<5 / 0	<5 / 0	<5 / 0	<5 / 0	<5 / 0	<5 / 0
HCl	<5 / 0	<5 / 0	303 / 400	93 / 121	<5 / 0	29 / 39
HBr	<10 / 0	<10 / 0	<10 / 0	<10 / 0	<10 / 0	<10 / 0
HCN	145 / 142	200 / 193	42 / 42	32 / 31	<2 / 0	39 / 39
NO _x	<15 / 0	<15 / 0	46 / 54	<15 / 0	<15 / 0	34 / 37
SO ₂	<10 / 0	<10 / 0	96 / 226	68 / 160	<10 / 0	72 / 170
CIT_G at 8 min	0.33	0.41	0.72	0.25	0	0.26

* For gas species not detected a zero value is used in the CIT equation.

Table 19 - Measured concentration at 8 min, continued.

Gas species	Test 7 ppm/mg/m ³	Test 8 ppm/mg/m ³	Test 9 ppm/mg/m ³	Test 10 ppm/mg/m ³	Test 11 ppm/mg/m ³
CO ₂	8370/13486	8325/12812	12250/18929	10446/16214	12519/20211
CO	367 / 376	365 / 358	1050 / 1032	1067 / 1054	1146 / 1177
HF	<5 / 0	<5 / 0	<5 / 0	<5 / 0	14 / 10
HCl	40 / 53	<5 / 0	<5 / 0	4090 / 5195	4844 / 6399
HBr	<10 / 0	<10 / 0	<10 / 0	<10 / 0	49 / 146
HCN	49 / 49	<2 / 0	<2 / 0	12 / 12	9 / 9
NO _x	39 / 43	<15 / 0	<15 / 0	<15 / 0	<15 / 0
SO ₂	77 / 180	<10 / 0	<10 / 0	<10 / 0	29 / 68
CIT_G at 8 min	0.31	0.04	0.08	5.67	7.17

* For gas species not detected a zero value is used in the CIT equation.

Appendix 2

Table 20 - Summary.

	Wall and ceiling lining, "X1"		Passenger seat, upholstery, "X1"		Floor, "X1"	
	Test 1	Test 2	Test 3	Test 4	Test 10	Test 11
Initial weight (g)	37.31	36.51	49.08	46.63	59.29	60.51
Final weight (g)	25.30	25.06	33.58	33.52	37.70	37.73
Mass lost (g)	12.01	11.45	15.50	13.12	21.59	22.78
CIT _G at 4 min*	0.11	0.16	0.32	0.10	4.63	5.97
CIT _G at 8 min*	0.33	0.41	0.72	0.25	5.67	7.17

* The condition that gives the worst result of CIT (mean of two test specimens) for either 4 min or 8 min sampling time shall be used for the purpose of classification.

Table 21 – Summary, continued

	Wall and ceiling lining + 1 mm Al. sheet, "C20/X10"	Passenger seat, upholstery, "C20/X10"		Passenger seat, back shell, "C20/X10"	
	Test 5	Test 6	Test 7	Test 8	Test 9
Initial weight (g)	51.41	52.38	51.62	54.41	53.83
Final weight (g)	45.47	45.57	44.15	31.49	31.23
Mass lost (g)	5.94	6.81	7.47	22.92	22.60
CIT _G at 4 min*	0	0.17	0.19	0.02	0.02
CIT _G at 8 min*	0	0.26	0.31	0.04	0.08

* The condition that gives the worst result of CIT (mean of two test specimens) for either 4 min or 8 min sampling time shall be used for the purpose of classification.

Appendix 2

Table 22 - Measured data

Test no	Specimen	Layer	Thickness (mm)	Area weight (kg/m ²)
1	Wall lining, "X1"	laminate	3.03	4.72
		insulation	18.02	0.25
2	Wall lining, "X1"	laminate	2.95	4.54
		insulation	17.10	0.25
3	Passenger seat, upholstery, "X1"	fabric	2.39	0.90
		foam	10.78	1.98
		cork wood	9.25	2.12
		painted wooden board	4.49	3.24
4	Passenger seat, upholstery, "X1"	fabric	2.43	0.88
		foam	9.21	2.01
		cork wood	10.51	2.08
		painted wooden board	4.58	3.34
10	Floor, "X1"	PVC carpet glued onto plywood	14.49	9.78
		Styrofoam	8.98	0.26
11	Floor, "X1"	PVC carpet glued onto plywood	14.33	10.14
		Styrofoam	9.11	0.27
5	Wall lining + Aluminium sheet, "C20/X10"	Aluminium sheet	0.52	1.31
		laminate	2.96	4.62
		insulation	20.10	0.25
6	Passenger seat, upholstery, "C20/X10"	fabric	4.36	0.98
		foam	18.00	2.24
		corrugated plastic board	2.92	5.56
7	Passenger seat, upholstery, "C20/X10"	fabric	4.03	0.99
		foam	18.00	2.33
		corrugated plastic board	2.78	5.49
8	Passenger seat, back shell, "C20/X10"	corrugated plastic board	2.92	5.80
		foam	18.00	2.39
		fabric	3.77	0.96
9	Passenger seat, back shell, "C20/X10"	corrugated plastic board	2.91	5.77
		foam	18.10	2.40
		fabric	3.69	0.97

Date of test

February 8-9, 2012.

Appendix 3

ISO 5660-1:2002, Reaction-to-fire tests - Part 1: Heat release rate (cone calorimeter method) with additional MARHE calculations according to CEN/TS 45545-2:2009

ISO 5660-1, the “Cone calorimeter-method”, specifies a method for assessing the heat release rate of a specimen exposed in the horizontal orientation to controlled levels of irradiance with an external igniter. The heat release rate is determined by measurement of the oxygen consumption derived from the oxygen concentration and the flow rate in the combustion product stream. The time to ignition (sustained flaming) is also measured.

In accordance with CEN/TS 45545-2:2009, average rate of heat emission at time t (ARHE), corresponds to the cumulative heat emission from t = 0 to t = t divided by t.

MARHE is the maximum value of ARHE during the time period t = 0 to t = end, expressed as kW/m² (heat emission rate per unit area).

Application

The test specimen is wrapped with aluminium foil which is cut away from the front side of the specimen as stipulated by the standard CEN/TS 45545-2, appendix D. The test specimens “Wall and ceiling liner, X1” was placed on a substrate of steel sheet. The test specimen then is loosely placed on to a layer of low-density (nominally 65 kg/m³) refractory-fibre blanket so that the total thickness of the test specimen is 50 mm.

During all tests a retainer frame was used, exposed surface area of test specimen was 0.009 m². No other backing than the non-combustible required in the standard was used. Upholstery material was tested using four metal wires cross the surface, according to the standard, in order to fix the material in the frame during the test.

Table 23 - Specimens

Test specimens	Test no	Irradiance, kW/m ²	Calibration constant (C), m ^{1/2} g ^{1/2} K ^{1/2}
Wall lining, “X1”	1, 2	50	0.04307
Passenger seat, upholstery “X1”	3, 4	25	0.04264
Wall lining, with surface layer of 1 mm Al. sheet, “C20/X10”	5	50	0.04307
Passenger seat, upholstery “C20/X10”	6, 7	25	0.04264
Passenger seat, back shell “C20/X10”	8, 9	50	0.04307
Floor, “X1”	10, 11	25	0.04330

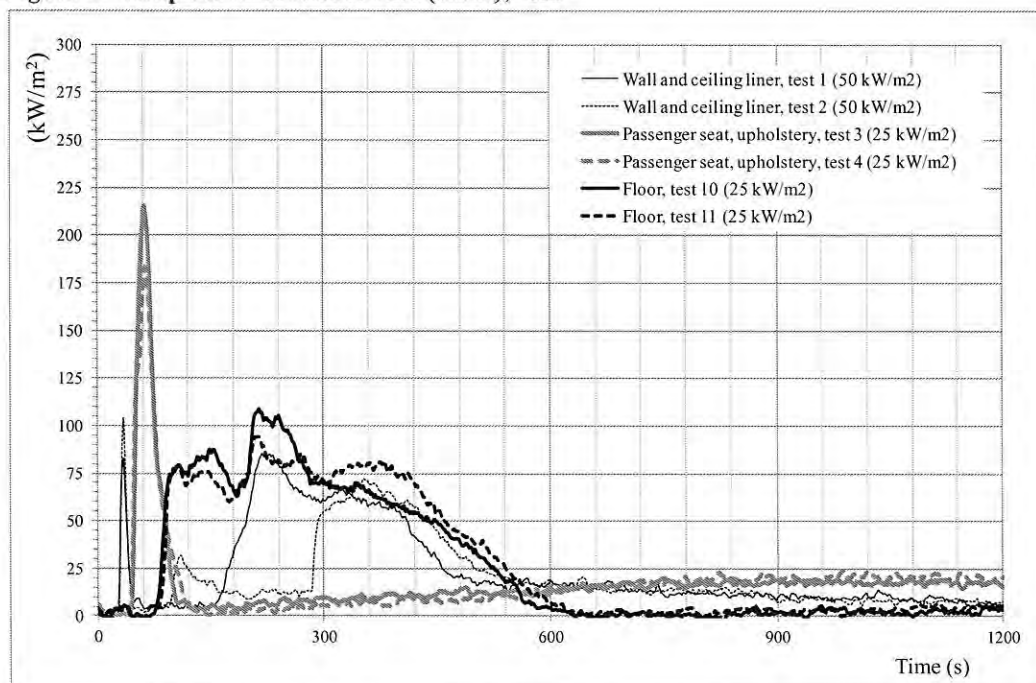
Appendix 3

Table 24 - Test results, "X1"

Variable	Wall lining		Passenger seat, upholstery		Floor	
	Test 1	Test 2	Test 3	Test 4	Test 10	Test 11
t_{flash}	-	-	-	-	-	-
t_{ign}	00:33	00:34	00:51	00:49	01:23	01:27
t_{ext}	17:59	14:42	01:57	02:18	10:14	10:31
t_{test}	20:00	20:00	20:00	20:00	20:00	20:00
q	<i>See figure 1</i>					
q_{max}	86	104	215	184	108	94
q_{180}	18	15	34	33	83	75
q_{300}	39	21	24	22	77	76
THR	27.1	23.3	20.6	20.5	31.7	33.2
M_0	64.0	64.6	134.5	132.0	109.4	109.4
M_s	50.5	51.1	134.0	131.3	108.2	108.3
M_f	24.6	24.9	109.4	107.3	60.6	59.0
$MLR_{ign-end}$	2.5	2.5	2.4	2.3	4.7	4.9
MLR_{10-90}	3.7	3.5	2.2	2.1	4.5	4.7
TML	2911	2938	2728	2657	5286	5469
ΔH_c	9.3	7.9	7.6	7.7	6.0	6.1
MARHE	40.4	30.7	62.1	57.6	61.1	60.6
V	24	24	24	24	24	24

Variable explanation given in table no 27.

Figure 4 - Graph of heat release rate (HRR), "X1"



Appendix 3

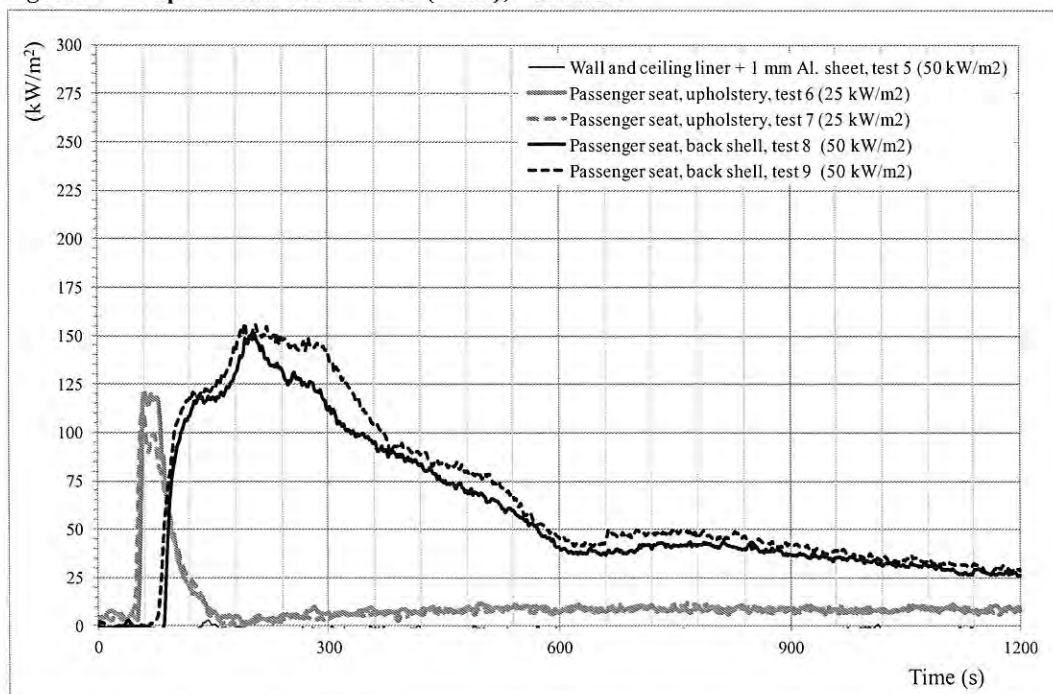
Table 25 - Test results, "C20/X10"

Variable**	Wall and ceiling lining + 1 mm Al. sheet	Passenger seat, upholstery		Passenger seat, back shell	
	Test 5	Test 6	Test 7	Test 8	Test 9
t_{flash}	-	-	-	-	-
t_{ign}	NI*	00:58	00:53	01:31	01:24
t_{ext}	-*	02:38	02:41	20:00	20:00
t_{test}	20:00	20:00	20:00	20:00	20:00
q	See figure 1				
q_{max}	3	120	110	151	156
q_{180}	-	29	28	124	130
q_{300}	-	20	19	116	128
THR	0.0	13.3	13.0	70.1	78.4
M_0	89.7	100.9	100.0	100.3	102.0
M_s	89.6	100.2	99.3	98.5	100.5
M_f	80.1	83.9	81.4	56.5	56.1
$MLR_{\text{ign-end}}$	-	1.6	1.7	4.3	4.5
MLR_{10-90}	1.4	1.5	1.7	4.8	5.1
TML	-	1802	1994	4735	4999
ΔH_c	-	7.4	6.5	14.8	15.7
MARHE	0.5	44.9	41.8	88.9	100.3
V	24	24	24	24	24

* NI = no ignition

** Variable explanation given in table no 27.

Figure 5 - Graph of heat release rate (HRR), "C20/X10"



Appendix 3

Table 26 - Measured data

Test no	Specimen	Layer	Thickness (mm)	Area weight (kg/m ²)
1	Wall lining, "X1"	laminate	2.98	4.69
		insulation	27.04	0.34
2	Wall lining, "X1"	laminate	3.00	4.68
		insulation	29.27	0.40
3	Passenger seat, upholstery, "X1"	fabric	2.52	0.91
		foam	32.40	6.83
		cork wood	8.66	2.25
		painted wooden board	4.42	3.45
4	Passenger seat, upholstery, "X1"	fabric	2.32	0.91
		foam	33.95	6.90
		cork wood	8.38	2.17
		painted wooden board	5.49	3.22
10	Floor, "X1"	PVC carpet glued onto plywood	14.40	9.95
		Styrofoam	34.30	0.99
11	Floor, "X1"	PVC carpet glued onto plywood	14.61	9.98
		Styrofoam	34.80	0.96
5	Wall lining + Aluminium sheet, "C20/X10"	Aluminium sheet	0.52	1.31
		laminate	2.98	4.67
		insulation	28.78	0.36
6	Passenger seat, upholstery, "C20/X10"	fabric	4.01	0.98
		foam	43.00	3.57
		corrugated plastic board	2.98	5.55
7	Passenger seat, upholstery, "C20/X10"	fabric	4.28	0.94
		foam	43.00	3.61
		corrugated plastic board	2.95	5.45
8	Passenger seat, back shell, "C20/X10"	corrugated plastic board	2.94	5.52
		foam	43.13	3.60
		fabric	3.79	0.91
9	Passenger seat, back shell, "C20/X10"	corrugated plastic board	2.95	5.56
		foam	42.49	3.67
		fabric	3.84	0.97

Date of test

February 7, 2012.

Appendix 3

Table 27 - ISO 5660-1: 2002, Parameter and variable explanation

Parameter	Variable	Explanation
t_{flash}	Flashing (min:s)	Time from test start until flames with shorter duration than 1 s.
t_{ign}	Ignition (min:s)	Time from test start until sustained flaming with duration more than 10 s.
t_{ext}	All flaming ceased (min:s)	Time from test start until the flames have died out.
t_{test}	Test time (min:s)	Test time. From test start until end of test.
Q_{max}	Peak heat release rate (kW/m ²)	Peak heat release rate during the entire test.
Q_{180}	Average heat release, 3 min (kW/m ²)	Average heat release rate during 3 minutes from ignition. If the test is terminated before, the heat release rate is taken as 0 from the end of test.
Q_{300}	Average heat release, 5 min (kW/m ²)	Average heat release rate during 5 minutes from ignition. If the test is terminated before, the heat release rate is taken as 0 from the end of test.
THR	Total heat produced (MJ/m ²)	Total Heat Released from test start until end of test.
M_0	Sample mass before test (g)	Mass of specimen.
M_s	Sample mass at sustained flaming (g)	Mass of specimen at sustained flaming.
M_f	Sample mass after test (g)	Mass of specimen at the end of the test.
$MLR_{\text{ign-end}}$	Average mass loss rate (g/m ² s)	Mass Loss Rate. Average mass loss rate from ignition until end of test.
MLR_{10-90}	Average mass loss rate (g/m ² s)	Mass Loss Rate. Average mass loss rate between 10% and 90% of mass loss.
TML	Total mass loss (g/m ²)	Total mass loss from ignition until end of test.
ΔH_c	Effective heat of combustion (MJ/kg)	Effective heat of combustion calculated as the ratio between total energy released and total mass loss calculated from ignition until end of test.
MARHE	Max average rate of heat emission (kW/m ²)	Maximum Average Rate of Heat Emission defined as the maximum of the function (cumulative heat release between $t = 0$ and $\text{time} = t$) divided by ($\text{time} = t$).
V	Volume flow in exhaust duct (l/s)	Volume flow rate in exhaust duct. Average during the test.

Appendix 4

ISO 9239-1:2010, Reaction to fire tests for floorings – Part 1: Determination of the burning behaviour using a radiant heat source

The test specimen is placed in a horizontal position below a gas-fired radiant panel inclined at 30° where it is exposed to a defined heat flux. A pilot flame is applied to the hotter end of the specimen. Following ignition, any flame front which develops is noted and a record is made of the progression of the flame front horizontally along the length of the specimen in terms of the time it takes to spread to defined distances. The results are expressed in terms of flame-spread distance versus time and critical heat flux at extinguishment.

Specimen

Floor consisting of, nearest to the radiant panel, PVC carpet glued onto plywood with overall thickness 14 mm, under the plywood is styrofoam of thickness 34 mm.

Application

The specimen was loosely put on to a particle board, having a density of 680 kg/m³ approximately, with "Bostik Golv- o Vägglim", glue amount 300 g/m² approximately.

Table 28 - Test results

Test no	1	2
The floor covering was ignited, min:s	02:03	02:03
The flames died out, min:s	13:30	14:03
The glow died out, min:s	-	-
Damage on the surface, mm	120	110
Damage in the underlay, mm	-	-
Maximum flame spread, mm	-	-
Time to maximum spread, min:s	12:36	12:48
Critical radiant flux (CHF), kW/m ²	10.40	10.51

Table 29 - Measured data

Test no	Specimen	Layer	Thickness (mm)	Area weight (kg/m ²)
10	Floor, "X1"	PVC carpet glued onto plywood	14.40	9.95
		Styrofoam	34.30	0.99
11	Floor, "X1"	PVC carpet glued onto plywood	14.61	9.98
		Styrofoam	34.80	0.96

Date of test

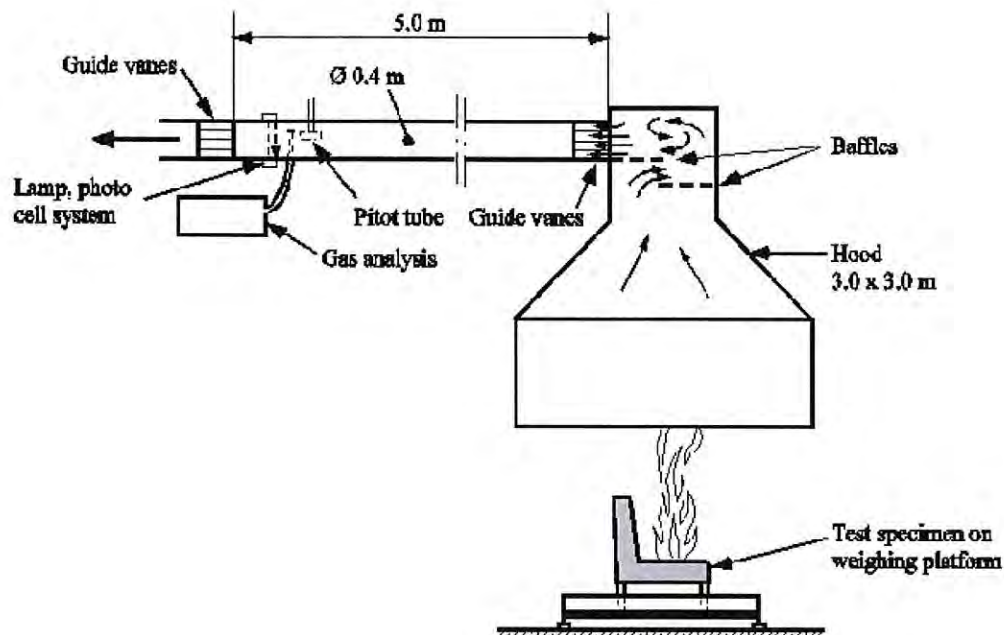
February 12, 2012.

Appendix 5

Rate of heat release of upholstered furniture when tested according to CEN/TS 45545-2:2009, furniture calorimeter.

Test procedure

The CEN/TS 45545-2, Annex B is used for the evaluation of fire behaviour of upholstered furniture in full scale. The specimen is ignited by a gas burner ignition source and burns freely under well ventilated conditions, see figure 1. The ignition source used is a square gas burner, conforming to CEN/TS 45545-2, Annex B. The ignition source is applied on top of the specimen during 3 minutes. The burner heat output is 7 kW. The smoke gases produced are collected by a hood and exhaust system from where samples are taken for gas analysis. Heat release rate is measured continuously.



Schematic drawing of the CEN/TS 45545-2, Annex B, furniture calorimeter equipment.

Ignition source

A square gas burner ignition source fed with propane gas at a mass flow rate of approximately 151 mg s^{-1} (7 kW), conforming to CEN/TS 45545-2, Annex B. It was placed approximately 10 mm from the seat and 85 mm from the back.

Vandalism of passenger seats

The seats were vandalised; the cover was cut and rolled up according to B.4.3 in CEN/TS 45545-2.

Appendix 5

Product, X1

The seat consisted of, from the top; fabric 3 mm, foam 32 mm, cork wood 9 mm and painted wooden board 4 mm. Downwards facing surfaces and also vertical surfaces where covered with steel sheet why only the upwards facing surface need to be tested.

Table 30 - Test results

Product	Time of evaluation [min]	MARHE (incl. burner heat output) [kW]	HRR _{peak} (incl. burner heat output) [kW]
X1	0 - 23	8	10

Figure 6 - Heat release rate (HRR), burner included (7 kW)

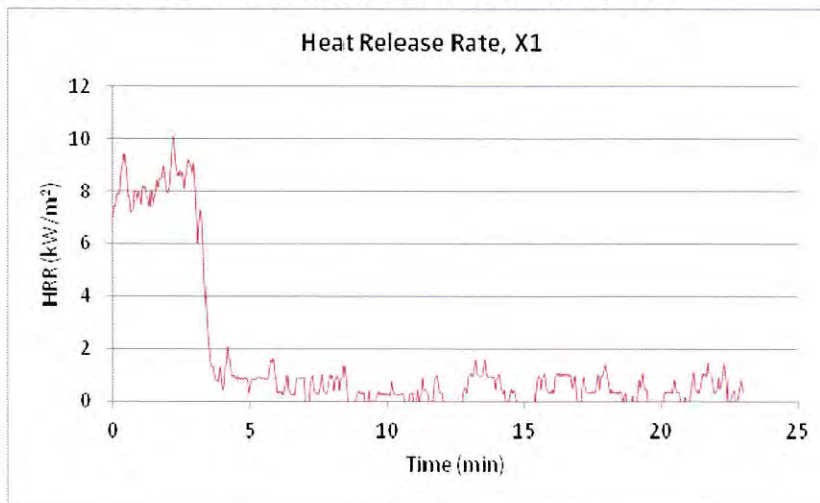
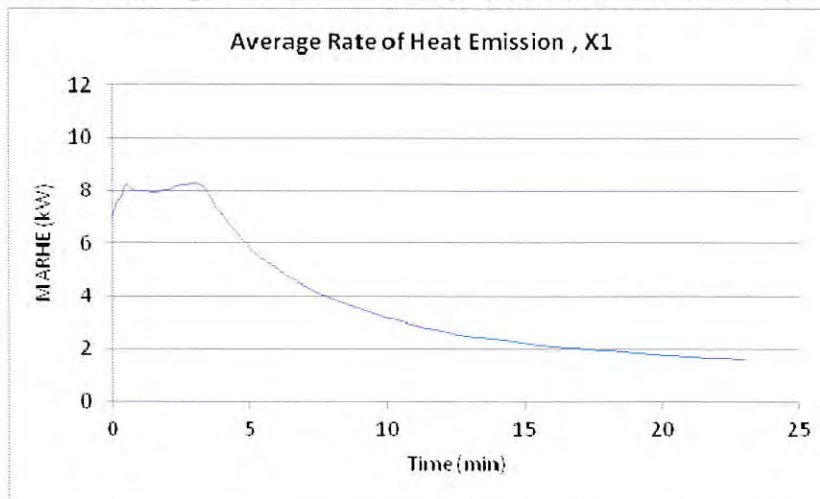


Figure 7 - Average Rate of Heat Emission (ARHE), burner included (7 kW)



Appendix 5

Table 31 - Observations during test

Time min:s	
-02:00	The gas burner was ignited.
00:00	The ignited gas burner was placed on top of the seat. See photo 2.
00:54	The fabric on the back of the seating part is igniting but is unable to support a constant combustion.
03:00	The gas burner was removed from the seat. See photo 4.
03:02	The flames cease but progressive smouldering is visible. See photo 5.
05:03	The smoke production has decreased. See photo 6.
08:56	The progressive smouldering has died out and no smoke is visible. See photo 7.
23:00	The measurements and test is terminated. See photo 8.

Observations after fire test

The upholstered X1 seat showed minor damage after the test, see photo no 9. Some charring is visible around the area where the burner was applied as well as on the lower part of the back.

Photos, X1



Photo 1 - Prior to test.



Photo 2 - Time 00:01. The burner has been applied.



Photo 3 - Time 01:45.



Photo 4 - Time 03:01. Burner just removed.

Appendix 5



Photo 5 - Time 03:08. The flames cease but progressive smouldering is visible.



Photo 6 - Time 05:00. The smoke production has decreased.



Photo 7 - Time 10:00. Smoke is no longer visible.



Photo 8 - Time 23:01. The test is terminated.



Photo 9 - After test. Some charring is visible around the area where the burner was applied as well as on the lower part of the back.

Appendix 5

Product, C20/X10

The material composition of the seat consisted of, from the top; fabric 4 mm, foam 43 mm and a plastic backing of corrugated plastic board 3 mm. The seat had Velcro fixing points.

Table 32 - Test results

Product	Time of evaluation [min]	MARHE (incl. burner heat output) [kW]	HRR _{peak} (incl. burner heat output) [kW]
C20/X10	0 - 23	16	21

Figure 8 - Heat release rate (HRR), burner included (7 kW)

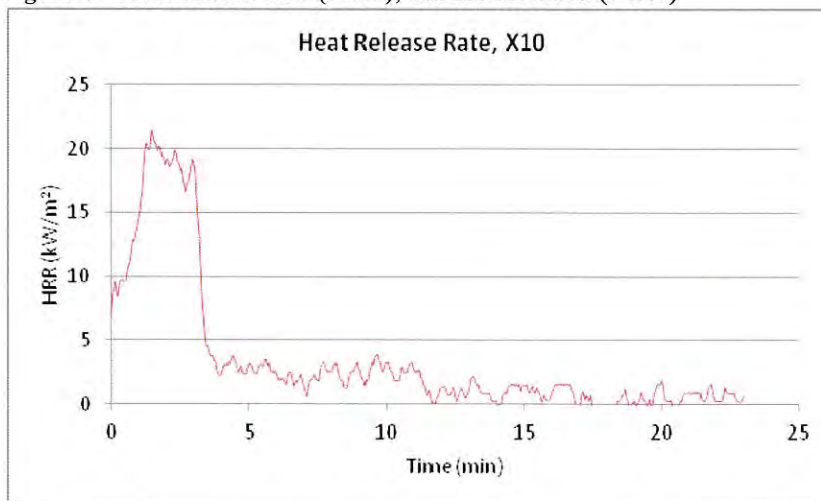
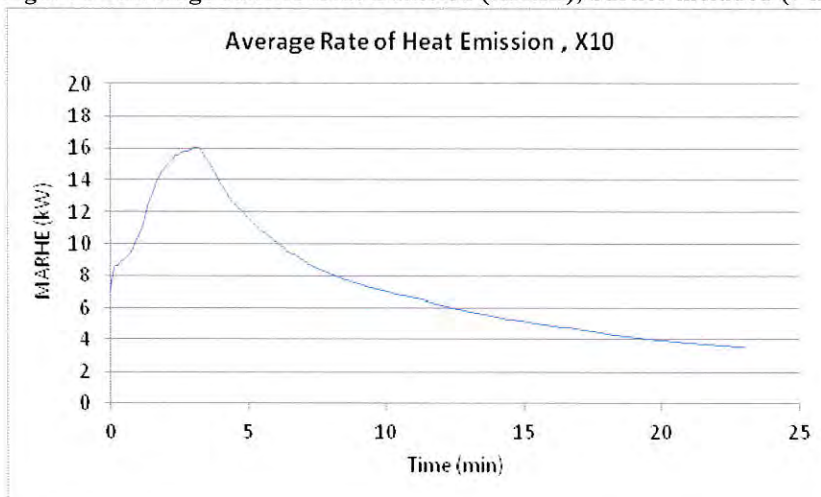


Figure 9 - Average Rate of Heat Emission (ARHE), burner included (7 kW)



Appendix 5

Table 33 - Observations during test

Time min:s	
-02:00	The gas burner was ignited.
00:00	The ignited gas burner was placed on top of the seat. See photo 2.
00:33	The foam on the backrest and parts of the seat is burning and small areas of the fabric have ignited. The flames are high and reaches over the top of the backrest. See photo 3.
01:05	All of the exposed foam is burning with large flames and thick, green smoke is coming out from under the seat. See photo 4.
03:00	The gas burner was removed from the seat. See photo 5.
03:05	The whole seat and back is burning.
04:40	The fire has lost in intensity and only parts of the foam around the Velcro as well as the Velcro is burning. See photo 6.
09:29	The Velcro is burning on the back underneath the pendant piece of fabric. See photo 7.
11:57	The flames on the backrest cease. See photo 8.
12:41	The flames on the seat cease. See photo 10.
23:00	The measurements and test is terminated. See photo 11.

Photos



Photo 1 - Prior to test.



Photo 2 - Time 00:02. The burner has been applied.

Appendix 5



Photo 3 – Time 00:38. The foam on the backrest and parts of the seat is burning and small areas of the fabric have ignited. The flames are high and reaches over the top of the backrest.



Photo 4 - Time 01:10. All of the exposed foam is burning with large flames and thick, green smoke is coming out from under the seat.



Photo 5 - Time 03:09. The burner has just been removed.



Photo 6 – Time 04:40. The fire has lost in intensity and only parts of the Velcro is burning as well as the foam around it.



Photo 7 - Time 09:30. The Velcro is burning on the back underneath the pendant piece of fabric.



Photo 8 - Time 12:00. The flames on the backrest cease.

Appendix 5



Photo 9 - Time 12:43. The flames on the seat cease.



Photo 10 - Time 15:00. The smoke production has stopped.



Photo 11 - Time 23:00. The test is terminated.



Photo 12 - After test.

Table 34 - Test parameter explanation

Parameter	Explanation
Test start	The specimen is exposed to the ignition source.
End of test	When all flaming and glowing combustion have ceased
HRR _{peak} , kW	Peak Heat Release Rate between test start and end of test, included contribution from ignition source.
MARHE, kW	Maximum average rate of heat emission between test start and end of test defined as the cumulative heat emission in the test period divided by the time t.

Appendix 6

CEN/TS 45545-1:2009, 5.1 Operation Category

Railway vehicles are classified under the operation categories 1, 2, 3 and 4.

Operation Category 1

Vehicles that are not designed or equipped to run on underground sections, tunnels and/or elevated structures and which may be stopped with minimum delay, after which immediate side evacuation to a place of ultimate safety is possible.

Operation Category 2

Vehicles that are designed or equipped to run on underground sections, tunnels and/or elevated structures, with side evacuation available and where there are stations or emergency stations that offer a place of ultimate safety to passengers, reachable within a short running time.

Operation Category 3

Vehicles that are designed or equipped to run on underground sections, tunnels and/or elevated structures, with side evacuation available and where there are stations or emergency stations that offer a place of ultimate safety to passengers, reachable within a long running time.

Operation Category 4

Vehicles that are designed or equipped to run on underground sections, tunnels and/or elevated structures, without side evacuation available and where there are stations or emergency stations that offer a place of ultimate safety to passengers, reachable within a short running time. If a vehicle is operating in more than one Operation Category, or changes its service, it shall fulfil the requirements of all the relevant operation categories.

CEN/TS 45545-1:2009, 5.2 Design categories

Railway vehicles are additionally classified under the following design categories:

A: vehicles forming part of an automatic train having no emergency trained staff on board

D: double decked vehicles

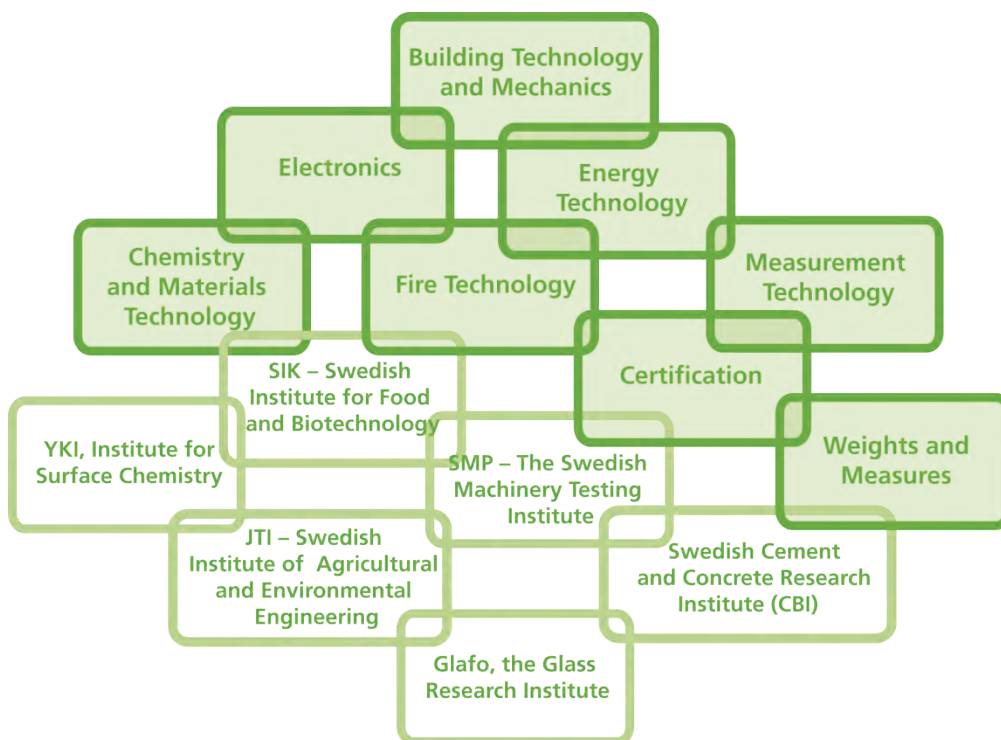
S: sleeping and couchette vehicles

N: all other vehicles (standard vehicles)

Freight transportation vehicles are not covered by CEN/TS 45545.

SP Technical Research Institute of Sweden

Our work is concentrated on innovation and the development of value-adding technology. Using Sweden's most extensive and advanced resources for technical evaluation, measurement technology, research and development, we make an important contribution to the competitiveness and sustainable development of industry. Research is carried out in close conjunction with universities and institutes of technology, to the benefit of a customer base of about 9000 organisations, ranging from start-up companies developing new technologies or new ideas to international groups.



SP Technical Research Institute of Sweden

Box 857, SE-501 15 BORÅS, SWEDEN

Telephone: +46 10 516 50 00, Telefax: +46 33 13 55 02

E-mail: info@sp.se, Internet: www.sp.se

www.sp.se

Fire Technology

SP Report : 2012:05

ISBN 978-91-87017-22-3

ISSN 0284-5172

More information about publications published by SP: www.sp.se/publ